1-1-2014

# Dual Delivery Systems Based On Polyamine Analog Benspm As Prodrug And Gene Delivery Vectors

Yu Zhu
*Wayne State University,*

# DUAL DELIVERY SYSTEMS BASED ON POLYAMINE ANALOG BENSPM AS PRODRUG AND GENE DELIVERY VECTORS

by

**YU ZHU**

**DISSERTATION**

Submitted to the Graduate School

of Wayne State University,

Detroit, Michigan

in partial fulfillment of the requirements

for the degree of

**DOCTOR OF PHILOSOPHY**

2014

MAJOR: PHARMACEUTICAL SCIENCES

Approved by:

_____

Advisor Date

_____

_____

_____

## ACKNOWLEDGEMENTS

I would like to express my sincere thanks to my advisor, Prof. David Oupický for all his guidance, encouragement, and patience during all these years. For me, his attitude to always find an answer for the unknown and his dedication as well as his passion to science explain what a real scientist should be. I am very lucky to have him as my PhD mentor.

My gratitude also goes to my committee members, Profs. Jing Li, Joshua Reineke and Randall Commissaris for their continuous guidance and suggestions during the course of my project. Special thanks also goes to Prof. Gensheng Wu for his expertise with the TNF-related apoptosis inducing ligand (TRAIL), and Prof. Jing Li for the help with LC-MS/MS. I would also like to thank Prof. Patrick Woster for the inspiration of combining BENSpm with our gene delivery systems. My deep thanks also goes to Prof. Hirata and Ms. Aiko Hirata for their help and training with molecular biology when I first started. I thank all our former and current group members, for their help, suggestions and encouragement throughout the years. I thank Dr. Yanmei Dong, for the synthesis of lipid BENSpm conjugates. My thanks also goes to Dr. Stuart Hazeldine, in particular, for teaching me everything about chemistry. Special thanks goes to Dr. Jing Li, for training me from the first day, and always being supportive from all aspects. I thank the Department of Pharmaceutical Sciences for offering me the great learning experience as a PhD student.

Finally, I would like to thank my family for their incredible love and encouragement, and all my friends for their company and support.

## TABLE OF CONTENTS

## LIST OF TABLES

## LIST OF FIGURES

## LIST OF SCHEMES

# CHAPTER 1

# INTRODUCTION

Please note that part of this chapter was taken from a book chapter titled "*Intracellular Delivery Considerations for RNAi Therapeutics*" published in *RNA Interference from Biology to Therapeutics*, K. A. Howard, Ed., Springer, New York 2012 [1]. The authors of the book chapter include Dr. Jing Li, Prof. David Oupicky and me. Part of this chapter was also taken from a review titled *"Recent advances in delivery of drug-nucleic acid combinations for cancer treatment"* published in the *Journal of Controlled Release* [2]. The authors of the review include Dr. Jing Li, Yan Wang, Prof. David Oupicky and me. All the authors agreed with including the work in this dissertation.

## 1.1 Gene Therapy

### 1.1.1 Overview

The U.S. Food and Drug Administration defines gene therapy as "the use of genetic material to treat, cure, or prevent a disease or medical condition". Ever since the first human gene transfer was approved in 1989 [3], the past two decades had witnessed the fast development of gene therapy from preclinical to clinical studies for a vast majority of diseases [4]. According to the data from Journal of Gene Medicine, more than 1,800 clinical trials have been approved worldwide (Figure 1). Although the field of gene therapy was under intense debate after the tragic death of Jesse Gelsinger

in 1999 in a gene therapy clinical trial, recently, the field was able to show promises with encouraging results in both pre-clinical and clinical studies [5].

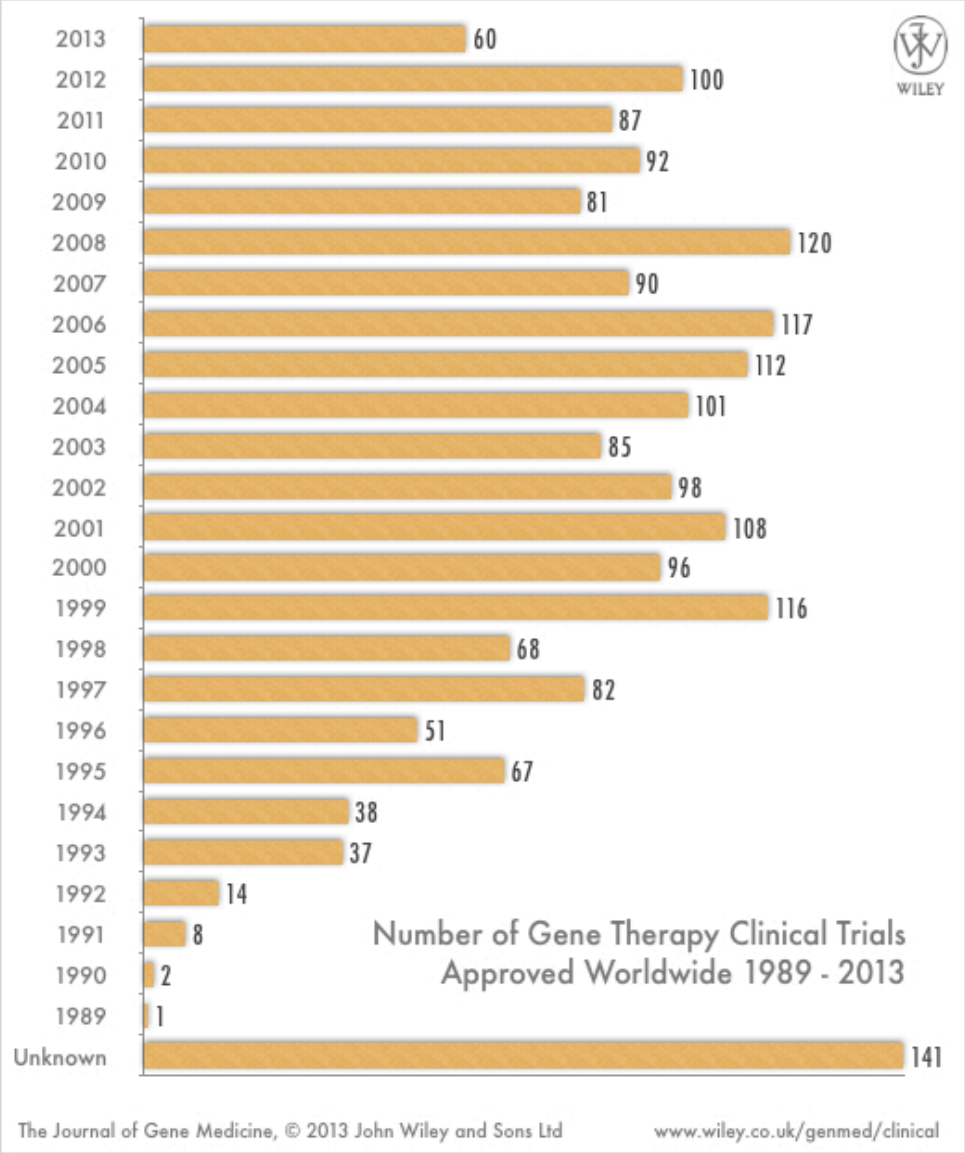


**Figure 1.** Number of gene therapy clinical trials approved worldwide, from 1989 to 2013. (Source: The Journal of Gene Medicine)

To date, clinical trials of gene therapy have been performed in more than 30 countries, with representatives from all five continents. The gene types transferred are

most frequently antigens, cytokines, tumor suppressors and suicide genes, which are generally used for cancer treatment [6]. These categories contributed to the 64.2% of clinical trials in gene therapy against cancer (Figure 2). Other major types of genes in use including growth factors, which were transferred in 7.5% of clinical trials and are mostly aimed at cardiovascular diseases; deficiency genes were used in 7.9 % of trials, which are used for the treatment of monogenic diseases. In all, gene therapy holds promise as a revolutionary approach for the treatment of various diseases.

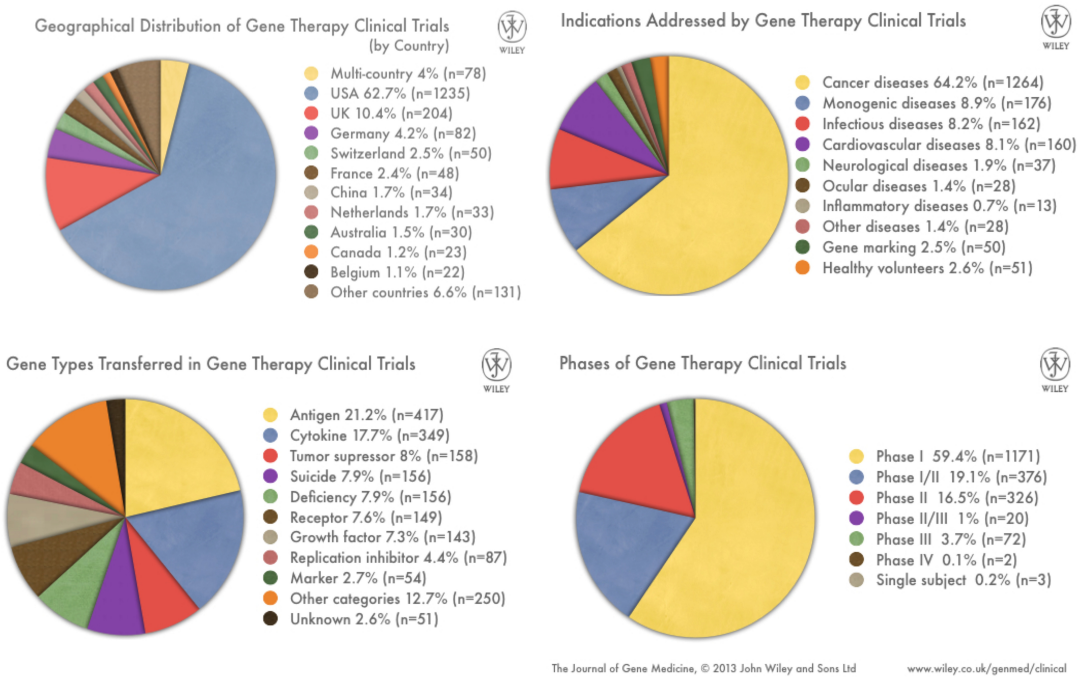


**Figure 2**. Distribution of gene therapy clinical trials categorized by countries, disease types, gene types and clinical phases.

### 1.1.2 Nucleic acids for gene therapy

Diverse genetic materials can be used in gene therapy, with the major types including nucleic acids such as DNA coding functional genes, and RNA interference. Plasmid DNA is a high molecular weight, double-stranded DNA construct with unique circular structure, which is commonly found in bacteria. It is physically separate from chromosomal DNA in cell nuclei, and can replicate independently. Artificial plasmids can be engineered as vectors carrying specific therapeutic genes for the expression in host cells. Examples of plasmids encoding therapeutic genes include tumor necrosis factor–related apoptosis-inducing ligand (TRAIL) gene against renal cell carcinoma, glioma cells and human lung cancer cells [7-9], interleukin-12 (IL-12) gene against malignant melanoma, renal cell carcinoma as well as human ovarian cancer [10-13], and p53 gene against human osteosarcoma, restenosis and endobronchial cancer [14-16]. More recently, minicircle DNA was developed as an effective alternative to conventional plasmid gene vectors. Conventional plasmid DNA contains bacterial backbone with resistance gene sequences and immunogenic motifs, which represent a potential risk for safe clinical application. The minicircle technology removes such sequences and demonstrates improved gene transfection efficiency [17-20]. For instance, Wu and coworkers investigated the antitumor effect of interferon (IFN)-γ gene on human nasopharyngeal carcinoma using minicircle DNA [21]. IFN-γ minicircle DNA demonstrated 11 times higher gene expression in nasopharyngeal carcinoma xenograft in mice, compared with the parental plasmids. Park et al. reported the application of minicircle DNA encoding adiponectin gene as a treatment of diet-induced obesity in mice. This strategy achieved a sufficient blood level of adiponectin in mice, whereas the parental plasmids showed no effect on the adiponectin expression [22].

Antisense oligodeoxynucleotides (AON) are short single-stranded segments of DNA that upon cellular internalization can selectively hybridize with the complementary mRNA and induce translational arrest of the target protein [23, 24]. AON demonstrate promise in gene therapy towards various diseases such as inherited neurodegenerative diseases, dysregulation of hepatic lipid metabolism and cancer [25-27]. For example, treatment with antisense oligonucleotides targeting superoxide dismutase 1 significantly slowed disease progression in a model of amyotrophic lateral sclerosis [28].

Small interfering RNA (siRNA) is a class of double-stranded RNA molecules with 20-25 nucleotides in length. siRNA conducts its silencing function in the cytoplasm by incorporating into RNA-induced silencing complex (RISC). RISC further pairs with the complementary mRNA molecule and leads to the cleavage of mRNA. The process is known as post-transcriptional gene silencing. Ever since the first discovery of siRNA-mediated gene silencing in 1998 [29], siRNA has been vigorously studied in the field of gene therapy. Therapeutics based on siRNA have emerged for the treatment of cancer, infectious diseases, and other diseases associated with specific gene disorders [30]. Current targets in clinical trials with siRNA include apolipoprotein B (ApoB) in patients with hypercholesterolemia [31]; vascular endothelial growth factor (VEGF) in solid tumors, diabetic macular edema and macular degeneration; polo-like kinase 1 (PLK1) in liver tumors [32].

Small hairpin RNA (shRNA) is a class of RNA interference (RNAi) agents with tight hairpin turn that can be cleaved by Dicer enzyme to generate 21-23 nucleotides long siRNA. shRNA can be introduced into host cells via plasmid vectors and further integrated into the host genome. Unlike siRNA, shRNA is usually delivered as the

relative gene inserted in plasmid DNA, which undergoes transcription process to form shRNA [33]. In 2002, Xia and coworkers published the first use of shRNA expressed in viral vector to achieve endogenous gene silencing and applied the strategy to a model system of polyglutamine diseases and demonstrated reduced polyglutamine aggregation in cells [34]. More therapeutic strategies based on shRNA emerged recently. Examples include clinical trials of FANG$^{TM}$ vaccine for the treatment of solid tumors, which contains furin bifunctional shRNA [35]. Orally delivered shRNA against β-catenin for the treatment of familial adenomatous polyposis is currently under Phase II study [36].

Other types of nucleic acids, such as mRNA, microRNA (miRNA) or antagomirs, are also under investigation as suitable components for gene therapy. Although it was generally accepted that mRNA is too unstable to be used for gene therapy, recent advances enabled the mRNA-mediated transfection and demonstrated its advantages as an alternative to plasmid DNA (pDNA) [37]. In addition, new members in the RNAi therapy include miRNA and antagomirs. The miRNA is a single strand RNA generated during endogenous transcription [38]. It is about 22 nucleotides in length, firstly transcribed in the nucleus as long primary transcripts (pri-miRNA), which can be processed to form mature miRNA by Dicer [39]. Depending on the level of complementarity with mRNA, miRNA may cause mRNA cleavage or it may bind imperfectly with the untranslated regions of mRNA, leading to translational repression. Opposing gene regulation can be achieved by antagomirs, which are single-stranded RNAs that can bind endogenous mature miRNA and block the function of miRNA-mediated silencing [40, 41].

### 1.1.3 Gene delivery vectors

Gene therapy shows promise for various diseases but its success requires efficient gene delivery systems. There are two major classes of delivery systems: viral vectors and synthetic nonviral vectors. Viral vectors that are capable of delivering nucleic acids into host cells can be used for gene therapy. Due to their long natural evolution, viruses typically exhibit higher delivery efficiency when compared with synthetic vectors. The most frequently used viral vectors are adenovirus (Ad), adeno-associated virus (AAV), retrovirus (RV), and lentivirus (LV). Ad and AAV are commonly used to deliver genes encoding therapeutic proteins, or encoding shRNA and miRNA. Neither Ad nor AAV integrates into the host genome, but they maintain their transient forms in the nucleus [42]. These virus types are able to infect both dividing and non-dividing cells. Both RVs and LVs can be integrated into the host genome but the major limitation of RV is their inability to infect non-dividing cells [43]. On the other hand, one advantage of LVs is that they favor integration into introns of active transcriptional units, which reduces the risk of insertional oncogenesis. Although viral vectors demonstrated effective gene delivery efficiency and are used in gene therapy clinical trials, their major drawbacks are safety concerns related to insertion mutagenesis and immunogenicity. Difficulties related to production scale-up are also a concern.

Compared with viral vectors, the synthetic delivery systems have several advantages, such as easier chemical modification, easier large-scale production and lower biological safety concerns associated with genome manipulations and host immunogenicity. Most studied synthetic vectors include polycations and cationic lipids.

Polycations bind with negatively charged nucleic acids and self-assemble via electrostatic interactions into nano-sized complexes termed polyplexes. Synthetic and natural polycations have been explored extensively for gene delivery, including polyethylenimine (PEI), poly(amido amine)s (PAA), cyclodextrins, and chitosan. Cationic lipids are amphiphilic molecules with a hydrophobic tail of long hydrocarbon chains (usually two alkyl chains) and a hydrophilic head of a charged group (e.g., quaternary amine) [44]. Plethora of cationic lipids is commercially available. Commonly used lipids for gene delivery include 1,2-di-O-octadecenyl-3-trimethylammonium propane (DOTMA), 1,2-dioleoyl-3-trimethylammonium propane (DOTAP), 1,2-dioleoyl-3-phosphatidylcholine (DOPC) and cholesterol [45]. Moreover, many commercial vectors for gene delivery are cationic lipids, including Lipofectamine, RNAifect and Oligofectamine. Upon hydration, the amphiphilic cationic lipids can spontaneously form complexes with nucleic acid molecules termed lipoplexes, or the lipids can self-assemble into lamellar vesicular structures as liposomes that can encapsulate pre-condensed nucleic acids (major precondensing agents are polycationic molecules such as polyamines and peptides with cationic amino acids) [46-49].

## 1.2 Combination Drug-Nucleic Acids Therapy in Cancer

As mentioned above, the major area of gene therapy application is cancer. Although gene therapy alone showed promise in treating cancer, most successful treatments rely on combination therapies. Heterogeneity of cancer and involvement of multiple pathways during tumor growth, progression and metastasis means that therapies that use only a single agent are unlikely to succeed. Most common types of

combination approaches include combinations of surgery with chemotherapy or radiation therapy, combinations of multiple chemotherapeutics, combinations of chemotherapy with immunotherapy, and more recently also drug-gene combinations [50]. The main rationale for combination therapies is to target different disease pathways to decrease the likelihood of developing drug resistance as well as to synergistically enhance activity of individual treatments and improve target selectivity [51]. Novel approaches that use drug-nucleic acid combinations in cancer treatment are described in the following sections.

### 1.2.1 Combining chemotherapy with nucleic acids to overcome multidrug resistance (MDR)

Drug resistance is one of the major issues causing failure and relapse of many tumors, which makes it a therapeutic target for combination cancer treatment. A typical approach to overcome multi-drug resistance (MDR) is to utilize RNAi to silence the expression of efflux transporter while at the same time giving an appropriate anticancer drug. In many cases, MDR is highly associated with P-glycoprotein (Pgp), also known as multidrug resistance protein 1 (MDR1). Pgp is a glycoprotein responsible for transporting a wide variety of substances across extra- and intracellular membranes. Importantly, Pgp is found overexpressed in various malignant tumor tissues, where it is actively involved in pumping chemotherapy drugs out of the cells. This active role in removal of the chemotherapeutic makes Pgp a prime target in combination approaches to overcome MDR. Numerous studies have shown that successful inhibition of Pgp expression by gene silencing with siRNA or AON dramatically increases the

accumulation of chemotherapy drugs in tumors and results in improved anti-tumor efficiency. However, efflux proteins like Pgp also play a crucial role in physiological regulation of endogenous substrates in healthy tissues throughout the body. It is important to control the silencing of Pgp expression specifically only in the tumor cells to avoid side effects caused by undesirable pharmacological activity in healthy organs and tissues [52]. Other MDR proteins such as MRP1, MRP2, BCRP and certain cell signaling pathways also contribute to chemoresistance. For example, in ovarian cancer, the Notch signaling pathway is a key regulator of tumor resistance to the treatment with cisplatin. Both *in vivo* and *in vitro* evidence showed that Notch 3 overexpression resulted in expansion of cancer stem cells and increased chemoresistance to cisplatin [53].

### 1.2.2 Combining chemotherapy with nucleic acids that promote apoptosis

One hallmark of cancer is its ability to escape apoptosis [54]. Pre-cancerous cells undergoing fatal mutations are usually eliminated from the body through apoptosis, which is a natural self-destruct mechanism. A complex, balanced network of pro-apoptotic and anti-apoptotic genes regulates apoptosis. However, this often becomes dysfunctional during tumor progression as a result of multiple gene mutations. Thus, delivery of gene therapy to reverse the apoptotic functionality of the mutated cells together with apoptosis-inducing chemotherapy is a possible strategy to avoid tumor recurrence and relapse.

The tumor suppressor p53 gene is a key regulator in cell cycle and functions in conserving genome stability. Malkin et al. demonstrated that treatment with wild-type

p53 delivered via an adenovirus significantly increased the sensitivity of various osteosarcoma cell lines to the chemotherapeutics cisplatin and doxorubicin (DOX) [55]. Introducing pro-apoptotic genes to cancer cells alone with the treatment of chemotherapy also showed beneficial outcome. In the treatment of head and neck squamous cell carcinoma, Zheng et al. demonstrated that local delivery of the TRAIL gene by adeno-associated virus-2 (AAV-2) synergized with cisplatin chemotherapy both *in vitro* and *in vivo*, and cisplatin pre-treatment significantly increased TRAIL-induced apoptosis [56]. In addition to TRAIL gene therapy, Wagner et al. described the application of a combined treatment using TNF-$\alpha$ gene and DOX. TNF-$\alpha$ is a cytokine involved in direct killing of tumor cells and promoting tumor angiogenesis, or the formation of new blood vessels. Multiple injections *in vivo* of combined TNF-$\alpha$ gene and DOX therapy significantly delayed tumor growth in subcutaneous murine neuroblastoma as well as liver metastases of human LS174T colon carcinoma [57]. In addition, another approach to promote apoptosis is to silence anti-apoptotic genes. Examples of suitable targets used in combination include Bcl-2 and survivin [58-60]. Bisen et al. investigated the effect of cisplatin in combination with survivin siRNA on apoptosis in head and neck cancer. The results confirmed that halting the function of the survivin gene through LV-mediated RNAi silencing therapy significantly increased the sensitivity of cancer cells to cisplatin-mediated apoptosis [59].

### 1.2.3 Other strategies in drug and nucleic acid combinations

In addition to chemosensitizing tumor cells using combinations of silencing agents and chemotherapeutics, other widely explored strategies are the combination of

anti-cancer drugs with nucleic acids for immunotherapy or anti-angiogenesis. For example, in resistant 4T1 and sensitive EMT-6 syngeneic mouse breast tumor models Kim et al. described the combined local interleukin-12 (IL-12) pDNA delivery with systemic paclitaxel (PTX) chemotherapy. This combination therapy showed improved inhibition of both the growth of the primary tumor as well as lung metastases compared with untreated and monotherapy-treated controls [61]. In another example, Huang et al. described co-delivery of VEGF siRNA and DOX using micelles composed of PEI grafted with stearic acid. Their result showed a promising effect on anti-tumor growth in a mouse model of human hepatocarcinoma [62].

### 1.3 Delivery Strategies for Drug-Nucleic Acid Combinations

Pharmacologic effects of various drug-nucleic acid combinations and the interactions between the signaling pathways involved are complicated and not necessarily well understood, therefore makes it difficult to optimize the delivery strategy, timing and dosing in combination treatment. However, co-delivery of chemotherapeutics and therapeutic nucleic acids in a single nanocarrier may offer benefits in terms of convenience, vehicle uniformity, ratiometric drug loading and temporal drug release [63]. Examples of proven simultaneous delivered drug-nucleic acid combinations are summarized in Table 1.

**Table 1.** Co-delivery of drug-nucleic acid combinations in cancer treatment.

| Nucleic acid | Drug | Target | Delivery method | Ref. |
|---|---|---|---|---|
| Bcl-2 siRNA | DOX | Human hepatic cancer (in vivo) | Polyplex | [64] |
| Bcl-2 siRNA | DOX | Rat glioma (in vivo) | Polyplex | [65] |

| | | | | |
|---|---|---|---|---|
| Bcl-2 siRNA | DOX | Human ovarian cancer (in vitro) | Silica nanoparticle | [66] |
| Bcl-2 siRNA | PTX | Human breast cancer (in vitro) | Polyplex | [67] |
| Bcl-2/MRP1 siRNA Bcl-2/MDR1 siRNA | DOX | Human MDR cancers (in vitro) | Lipoplex | [68] |
| c-Myc /VEGF siRNA | DOX | Human fibrosarcoma (in vivo) | Lipid-polymer nanoparticle | [69] |
| c-Myc siRNA | DOX | Human fibrosarcoma (in vivo) | Lipid-polymer nanoparticle | [70] |
| EGFR siRNA | DSGLA lipid | Human lung carcinoma (in vivo) | Lipid-polymer nanoparticle | [71] |
| EGFR siRNA | SAHA | Human glioblastoma (in vitro) | Polyplex | [72] |
| Mcl1 siRNA | SAHA | Nasopharynx carcinoma (in vivo) | Lipoplex | [73] |
| Mcl1 siRNA | Mitoxantrone | Human nasopharynx carcinoma (in vivo) | Lipoplex | [74] |
| Mcl1 siRNA | PTX | Human nasopharynx carcinoma (in vivo) | Lipoplex | [75] |
| MDR-1 siRNA | DOX | Human breast carcinoma (in vivo) | Polyplex | [76] |
| MDR1 siRNA | DOX | Human cervical carcinoma (in vitro) | Quantum dot | [77] |
| MVP siRNA | DOX | Human breast cancer (in vivo) | Polyplex | [78] |
| P-gp siRNA | PTX | Mouse mammary gland adenocarcinoma (in vivo) | Polyplex | [79] |
| P-gp siRNA | DOX | Human cervix carcinoma (in vitro) | Silica nanoparticle | [80] |
| Plk1 siRNA | PTX | Human breast carcinoma (in vivo) | Polyplex | [81] |
| Survivin shRNA | PTX | Human ovarian cancer (in vivo) | Polymer micelle | [82] |
| TRAIL plasmid | DOX | Human liver cancer (in vivo) | Polyplex | [83] |
| TRAIL plasmid | DOX | Human brain gliomas (in vivo) | polyplex | [84] |
| VEGF siRNA | PTX | Human prostate adenocarcinoma (in vitro) | Polyplex | [85] |
| VEGF siRNA | DOX | Human hepatoma (in vivo) | Polymeric micelle | [62] |

DOX: doxorubicin

PTX: paclitaxel

An interesting type of the co-delivery vectors emerging in recent years is the carrier doubles as a nucleic acid delivery vector and a prodrug that can enhance the therapeutic outcome of nucleic acids. A growing number of examples of such carriers successfully combine the delivery function of vectors with pharmacologic activity. Pluronic block copolymers are probably the best-known and most-investigated example of such carriers. These copolymers chemosensitize MDR cancer cells through multiple mechanisms, including inhibition of the Pgp drug efflux system [86], depletion of cellular ATP pools [87], and dysfunction of mitochondria [88]. While most of the available reports address the use of Pluronics for delivery of chemotherapeutics, importantly, the copolymers can be also used to deliver nucleic acids. Namely, it has been demonstrated that Pluronics can activate the nuclear factor kappa-light-chain-enhancer of activated B cells (NFκB), which is a transcription factor that enhances gene expression [89]. By introducing Pluronics into existing polyplexes, the gene delivery efficiency can be significantly improved, without causing cytotoxicity, as a result of increased cell uptake and nuclear transport of pDNA.

In most cases, dual-function carriers are rationally designed for specific applications. For example, Huang et al. developed a novel cationic lipid named DSGLA that is capable of delivering siRNA while simultaneously down-regulating the phosphorylated extracellular signal-regulated kinase (pERK) to enhance anti-cancer activity of the delivered siRNA [71]. The lipid, which contains guanidinyl and lysyl headgroups, has been shown to efficiently down-regulate pERK in H460 human lung carcinoma cells and to induce their apoptosis. Furthermore, a significant enhancement in tumor growth inhibition was observed in a mouse model of lung tumors after

intravenous (i.v.) administration of DSGLA/siRNA lipoplexes containing EGFR siRNA.

In addition to the use of lipoplexes as a dual-function vector, Rice et al. designed a type of novel cationic polypeptide capable of incorporating peptides with an intrinsic proteasome inhibitory function in order to improve transfection activity of plasmid DNA [90]. Proteasomes are important cellular enzymes responsible for the degradation of a variety of proteins. Inhibition of proteasomes has been shown to enhance transfection efficiency. Interestingly, in human hepatocellular carcinoma HepG2 cells, Rice et al. incorporated a tripeptide aldehyde proteasome inhibitor into the C-terminal end of a cationic gene delivery peptide (Cys-Trp-Lys18), and the resulting carrier showed elevated gene expression. Rice et al. note that using peptides with a proteasome inhibitory function as the carrier for pDNA delivery is more beneficial than concurrent treatment with pDNA polyplexes and free proteasome inhibitors. Thus, introducing intrinsic proteasome inhibitory activity has shown potential to boost the efficiency of anti-cancer gene therapy.

We have recently reported synthesis of biodegradable polycations that can function dually as gene delivery vectors and as antagonists of the CXCR4 chemokine receptor [91]. As a result of CXCR4 inhibition, the synthesized polycations were able to block the invasion of cancer cells, while simultaneously mediating efficient transfection in vitro. Evidence shows that the chemokine receptor CXCR4 and its cognate ligand SDF-1 (CXCL12) play critical roles in tumor invasion and metastasis. Likewise, many clinical studies have revealed that CXCR4-positive tumors metastasize to distant sites with high levels of SDF-1. Blocking the CXCR4/SDF-1 axis either by CXCR4 antagonists or by siRNA silencing of the CXCR4 gene has been shown to be capable of

preventing metastasis [92]. Such dual-function delivery vectors are expected to enhance anti-metastatic efficacy in a variety of cancer gene therapy methods.

## 1.4 Polyamine Pathway in Cancer

Years of research in the field of cancer treatment promoted the elucidation of the molecular basis of cancer, and led to the identification of valuable therapeutic targets [93]. One typical example is the polyamine pathway, which is generally up-regulated in cancer and therefore holds promise for the chemotherapy and chemoprevention.

### 1.4.1 Natural polyamines and their biological functions

Natural polyamines, including spermine (SPM), spermidine (SPD) and their diamine precursor putrescine (PUT), are alkylamines that exist in all eukaryotes [94-96]. In 1678, SPM and SPD were first discovered by Leeuwenhoek in human semen [97]. Later in 1885, Brieger reported the discovery of PUT [98]. These polyamines are essential for cell growth, differentiation, survival and mammalian development [99]. In general, the intracellular concentration of all polyamines is in millimolar range and most of the polyamines exist in the form bound to nucleic acids (DNA, RNA) or other negatively charged molecules, such as proteins and phospholipids [100, 101]. The majority of polyamines exists as polyamine-RNA complexes, thus influencing protein synthesis [102]. It is generally believed that polyamines exhibit its main function in supporting cell growth and cell survival at the transcriptional, translational and post-translational levels, through the regulation of gene expression, free-radical scavenging, ion-channel regulation and maintenance of chromatin structure [103]. The dynamic

balancing of polyamine levels inside the cells is important for maintaining the healthy status of the cells, and the intracellular polyamine concentration is strictly regulated through the biosynthesis, catabolism pathway, cell uptake and efflux [94]. Dysregulation of polyamine levels is usually associated with various diseases, as the polyamine depletion leads to inhibition of cell growth and accelerates aging [104], while increased level of polyamines is associated with hyper-proliferative diseases such as cancer [105].

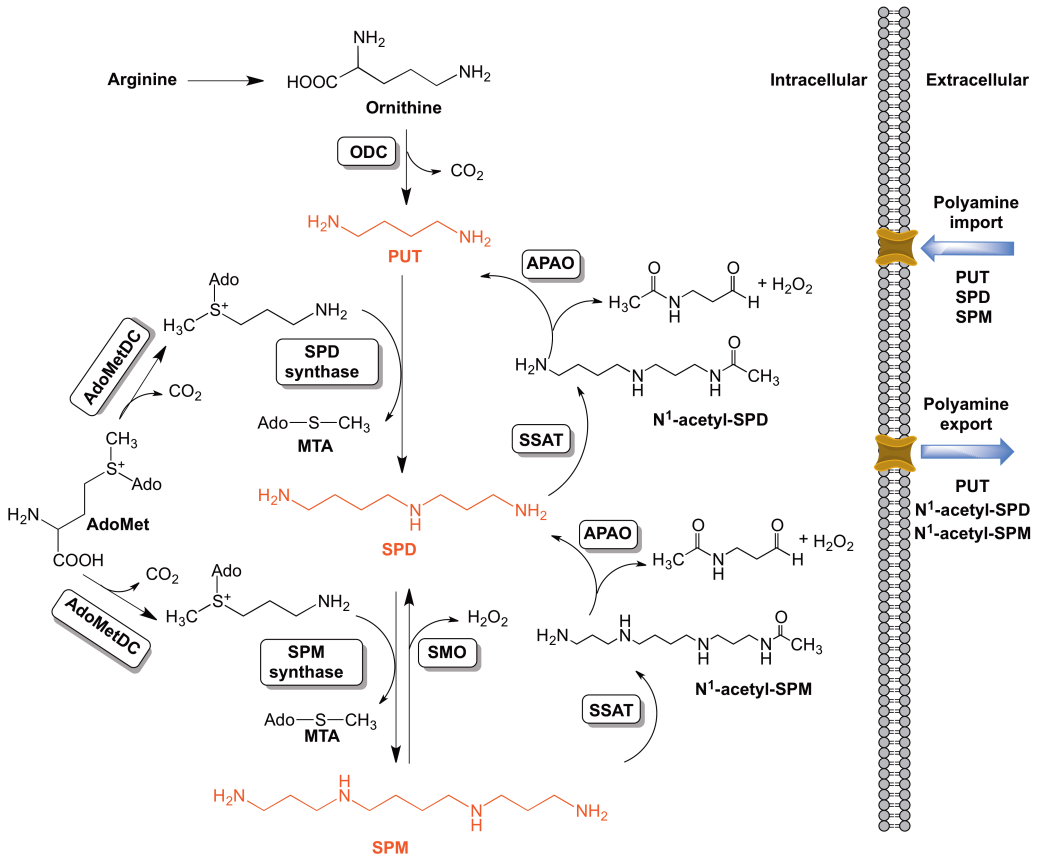


**Figure 3.** The polyamine pathway. Ornithine, the precursor for polyamine synthesis, is the product of arginine generated from urea cycle. Ornithine is converted to PUT by ornithine decarboxylase (ODC). PUT is then converted to higher molecular weight SPD by addition of propyl amine. The process is catalyzed by SPD synthase. SPD can be further converted to SPM by SPM synthase. Notably, the product of propyl amine involved in the synthesis of SPD and SPM is generated from the decarboxylation of S-adenosylmethionine (AdoMet) by S-adenosylmethionine decarboxylase (AdoMetDC). Catabolism of SPD and SPM is mediated by three major enzymes: spermine/spermidine $N^1$-acetyltransferase (SSAT); polyamine oxidase (APAO) and spermine oxidase (SMO). SMO can oxidize SPM to form SPD; SSAT catalyzes the acetylation of SPM and SPD to form the $N^1$-acetyl-SPM or $N^1$-acetyl-SPD, respectively. Acetylated polyamine product can be further exported out of the cell, or it can be oxidized by APAO to form the precursor polyamine (PUT or SPD).

### 1.4.2 Polyamine biosynthesis

Polyamines can be imported from extracellular resources, such as directly from food, or generated by gut bacteria [106], although the mechanism of cellular polyamine

uptake is not yet fully characterized. On the other hand, endogenous polyamines are generated from the biosynthesis pathway. As shown in Figure 3, the first rate-limiting enzyme in the polyamine biosynthesis pathway is ODC, which catalyzes the conversion of ornithine to PUT. Ornithine, the substrate for ODC is an amino acid intermediate in the urea cycle generated from arginine by arginase [107]. In mammals, ODC has a very short half-life around 10 min, and it is one of the best-characterized proteins that is subjected to ubiquitin-independent degradation process [96]. The degradation of ODC is mediated by ODC antizyme, and the process is negatively regulated by the feedback loop of polyamine products [108].

The second rate-limiting step in the polyamine synthesis is the decarboxylation of AdoMet by AdoMetDC to generate the amino propyl donor (decarboxylated AdoMet) for the synthesis of SPD and SPM. SPD is synthesized from PUT by incorporating the aminopropyl moiety from decarboxylated AdoMet, and the reaction is catalyzed by SPD synthase. SPM is synthesized in presence of SPM synthase by aminopropylation to the aminobutyl end of SPD [109].

### 1.4.3 Polyamine catabolism

Several enzymes, such as SMO, SSAT and APAO, mediate the catabolism of polyamines. SSAT is a rate-limiting enzyme in the catabolic pathway. It catalyzes the $N^1$-acetylation of SPD and SPM, by transferring the acetyl group from acetyl coenzyme A. SSAT is a highly inducible enzyme, and its expression can be regulated by a variety of stimuli such as polyamine levels, hormones, toxins, drugs, cytokines and stress pathways [110]. Oppositely, APAO is constitutively expressed in most tissues with its

high activity and slow turnover rate [111]. SMO specifically oxidizes SPM. It is also highly inducible by a variety of stress stimuli, and is often up-regulated during cellular stress such as inflammation, cell differentiation and DNA damage [112].

SPD and SPM can be acetylated by SSAT and further exported out of the cells. Alternatively, the acetylated products from SPD and SPM are also subjected to oxidation by APAO, which leads to the formation of lower molecular weight polyamines (PUT or SPD), as well as the product of 3-acetylaminopropanal and hydrogen peroxide ($H_2O_2$). In contrast to the function of APAO, which oxidizes the acetylated product of SPD and SPM, SMO catalyzes the oxidation of unsubstituted SPM to SPD, and releases 3-aminopropanal and $H_2O_2$. It is also worth noting that reaction with APAO and SMO in the polyamine pathway causes oxidative stress to the cell by generating $H_2O_2$ and aldehydes. The production of reactive oxygen species (ROS) together with increases in acetylated polyamines and the enzyme activities are reported to be responsible for apoptosis and ROS damage to the host cells [113, 114].

### 1.4.4 Polyamine regulation in cancer

Considering the essential role of polyamine pathway in cell growth and development, it is not surprising to find that occurrence of cancer usually correlates with dysregulation of polyamine pathway. Indeed, higher expression of natural polyamines, elevated activity of the polyamine synthesis enzymes or reduced activity of polyamine catabolism are normally found in various cancers, including breast, prostate, renal, colorectal, pancreatic, hepatocellular carcinoma, lung and brain cancers [115]. Moreover, SPD and SPM are acetylated when they are accumulated in excess amount

during carcinogenesis, therefore the urinary acetylated SPD and SPM has become a sensitive marker for human cancers [100].

In 1968, Russell et al. first showed that increased ODC activity was associated with sarcomas and hepatomas [116]. ODC is a transcriptional target of the oncogene *c-Myc* and *Ras* [117], and it is shown to be overexpressed in gastric cancer [118], breast cancer [119], lymphoma [120], non-small-cell lung cancer [121] and prostate cancer [122]. Deng et al. examined the expression of ODC in breast cancer tissues and four breast cancer cell lines, and found that ODC was upregulated in all breast cancer tissues and cell lines compared with non-tumor tissue and normal breast epithelial cells [123]. They also demonstrated that down-regulation of ODC expression with antisense ODC resulted in suppression of cancer proliferation and cell cycle arrest. More significantly, O'Brien and coworkers were able to demonstrate that overexpression of ODC is sufficient for the promotion of skin tumor [124]. They developed the ODC transgenic mice model for skin tumorigenesis experiment. Results showed much higher sensitivity of the transgenic mice to develop skin tumors with a single administration of carcinogen, compared with the normal control mice. Similarly, AdoMetDC, the second rate-limiting enzyme in the biosynthesis pathway of polyamine has also been reported to be up-regulated in certain types of cancer [125]. Ravanko et al. proved that AdoMetDC alone is sufficient for the transformation of NIH 3T3 cells into highly invasive tumors in nude mice [126]. Furthermore, the inhibition of AdoMetDC by small molecule inhibitor SAM486A led to the suppression of breast cancer invasiveness both *in vitro* and *in vivo* [127]. Other enzymes involved in the polyamine biosynthesis such as SPM

and SPD synthases are constitutively expressed in the cells, and are considered to be less relevant to the tumorigenesis in human [128].

Additionally, dysregulation of enzymes in polyamine catabolism also contributes to the tumorigenesis. Increased activity of SMO is often observed in inflammation-associated tumors. In this case, production of ROS by SMO is directly linked with DNA damage and activation of inflammation cytokines. Chronic inflammation with sustained elevation of ROS produced by SMO increases the risk of tumorigenesis [112]. For example, development of prostate cancer is considered to be associated with inflammation [129]. This statement is supported by Goodwin et al. that significantly higher expression of SMO is observed in tissue samples of prostate cancer patients [130]. Another interesting example is that certain infection events that lead to the up-regulation of SMO activity will later contribute to the carcinogenesis. Xu et al. reported that *Helicobacter pylori,* a human gastric pathogen, could up-regulate the enzyme activity of SMO, thus causing the production of ROS and consequently, result in mutagenic DNA damage that may contribute to the development of gastric cancer [131]. It is also worth mentioning that SMO seems to play an opposite role in the development of breast cancer. Report showed that SMO activity is much lower in the tumor tissue samples than in the normal tissue samples from breast cancer patients [132]. This result is in good correspondence with another report that decreased APAO activity was observed in breast cancer tissues [133]. Possible explanation for the decreased activity of polyamine catabolic enzymes in breast cancer is that lower expression of SMO and APAO leads to reduced amount of ROS in the local tumor tissue, thus promotes the survival of tumor cells [112]. The role of SSAT enzyme in tumorigenesis is also

complicated and requires more investigation. Mouse model with systemic overexpression of SSAT demonstrated resistance to the development of skin cancer after being challenged by carcinogen [134]. However, local induction of SSAT expression in the mice skin resulted in accelerated tumor progression [135]. Elevated SSAT was observed in tumor tissue from breast cancer patients [133]. In contrast, in the case of human colon cancer or other gastrointestinal cancers that are associated with *Ki-ras* oncogene, SSAT activity was suppressed by *Ki-ras*, which resulted in suppression of polyamine catabolism and elevated polyamine content [136].

In all, dysregulation of enzymes involved in the polyamine pathway results in accumulation of polyamines, which promotes tumorigenesis and tumor progression. Elevated polyamine levels are reported to enhance the malignant potential of cancer cells and decrease anti-tumor immunity [137]. Alteration in the polyamine pathway is also associated with poor prognosis of certain cancers [138]. Therefore, targeting the polyamine pathway holds great potential in cancer chemotherapy and chemoprevention [139].

### 1.4.5 Targeting polyamine pathway in cancer

Realizing the importance of polyamine pathway in cancer, extensive effort has been made to develop therapeutic agents against the polyamine metabolism. Earlier work starting from 1970s was mainly focusing on developing inhibitors of polyamine biosynthesis enzymes. Structures of representative inhibitors are shown in Figure 4. Methylglyoxal bis(guanylhydrazone) (MGBG), a drug used for treatment of leukemia, was demonstrated to be a competitive inhibitor for AdoMetDC by Williams-Ashman et

al. in 1972 [140]. Treatment with MGBG leads to the depletion of SPM and SPD, however, accumulation of excess PUT was observed [141]. Although *in vitro* results showed that MGBG treatment led to cell growth inhibition, clinical use of this drug is limited by the significant toxicity to mitochondria [142]. Based on the structure of MGBG, researchers later developed other AdoMetDC inhibitors, such as SAM486A, with reduced mitochondrial toxicity [143]. Unfortunately, no clinical benefit was shown in Phase I and Phase II studies [144, 145].

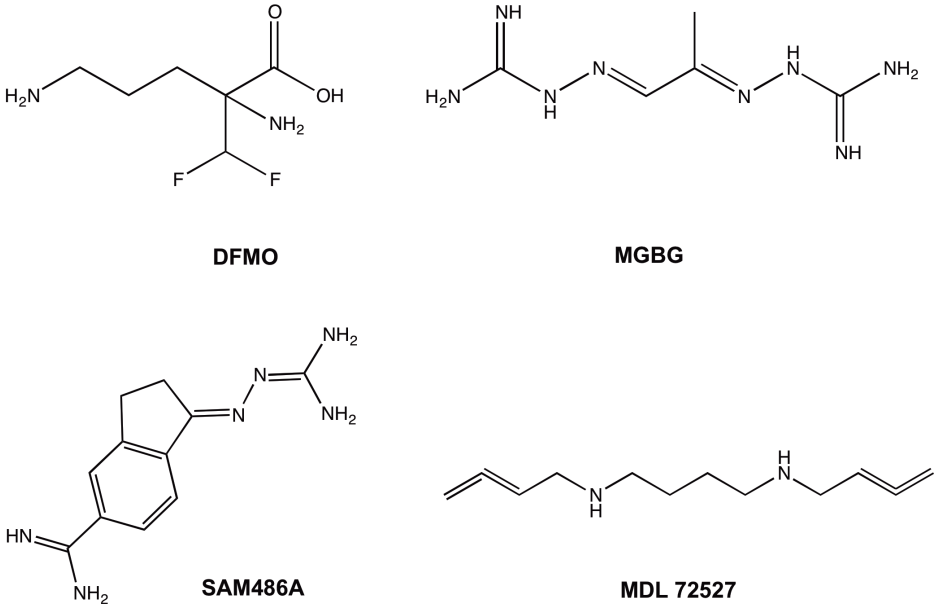


**Figure 4.** Representative inhibitors for polyamine metabolic enzymes. DFMO is an irreversible inhibitor for ODC; MGBG is a competitive inhibitor for AdoMetDC; SAM486A is a competitive inhibitor for AdoMetDC with lower mitochondrial toxicity than MGBG; MDL 72527 is an enzyme-activated inhibitor for APAO, which can also inhibit SMO. Modified from [101].

One of the most well-known inhibitors for polyamine biosynthesis is difluoromethylornithine (DFMO), an irreversible inhibitor of ODC that binds to the active site of this enzyme [146, 147]. Results from *in vitro* studies showed that treatment of

cells with DFMO led to depletion of PUT and SPD, but the level of SPM often remained less affected [148]. Generally, DFMO leads to cytostatic growth inhibition, rather than cytotoxic effect towards cancer cells. Clinical trials demonstrated that DFMO was ineffective as a single chemotherapy agent against several tumor models, including gliomas, melanomas, breast and prostate cancers [101]. Possible explanation for the disappointing result is that DFMO is poorly transported into the cell thus limiting the ODC inhibition and polyamine depletion effect. Additionally, activation of compensatory mechanism in polyamine pathway and incomplete depletion of SPM after the treatment with DFMO may also compromise the treatment outcome [149]. ODC inhibitors with higher potency were also synthesized, however, no significant advantage in clinical studies was shown so far [150]. Furthermore, inhibitors targeting the SPM and SPD synthase were also explored as chemotherapy agent. For example, S-adenosyl-3-thio-1,8-diaminooctane was synthesized as a specific inhibitor of SPD synthase. A similar analogue, S-adenosyl-1,12-diamino-3-thio-9-azadodecane was developed as inhibitor for SPM synthase. However, both inhibitors demonstrated limited effect on cell growth inhibition [151, 152]. Also worth mentioning are inhibitors developed for targeting other enzymes such as APAO. Although APAO was thought to be constitutively expressed in the cells, thus having less importance as a therapeutic target, recent developments in inhibiting APAO activity showed promising cell killing effect towards cancer cells [149]. The most successful inhibitor for APAO is $N^1$,$N^4$-bis(2,3-butadienyl)-1,4-butanediamine (MDL 72527), which is also considered an inhibitor for SMO. MDL 72527 has shown toxic effect towards leukemia cells and appears to be effective when combined with DFMO in *in vivo* cancer models [128, 149].

As discussed above, initial efforts of developing anti-cancer reagent based on the inhibition of polyamine biosynthesis enzymes yielded limited clinical success. The ineffectiveness of the inhibitors targeting biosynthesis of polyamines is partially due to the incomplete depletion of all the natural polyamines. In recent years, more emphasis has been put on developing polyamine analogues that are capable of competing with natural polyamines for the transport, biosynthesis and catabolism. Theoretically, ideal polyamine analogues would possess the following features: (i) capable of competing with natural polyamines for the polyamine transport system thus reducing the import of natural polyamines; (ii) despite the structural similarity with natural polyamines, the analogues should not have the same biological functions as natural polyamines; (iii) intracellular accumulation of the polyamine analogues should act as a feedback to the polyamine metabolism, resulting in down-regulation of polyamine biosynthesis and up-regulation of catabolism [103].

Synthesis of polyamine analogues that met the above criteria was first attempted by Bergeron and coworkers in 1988 [153]. Since then, considerable amount of polyamine analogues mimicking the structures of SPD and SPM was synthesized and tested over the past 20 years. The analogues can be grouped into the following categories based on the chemical structure: symmetrically substituted bis(alkyl) polyamine analogues; asymmetrically substituted analogues; conformationally restricted analogues; oligoamines and macrocyclic analogues [154]. Representative examples of polyamine analogues are shown in Figure 5. Among the most successful of the developed polyamine analogues is $N^1$,$N^{11}$–bisethylnorspermine (BENSpm). BENSpm has shown promising antitumor activity against a wide range of cancers, including

melanomas, ovarian, breast, and pancreatic cancers [155-158]. BENSpm induces SSAT, down-regulates ODC and AdoMetDC [159], and ultimately causes cell growth inhibition and apoptosis [160-162]. The mechanism of action as well as preclinical and clinical outcomes of BENSpm will be discussed in detail in the following section. In addition, asymmetrical polyamine analogues $N^1$-propargyl-$N^{11}$-ethylnorspermine (PENSpm) and $N^1$-cyclopropyl-methyl-$N^{11}$-ethylnorspermine (CPENSpm) possess similar backbone as BENSpm and also showed significant anti-proliferation activity and SSAT induction. The similar antitumor effect of asymmetrical analogues with BENSpm demonstrates that active functional moieties could be linked to the same polyamine backbone, which may offer potential targeting capability [103]. Synthesis of conformational restricted analogues also generated encouraging results. Most promising agents in this group are CGC-11047 and CGC-11093, which are derivatives of $N^1$,$N^{12}$-bisethylspermine (BESpm) and $N^1$,$N^{14}$-bisethylhomospermine (BEHSpm), respectively. CGC-11047 and CGC-11093 showed increased anti-proliferative activity and reduced nonspecific toxicity compared with the parent compounds [101]. Notably, despite the structural similarities, CGC-11047 and CGC-11093 showed discrepancy in the profile of regulating polyamine catabolic enzymes. CGC-11047 significantly induced SSAT and SMO, whereas CGC-11093 showed little effect on the expression of both enzymes [103]. The fact that both compounds are active anti-cancer agents implied the complexity of the mechanism for polyamine regulation and indicated the diverse influences of polyamine analogues on polyamine pathway, other than affecting the enzyme activities.

Synthesis of oligoamines as effective antitumor agents is guided by the hypothesis that increased number of amines in the polyamine analogue contributes to increased affinity for DNA. The interactions between the polyamine analogue and nucleic acids in the cancer cells are then responsible for the antiproliferative effect [163]. For example, CGC-11144 is a representative oligoamine with significant antitumor activity. CGC-11144 demonstrated growth inhibition in a panel of prostate cancer cells, and showed antitumor effect *in vivo* in a breast cancer model [164]. CGC-11144 showed broad effect on cellular functions. Treatment with CGC-11144 not only leads to decrease in all three natural polyamines and inhibition of ODC activity, but also results in multiple genetic changes such as activation of caspase 3 and suppression of the expression of estrogen receptor [165]. Another unique class of polyamine analogues is macrocyclic polyamine. Unlike other polyamine analogues that generally target the polyamine pathways, macrocyclic polyamines exhibit its antitumor function through other mechanisms such as DNA cleavage and depletion of ATP. Representative molecule from this subset of compounds, such as CGC-11199, demonstrated antitumor activity in human prostate cancer. However, the mechanism of action is considered less relevant with the polyamine regulation [166].

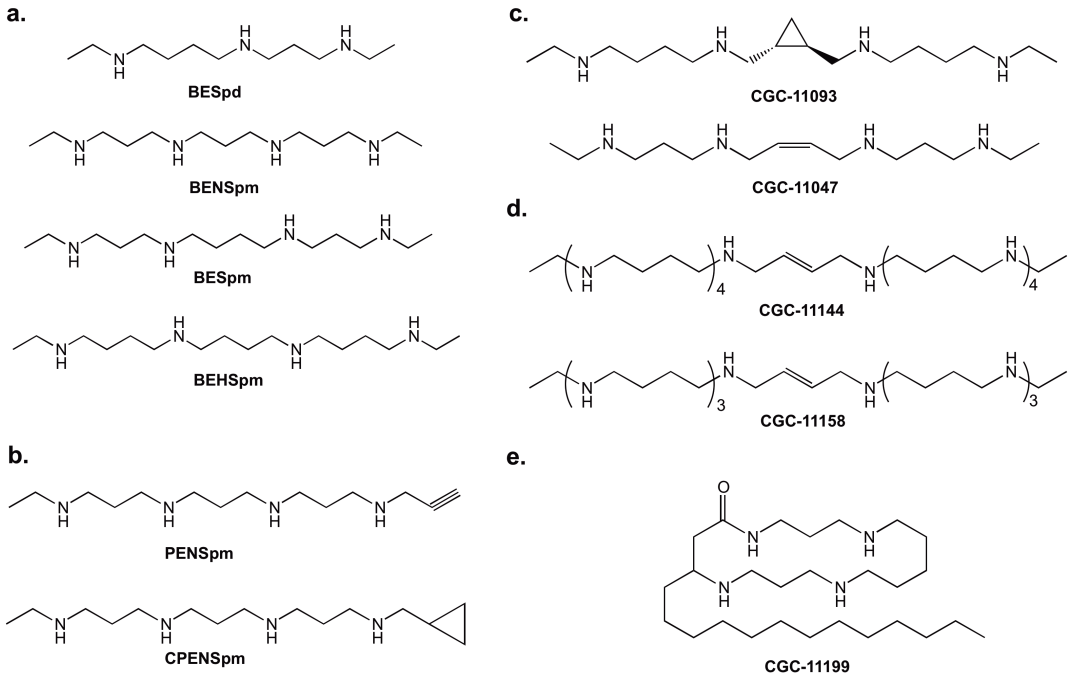


**Figure 5.** Examples of polyamine analogues with antitumor activity. (a) Symmetrically substituted polyamine analogues; (b) asymmetrically substituted polyamines; (c) conformational restricted polyamine analogues; (d) oligoamines and (e) macrocyclic polyamine.

### 1.4.6 BENSpm as anticancer drug targeting polyamine pathway

As discussed above, BENSpm is one of the most successful antitumor agents developed in the field of polyamine research. BENSpm mimics the structure of SPM, but differs from SPM in that the terminal primary amines of BENSpm are modified with ethyl groups, thus preventing the oxidation by multiple oxidases such as APAO. BENSpm exhibits multiple functions in the regulation of intracellular polyamines. It is shown that BENSpm can highly induce the activity of catabolic enzyme SSAT. It also induces SMO and downregulates both ODC and AdoMetDC [164]. Unlike single enzyme inhibitors, BENSpm demonstrates complete depletion of all three natural polyamines and shows

significant antitumor activity in vitro [165]. Using a transgenic model of primary fibroblast derived from transgenic mice overexpressing SSAT, Alhonen et al. demonstrated that the growth inhibition effect of BENSpm was largely dependent on the depletion of polyamine pools, and the massive induction of SSAT activity mainly happened at the post-transcription level [167, 168]. It was also reported that BENSpm is a potent inducer of SMO, especially in non-small-cell lung cancers [169]. Investigations in BENSpm-treated SK-MEL-28 human melanoma cells revealed that BENSpm caused depletion of intracellular polyamine pools and triggered G1 phase cell cycle arrest. Besides the effect on cell growth inhibition, BENSpm also induced apoptosis in the melanoma cells by activating the mitogen-activated protein kinase (MAPK) pathway, inducing cellular oxidative stress and activating the mitochondrial apoptotic pathway [113, 170]. BENSpm is also reported to exhibit gene regulation functions. Shah et al showed that BENSpm downregulated the gene expression of two transcription factors: NFκB and estrogen receptor-alpha in breast cancer cells, and resulted in apoptosis in the tested MCF-7 breast cancer cell line [171].

**Table 2.** Applications of BENSpm in cancer therapy.

| Treatment | Model | Cancer type | Effect | Ref. |
|---|---|---|---|---|
| BENSpm | in vitro | Breast tissue explants | ↑SSAT | [172] |
| BENSpm | in vitro | L56Br-C1 breast cancer cells | ↑SSAT; Apoptosis; ↓ Cell proliferation; ↑caspase-3 and 9 | [173] |
| BENSpm | in vitro | MALME-3M melanoma cells | ↑p53-p21WAF1/CIP1-Rb; G1 cell cycle arrest | [158, 174] |
| BENSpm | in vitro | MCF-7 breast cancer cells | G1 cell cycle arrest; ↑p53 and p21 expression; Cell growth inhibition and apoptosis | [160] |
| BENSpm | in vitro | MCF-7, L56Br-C1 and HCC1937 breast | Polyamine depletion; DNA strand | [175] |

| | | | | |
|---|---|---|---|---|
| | | cancer cells | breakage | |
| BENSpm | in vitro | MDA-MB-231, Hs578t, MCF-7, T47D breast cancer cells | ↑SSAT and SMO; Growth inhibition; ↓ODC; Polyamine depletion | [176] |
| BENSpm | in vitro | Panc-1 and BxPC-3 pancreatic cancer cells and xenograft mice model | ↑SSAT; ↓ODC and AdoMetDC; ↓polyamine pool; antiproliferation; in vivo antitumor effect | [177, 178] |
| BENSpm | in vitro | SH-SY5Y neuroblastoma cells | Polyamine depletion; cell growth inhibition and apoptosis; ↑survivin | [179] |
| BENSpm | in vitro | SK-BR-3, MCF-7, L56Br-C1 and HCC1937 breast cancer cells | Polyamine depletion; Cell growth inhibition; Regulation of cell cycle | [180] |
| BENSpm | in vitro | SK-MEL-28 melanoma cells | ↑SSAT and ROS; Apoptosis; ↑caspase-3 and 9; cytochrome c release | [113] |
| BENSpm | in vitro | SK-MEL-28, MALME-3M, A375 and LOX melanoma cells | ↑SSAT; Apoptosis and growth inhibition; ↓survivin and ML-IAP proteins; Activation of MAPK pathway | [170, 181] |
| BENSpm | in vitro | U87, LN229 glioblastoma cells | ↑SSAT; ↑Cell apoptosis and detachment; Inhibition of mTOR-mediated protein synthesis | [182, 183] |
| BENSpm | in vitro and in vivo | AT3.1, AT6.1, AT6.3, DU145, DuPro-1 and TSU-Pr1 prostate cancer cells; DU145, DuPro-1 and PC-3 xenograft mouse model | Cytotoxicity; Tumor growth inhibition | [184] |
| BENSpm | in vitro and in vivo | PC-3, TSU-pr1, DU-145, and JCA-1 prostate cancer cells; DU-145 xenograft mouse model | ↑SSAT; ↓ODC; ↓Polyamines; Tumor growth inhibition | [185] |
| BENSpm | in vitro and in vivo | U87, LN229 glioblastoma cells; U87 intracerebral mouse model | ↑SSAT and ROS; Prolonged survival of tumor-bearing mice | [186] |
| BENSpm | in vivo | A121 ovarian carcinoma, A549 lung cancer, MALME-3M melanoma, and SH-1 melanoma xenografts mice model | Tumor regression | [187, 188] |
| BENSpm | in vivo | BL13 bladder carcinoma xenograft mouse model | Tumor regression | [189] |
| BENSpm | in vivo | PANUT-3 and MALME-3M melanoma xenograft mice model | ↑SSAT in tumor tissue; polyamine depletion in tumor; antitumor activity | [190] |
| BENSpm | in vivo | Transgenic mouse model with neu/erb-B2 overexpression | ↑SSAT; ↓number of tumor; ↓tumor volume | [191] |
| BENSpm | Phase I trial | Advanced solid tumors patients | Central nervous system toxicity | [192, 193] |
| BENSpm | Phase I trial | Hepatocellular carcinoma patients | Dose well tolerated in patients; Lack of efficiency | [194] |
| BENSpm | Phase I trial | Non-small cell lung cancer patients | MTD was 185 mg/m$^2$ for 5 days; Gastrointestinal toxicity | [195] |
| BENSpm | Phase II trial | Metastatic breast cancer patients | Dose well tolerated in patients; Lack of efficiency | [196] |
| BENSpm and 2ME | in vitro | MCF-7 breast cancer cells | Synergism; Polyamine depletion; Cell apoptosis | [197] |
| BENSpm with 5-FU | in vitro | HCT116 colon carcinoma cells | ↑SSAT; ↑Apoptosis; ↓Polyamines; Synergism | [198] |
| BENSpm with | in vitro | MCF-7, Hs578t, T47D and MDA-MB-231 | Strong synergism; ↑SSAT and SMO; | [199] |

| | | | | |
|---|---|---|---|---|
| 5-FU or PTX | | breast cancer cells | Cytotoxicity | |
| BENSpm with cisplatin | in vitro and in vivo | L1210 leukemia cells and B16F1 melanoma cells; L1210 and B16F10 mice model | Cytotoxicity; ↑ Lifespan | [200] |
| BENSpm with OXP | in vitro | A2780 ovarian cancer cells | ↑Strong synergism; ↑SSAT; Polyamine depletion; Cell growth inhibtion and cytotoxicity | [201, 202] |
| BENSpm with OXP and 5-FU | in vitro | HCT-116 colorectal cancer cells | Polyamine depletion; ↑SSAT and SMO; ↓cell resistance | [203, 204] |

5-FU: 5-fluorouracil

PTX: paclitaxel

OXP: oxaliplatin

2ME: 2-Methoxyestradiol

BENSpm demonstrated promising antitumor effect in both *in vitro* and *in vivo* models of a variety of cancers. Application of BENSpm in preclinical and clinical cancer therapy is summarized in Table 2. For *in vitro* studies, BENSpm showed promising outcome as antitumor agent towards glioblastoma U87 and LN229 cells [182], neuroblastoma SH-SY5Y cells, breast cancer MDA-MB-231 and MCF-7 cells [176], SK-MEL-28 human melanoma cells [113] and human prostate cancer PC-3, TSU-pr1, DU-145, and JCA-1cell lines [185]. More significantly, several studies pointed out the effectiveness of BENSpm for *in vivo* antitumor therapy. For example, BENSpm significantly inhibited tumor growth of breast cancer MDA-MB-231 xenografts mouse model, following the treatment schedule of 5 times each week (100 mg/kg for each dose) for constitutively 4 weeks [199]. In a FVB/NTgN transgenic mouse model with neu/erb-B2 oncogene overexpression, treatment with 20 mg/kg BENSpm once a week for 10 weeks resulted in a 40% reduction in the average number of tumors per mouse [191]. Similarly, significant antitumor efficacy was also observed in *in vivo* mouse models including bladder BL13 carcinoma, SH-1 melanoma, MALME-3M melanoma,

A549 lung adenocarcinoma, A121 ovarian carcinoma, pancreatic Panc-1 and BxPC-3 adenocarcinoma xenografts [178, 187, 189].

Because of the promising results from *in vitro* and *in vivo* studies, BENSpm was evaluated as a single agent with antitumor activity in phase I and phase II clinical trials. In a phase I clinical trial, BENSpm was tested in patients with advanced hepatocellular carcinoma [194]. Although the drug was relatively well tolerated at 75 $mg/m^2$ by i.v. injection every other weekday for two weeks in a 28-day cycle, BENSpm failed to demonstrated effectiveness against the disease and was not recommended for further evaluation as a monotherapy agent. In another phase I study, BENSpm was administered in patients with non-small cell lung cancer but, again, no significant disease response was observed [195]. Another phase I trial was designed to determine the maximum tolerated dose (MTD) and dose-limiting toxicities of BENSpm. The results demonstrated significant central nervous system toxicity at dose levels above 94 $mg/m^2$/day, and BENSpm was not recommended for phase II study [192]. The only reported phase II study used BENSpm in patients with metastatic breast cancer. Again, the results yielded no clinical activity, with all patients showing disease progression by 4 months [196].

Although as a single agent BENSpm did not show satisfactory clinical outcome, recent studies demonstrated that it could be beneficial to combine BENSpm with other chemotherapy drugs. For example, BENSpm act synergistically in combination with platinum drugs, such as oxaliplatin and cisplatin in A2780 human ovarian carcinoma cells [202]. More importantly, BENSpm was tested in combination with six standard chemotherapy agents in a panel of four human breast cancer cell lines. The most

promising combinations were BENSpm with 5-fluorouracil or paclitaxel in human breast cancer cell lines MDA-MB-231 and MCF-7 [199]. In all, encouraging preclinical results support the continuing evaluation of BENSpm in combination chemotherapy and chemoprevention.

## 1.5 Prodrugs

### 1.5.1 Definition and advantages

Depending on the final application, modifications of the parent drug molecules to produce corresponding prodrugs may offer additional advantages over the free drug alone. Prodrugs are chemically modified drug molecules that are inactive or less active than the parent drug. However, after *in vivo* administration, prodrugs will undergo enzymatic metabolism or chemical transformation to release the active parent drug and exert its desired pharmacological effect [205]. Prodrug strategy can be used to improve the drug absorption, distribution, metabolism and elimination (ADME). In chemotherapy, designing prodrugs also helps to improve the tumor selectivity and to minimize the off-target toxicity [206]. In general, a prodrug is composed of three components: (1) the active drug molecule; (2) degradable linker bridging the drug and the rest part of the prodrug named “promoiety”; (3) the promoiety that enabled the prodrug with additional properties such as improved solubility, targeting and decreased toxicity [206].

In the design of a successful prodrug, the chemical linker needs to be carefully selected. Theoretically, the linker should self-immolate or cleave at the pharmacological site of action [207]. The linker should be either enzymatically degradable or stimuli-responsive to the disease-related environment such as changes in pH and redox

potential. Commonly used linkers include esters, carbamates, carbonates, and amides. More recently, a variety of self-immolative linkers were developed with improved degradation kinetics. Common prodrug linkers and proposed degradation mechanisms are summarized in Scheme 1.

Ester prodrugs are the most widely used because esters are degraded easily by ubiquitous plasma esterases or chemical hydrolysis. Synthesis of ester prodrugs is straightforward, with the required carboxylic acid and hydroxyl groups often existing in drug backbones. Ester prodrugs can be readily cleaved in the blood, liver and other organs to release the functional drug molecule [208]. The most important esterases are carboxylesterase, acetylcholinesterase, butyrylcholinesterase, paraoxonase, and arylesterase [208]. These enzymes are widely distributed throughout the body, thus rendering the ester prodrug quite labile *in vivo.* One major problem associated with the ester prodrug is the difficulty in controlling the site of prodrug conversion. Because of the ubiquitous existence of esterases, it is hard to predict the rate and the site of hydrolysis, and further, the pharmacological outcomes. Carbonates and carbamates are enzymatically more stable compared with hydroxyl esters. The degradation of these types of prodrugs is mediated by selective carboxylesterase.

Another type of commonly used prodrug strategy is amide. Although amide bond can be hydrolyzed by carboxylesterases, peptidases or proteases [205], it is generally more stable than the corresponding esters and carbamates. In fact, amide prodrugs exhibit high enzymatic stability *in vivo*, with the observation that amide prodrugs can be stable in the plasma for several days [207]. Therefore, the application of amide prodrugs is limited to designing specific enzyme-cleavable amides for improved targeting [209].

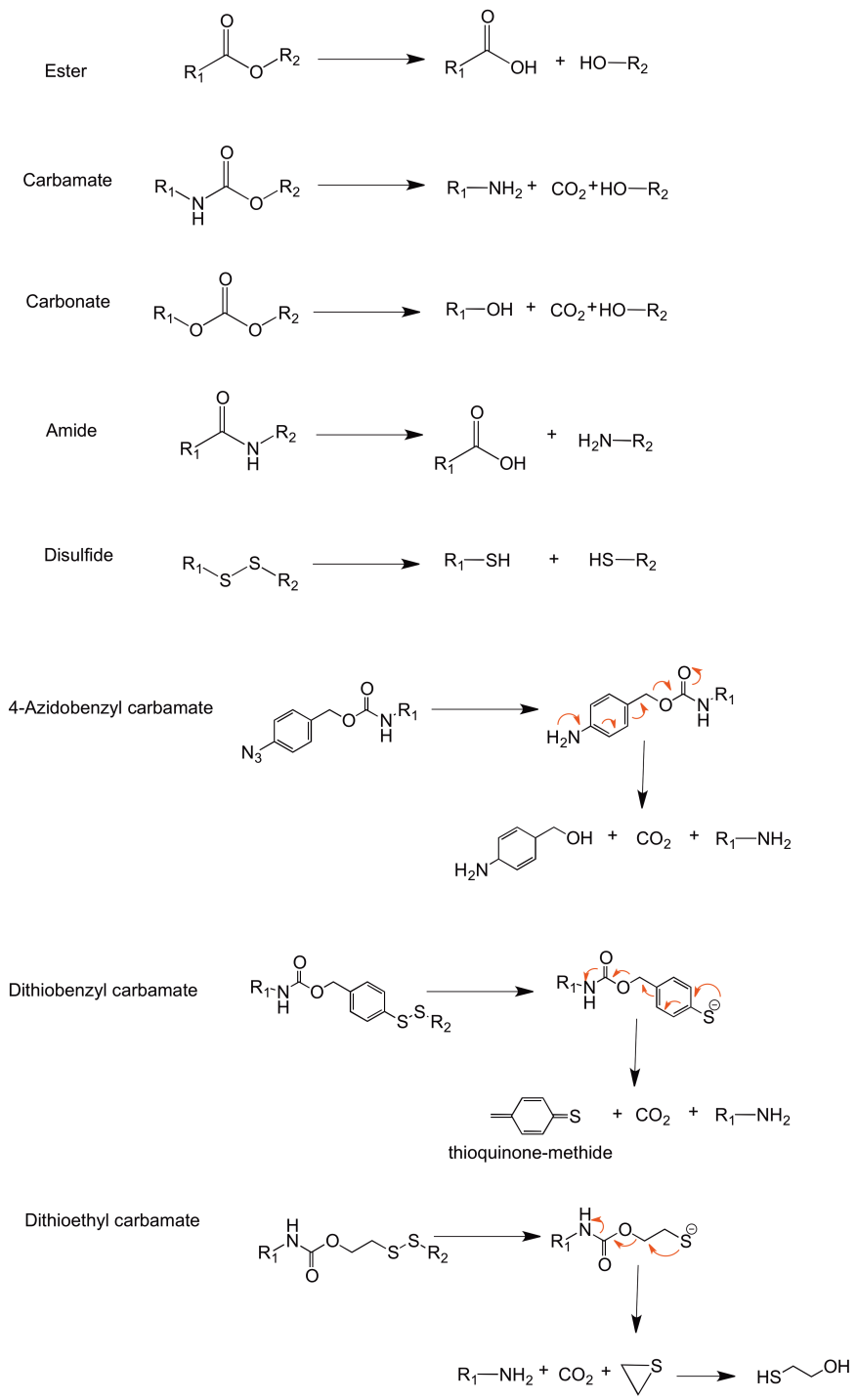


**Scheme 1.** Structures of common linkers used in prodrug conjugations and the proposed release mechanisms ($R_1$ and $R_2$ stand for either the drug molecule or the promoiety). Modified from [210-212].

In addition, other types of linkers include hydrazones, oximes, and disulfides. Each linker endows the prodrug with different environmental responsive properties. For example, hydrazone prodrugs are pH sensitive, with the degradation that takes place at pH < 5. Thus this type of prodrug is expected to be cleaved in the acidic endosome and lysosome compartments [213]. Disulfide prodrugs are redox responsive molecules and the reduction-triggered drug release is favored in tumor tissues with elevated levels of intracellular reducing agents like glutathione (GSH), thus improving the targeting in chemotherapy [214].

### 1.5.2 Prodrugs of amine drugs

Although prodrug strategy is widely used and accounts for approximately 10% of all the marketed medicine globally [215], application of such strategy in amine drugs is limited by the high stability of amide bonds. As we discussed above in the polyamine pathway section, polyamine analogues like BENSpm offer great therapeutic potential in cancer treatment. Conversion of this type of amine drug molecules into prodrug would be beneficial in the following aspects: (1) masking the amine groups, which are highly ionized at physiological conditions improves the lipophilicity of the drug and promotes the passive diffusion of the drug through membrane barriers; (2) temporary protection of the amine functional groups reduces the tendency to undergo first-pass metabolism; (3) careful selection of the promoiety of the prodrug enables the tissue targeting of amine drug, especially for targeting the tumor site.

Besides the amide and carbamate bond, self-immolative linker strategies are utilized in designing amine prodrugs with improved degradation profile. One interesting

approach is to use 4-azidobenzylcarbamate as the modification strategy for amine drugs [216]. The 4-azidobenzylcarbamate was shown to undergo rapid reduction in the presence of reducing molecule such as dithiothreitol (DTT), and the reduction product 4-aminobenzylcarbamate triggers immediate cascade degradation to release the functional amine drug [210]. Additionally, disulfide reduction-triggered self-immolative systems are also under vigorous investigation. Valhov et al. reported the disulfide-triggered linker system based on dithiobenzyl carbamate (Scheme 1). Following the disulfide reduction by GSH, this linker system will undergo thioquinone-methide 1,6-elimination and further release the amine free drug [211]. Another interesting approach is to use simple dithioethyl carbamate linker that can undergo 2-mercaptoethanol 1,2-elimination [212]. Activation of this prodrug contains two steps, first is the reduction of disulfide, and then the electronic rearrangement of the reduction product resulting in self-fragmentation of the remaining linker and release of the active amine drug. During the 1,2-elimination process, an intermediate of thiirane is generated from intramolecular cyclization (Scheme 1), which is further hydrolyzed to form the 2-mercaptoethanol [211]. In all, this type of self-immolative linker offers feasible solution for designing amine prodrugs. Furthermore, advanced modifications such as to incorporate space hindering moieties to the linker systems allow for easy control of the drug release rate.

### 1.5.3 Polymeric prodrug conjugates in chemotherapy

Depending on the types of promoieties, prodrugs can be categorized as targeting ligand-conjugated prodrugs, stimuli-responsive prodrugs, double prodrugs, membrane transporter-conjugated prodrugs, and polymeric prodrugs [206, 207, 217]. Among these,

polymeric prodrugs draw increasing attention in the field of chemotherapy. In general, the most prominent advantage of polymeric prodrugs is that they allow for passive targeting to the tumor site. Due to the rapid growth and elevated angiogenesis of the tumor tissue, the blood vessels associated with the tumor are usually poorly developed and thus facilitate leakage of macromolecular drugs to the tumor tissue. In addition, tumor tissues usually lack effective lymphatic drainage systems, thus increasing the accumulation of macromolecules in the tumor site. This phenomenon is known as the enhanced permeability and retention (EPR) effect [218]. One successful prodrug designed to utilize this advantage was PK1: N-(2-hydroxypropyl)methacrylamide (HPMA)-DOX prodrug with a peptide linker [219]. Phase I clinical trial showed that the polymeric prodrug can significantly decrease the DOX dose-limiting toxicities, with no sign of cardiotoxicity observed in patients at the DOX equivalent dose of 1680 mg/m$^2$. In another study, the influence of molecular weight of HPMA in the HPMA-DOX conjugates was evaluated. Results showed that DOX prodrug with higher molecular weight HPMA (~1000 kDa) has 28 fold longer blood half-life, with concomitant enhancement in tumor accumulation and significant higher efficacy in tumor inhibition, compared with the free DOX [220].

Polymeric prodrug conjugates are generally much larger in size than the parent drug, which leads to reduced urinary excretion, prolonged circulation half-life and modified biodistribution profile. The most commonly used polymer for this purpose is poly(ethylene glycol) (PEG). PEG is a water-soluble, nontoxic polymer that is approved by FDA in several products for *in vivo* administration [221]. Several PEGylated prodrugs are already on the market and more are undergoing clinical trials. NKTR-102, for

instance, is a PEGylated irinotecan prodrug that is currently in phase 3 clinical trial for patients with metastatic breast cancer. NKTR-102 demonstrated significant enhancement in antitumor activity and reduced hematopoietic toxicity compared with parent irinotecan [222].

More complex systems, such as liposome-encapsulated polymeric prodrugs, self-assembled polymer-drug nanoparticles and micelles, are also developed with increased half-life and promising antitumor activity [223, 224]. One representative example is the design of folate receptor-targeted lipid nanoparticle formulation for PTX-cholesterol prodrug [225]. PTX has poor aqueous solubility and limited lipid solubility. Cholesterol was first conjugated to PTX to form the prodrug with improved lipophilicity. The prodrug was then incorporated into a lipid nanoparticle, which also contained folate as a tumor targeting ligand. This PTX nanoparticle showed prolonged systemic circulation and exhibited excellent colloidal stability. Treatment with this novel formulation in mouse xenograft tumor model showed significantly greater tumor growth inhibition and prolonged animal survival. In all, incorporating polymer based prodrug strategy into chemotherapy offers great potential for cancer treatment.

## 1.6 Conclusions

As described above, gene therapy in combination with chemotherapy has shown significant promise in cancer treatment. However, current chemo drugs used in drug-nucleic acids combinations are merely limited to several candidates such as PTX and DOX. To further utilize the possible synergism by targeting various cellular pathways in cancer, identification of novel drug-gene pairs is of great need. Considering the

importance of polyamine pathway in cancer development, it is of great interest to identify effective drug targets in this pathway for combination therapy. Identification of synergistic therapeutic agents will be discussed in Chapter 2.

Furthermore, from the point of view of delivery systems, advances in the field of drug-nucleic acid combination require efficient delivery strategies for both chemotherapy drug and nucleic acids. It would be beneficial to design dual delivery systems for such applications. Considering the effectiveness of polymer-based delivery systems in nucleic acid delivery, and the possible advantages of designing polymeric prodrugs, it is favorable to design a dual delivery system that combines the prodrug functionality and gene delivery capability. The design of such dual delivery platforms will be the major topic of Chapter 3, 4 and 5.

# CHAPTER 2

# IDENTIFICATION OF SYNERGISTIC EFFECT OF BENSPM WITH OTHER THERAPEUTIC AGENTS

## 2.1 Introduction

As discussed in Chapter 1, BENSpm is one of the most successful polyamine analogues developed to target polyamine pathway [188, 226]. The general mechanism of action of BENSpm is to up-regulate metabolism enzymes SSAT and SMO, while at the same time, down-regulate biosynthesis enzyme ODC. BENSpm depletes all natural polyamines (SPM, SPD and PUT) and leads to apoptosis and cell growth inhibition in a wide range of cancers [158, 176, 177, 180, 182]. Recent advances in polyamine research reveal that BENSpm can act synergistically with various chemotherapy drugs [197, 227], thus providing the rationale for us to expand the knowledge of BENSpm synergism with other kinds of therapeutic agents.

### 2.1.1. Tumor necrosis factor-related apoptosis-inducing ligand (TRAIL)

One promising candidate in combination cancer therapy is called TRAIL, which is a therapeutic protein from the TNF family. In human, there are five TRAIL receptors: DR4, DR5, DcR1, DcR2 and osteoprotegerin (OPG) [228]. DR4 and DR5 are the death receptors capable of inducing apoptosis, while the other three are decoy receptors to antagonize apoptosis by competing for ligand binding. TRAIL is attractive in cancer treatment because transformed cells are generally more sensitive to TRAIL-induced

apoptosis, compared with normal cells. One possible explanation for TRAIL selectivity is that TRAIL's death receptors (DR4 and DR5) are mainly expressed in transformed cells while its decoy receptors (DcR1, DcR2 and OPG) are expressed in normal cells [229], which renders the cancer cells more sensitive to TRAIL treatment. Recombinant human TRAIL protein (rhTRAIL) was tested as a single anti-cancer agent in phase I clinical trial in advanced cancer patients and demonstrated no apparent toxicity [230]. In another phase I clinical trial, rhTRAIL was tested in combination with rituximab, an anti-CD20 antibody, in non-Hodgkin lymphoma patients, which yielded 2 complete and 1 partial response in patients [231, 232]. Although a recent phase II study demonstrated unsatisfactory outcome in non-small-cell lung cancer patients by combination treatment of rhTRAIL with three different chemotherapy drugs (paclitaxel, carboplatin and bevacizumab), most recent preclinical and clinical studies of TRAIL are still focusing on combination strategies [231]. Preclinical studies revealed that some cancer cells are able to gain resistance to TRAIL after repeated exposure [233]. Therefore it would be more efficient to administer TRAIL in combination with other chemotherapy agents, which may sensitize the cells to TRAIL treatment and minimize the possibility of resistance. Although it has been reported that combining TRAIL with various drugs such as kinase inhibitors, histone deacetylase inhibitors and genotoxic drugs is beneficial [234], combination of TRAIL with agents targeting polyamine pathway has never been explored.

### 2.1.2. RNAi targets

RNAi targets are also being extensively studied in combination therapy. We are

mainly focusing on three popular RNAi targets, Akt-2, Poly (ADP-ribose) polymerase (PARP) and survivin, due to their active role in cancer. Akt-2 gene is known as a putative oncogene encoding a serine/threonine-protein kinase. It belongs to the PI3K/AKT/mTOR signaling pathway and plays an important role in balancing cell survival and apoptosis. Reports showed that this gene is amplified in human breast cancer cells, human ductal pancreatic cancers and human ovarian carcinoma cell lines [235-238]. Overexpression of Akt-2 is associated with up-regulation of metastasis in breast cancer [239, 240]. Therefore Akt-2 is expected to be a good target for RNAi therapy, especially in the treatment of metastatic cancer cells with Akt-2 overexpression. PARP is a protein involved in DNA repair process. It helps to maintain cell survival and overexpression of PARP is observed in different cancers such as breast cancer, ovarian cancer, colon cancer and melanoma [241]. Inhibition of PARP using either siRNA or small molecule inhibitors has shown promising therapeutic effect for breast/ovarian cancer treatment [242-245], thus rendered PARP as a promising therapeutic target. Survivin is known to negatively control cell apoptosis pathway by inhibiting caspase activation. It is highly expressed in different cancer cells such as breast cancer and colon cancer [246, 247]. Silencing of survivin gene by RNAi is reported to effectively suppress tumor growth [248, 249]. To date, all the three targets are being vigorously investigated in combination with chemotherapy drugs [250-255], thus attracts our attention to test them in combination with polyamine analogue BENSpm.

### 2.1.3. Evaluation of combination effect

In order to evaluate the combination effect of BENSpm with the above-mentioned therapeutic agents, it is necessary to use a suitable statistical method. We employed the Chou-Talalay method for quantification of synergism [256, 257]. This method is based on the median-effect equation, which is a unified general theory to describe the dose-effect relationships:

$$\frac{f_a}{f_u} = \left( \frac{D}{D_m} \right)^m \quad (1)$$

Where $f_a$ and $f_u$ are the fractions of cell population that are affected or unaffected, respectively. Therefore, ($f_a$ + $f_u$) equals 1 by definition. $D$ is the dose used to achieve the certain effect, and $D_m$ is the required dose to achieve median effect ($IC_{50}$ in the case of cell killing). Depending on the value of $m$, the median-effect equation described various relationships between dose and response: $m$ = 1 indicates hyperbolic dose response; $m$ > 1 indicates sigmoidal and $m$ < 1 indicates flat sigmoidal dose response curve [258].

When applied to multiple drugs, for example, the combinations of two drugs (D1 and D2) with mutually exclusive drug effect, the drug-effect equation can be derived in the following form:

$$\left[ \frac{(f_a)_{1,2}}{(f_u)_{1,2}} \right]^{1/m} = \left[ \frac{(f_a)_1}{(f_u)_1} \right]^{1/m} + \left[ \frac{(f_a)_2}{(f_u)_2} \right] = \frac{(D)_1}{(D_m)_1} + \frac{(D)_2}{(D_m)_2} \quad (2)$$

Where $(f_a)_{1,2}$ is the fraction of population effect in combination of the two drugs; $(f_a)_1$ and $(f_a)_2$ are the fractions of affected cell population in the presence of single drug D1 and D2, respectively. Detailed description of how the equation was derived was published by Chou et al. in 1981 [259]. Based on this equation, Chou and Talalay later introduced

the combination index (CI) for quantitative evaluation of synergism between two drugs, where the CI value was defined as:

$$CI = \frac{(D)_1}{(D_x)_1} + \frac{(D)_2}{(D_x)_2} \quad (3)$$

The value of $(D_x)_1$ and $(D_x)_2$ indicates the doses of drug D1 or D2 alone to achieve a certain effect *x*, respectively. $(D)_1$ and $(D)_2$ are the doses of drug D1 and D2 in combination to achieve the same effect. CI < 1, = 1, and > 1 indicate synergism, additive effect, and antagonism, respectively. The isobologram, a 2-dimensional diagram showing varying concentrations of two drugs that resulted in constant effect, is usually used to demonstrate the combination effect (Figure 6a) [260]. To achieve a certain cell killing effect, for example 50% cell killing, doses of drug D1 and D2 used in combination can be plotted on the isobologram as a point (x,y), where the x and y-coordinates indicate the respective doses of both drugs. When single drug is used, the doses can be plotted on the axes where y = $(IC_{50})_1$ and x = $(IC_{50})_2$. The line connecting these two points is the line of additivity. Synergism, additive effect, or antagonism is indicated when the doses used in combination (x,y) are located below, on, or above the line, respectively. Normalizing the x- and y-axis by dividing the value of drug D1 and D2 doses in combination by the constant of single drug dose to achieve the same effect generates the normalized isobologram, where the sum of the x and y-coordinates indicates the CI value (Figure 6b) [261]. It can be observed from this graph that smaller CI value indicates stronger synergism. The opposite applies to antagonism, where the larger the CI value is, the stronger antagonism is indicated. In fact, CI value can be categorized as follows: CI < 0.1 very strong synergism; 0.1-0.3 strong synergism; 0.3-

0.7 synergism; 0.7-0.9 moderate/slight synergism; 0.9-1.1 additive; 1.1-1.45 slight/moderate antagonism; 1.45-3.3 antagonism; 3.3-10 strong antagonism; CI > 10 very strong antagonism [261]. In addition to CI, another important parameter that can be obtained from the median effect/CI model is the dose-reduction index (DRI), which is defined as:

$$\left(DRI\right)_1 = \frac{\left(D_x\right)_1}{\left(D\right)_1} \tag{4}$$

DRI indicates how many fold the dose of each drug in combination can be reduced, compared with the doses of each drug alone [261]. In summary, CI and DRI values allow the quantitative determination of synergistic effect between two agents. This model will be used in our study of agents that synergize with BENSpm in cancer therapy.

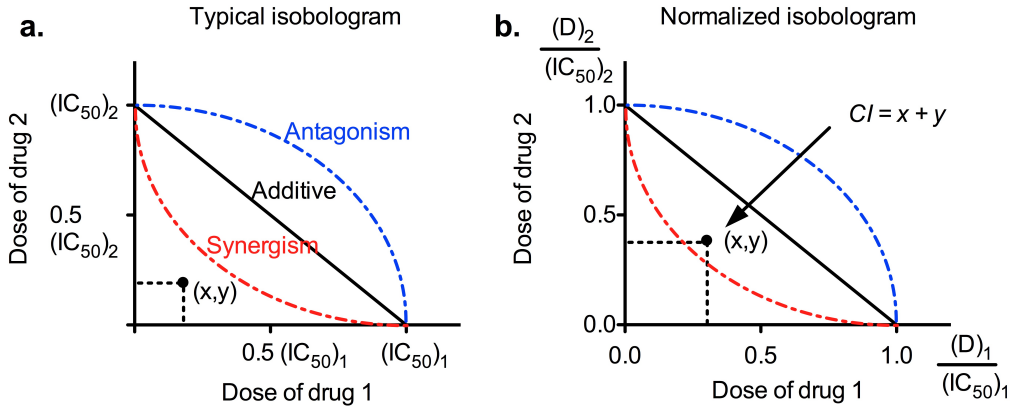


**Figure 6.** Isobologram of $IC_{50}$. (a) A typical isobologram for two drugs with the doses indicated at x- and y-axis. (b) Normalized isobologram of two drugs with the doses normalized as the ratio compared with $IC_{50}$ of single drugs. Modified from [261].

## 2.2 Materials and Methods

### 2.2.1 Materials

Trypsin-like enzyme (TrypLE Express) was purchased from Gibco (Invitrogen, Carlsbad, CA). Fetal bovine serum (FBS), Dulbecco's phosphate buffered saline (PBS), RPMI 1640 Medium and Penicillin-Streptomycin were purchased from Thermo Scientific (Logan, UT). Recombinant human TRAIL/Apo2L protein was purchased from PeproTech (Rocky Hill, NJ). Negative control siRNA (ON-TARGET plus Non-targeting siRNA #1) was purchased from Dharmacon (Lafayette, CO). SignalSilence® siRNAs: Akt-2, survivin, and PARP with the corresponding antibodies: Akt-2 rabbit mAb, survivin mouse mAb and PARP rabbit mAb were from Cell Signaling Technology (Beverly, MA). Lipofectamine™ RNAiMAX transfection reagent was purchased from Invitrogen (Grand Island, NY). N,N'-Bis(3-aminopropyl)-1,3-propanediamine (norspermine) and di-tert-butyl dicarbonate ($Boc_2O$) were from Alfa Aesar (Ward Hill, MA). Triethylamine (TEA) was purchased from Acros Organic (Fair Lawn, NJ). Sodium hydride (NaH, 60% suspension in oil) and magnesium sulfate ($MgSO_4$) were from Sigma-Aldrich (St. Louis, MO). All other reagents and chemicals were obtained from Fisher Scientific or VWR International unless otherwise noted.

### 2.2.2 Synthesis of BENSpm

$^1H$ NMR spectra were recorded on Mercury-400 MHz Spectrometer and chemical shifts ($\delta$) were expressed in ppm. BENSpm was synthesized following published procedure via three step reaction [155]:

*Boc-protected norspermine.* Briefly, norspermine (6.16 g, 32.7 mmol) and TEA (16.6 g, 101.2 g/mol, 164 mmol) were dissolved in 200 mL methanol. $Boc_2O$ (32.3 g, 148 mmol) was dissolved in 80 mL methanol in dropping funnel and then add to the solution of norspermine and TEA as the rate of 1 drop/sec. Reaction was kept overnight in water bath at room temperature. Thin layer chromatography (TLC) was used to monitor the reaction till completion (hexane: ethyl acetate = 2: 1, $R_f$ = 1/3). Methanol was then completely removed in vacuo. Product was further run through silica gel column for purification (hexane: ethyl acetate = 3: 1, column size = 1000 mL, yield = 95%).

*Alkylation of Boc-protected norspermine.* Boc-protected norspermine (19.26 g, 33 mmol) and iodoethane (20.4 g, 10.5 mL, 131 mmol) were dissolved in dry DMF/THF (1: 4, 350 mL), to which solution NaH (4.8 g, 198 mmol, equals to 8 g 60% oil dispersion) was carefully added. Reaction was kept in ice bath during NaH addition and then moved to room temperature and stirred overnight. TLC was used to verify the completion of reaction (hexane: ethyl acetate = 2: 1, $R_f$ = 0.4). Water was then added to the reaction mixture dropwise to consume the excess of NaH (50 mL DW). The reaction mixture was then extracted with hexane. Hexane layer was then washed with saturated sodium chloride (140 mL) and dried with $MgSO_4$. Solution was concentrated on rotary evaporator and purified by silica gel column (hexane: ethyl acetate = 3: 1, column size = 1000 mL) to give the Boc-protected BENSpm.

*Boc deprotection.* Boc-protected BENSpm (20.6 g, 32 mmol, 640 g/mol) was dissolved in 200 mL isopropanol. HCl solution in isopropanol (6 N HCl, 26 mL) was added. The reaction mixture was refluxed overnight. White solid formed during the

reaction. The reaction mixture was then kept at -20 °C to facilitate the precipitation. The solid was then filtered and dried in vacuum. Solid was suspended in 150 mL methanol with 13 mL HCl (6 N in isopropanol) added. The mixture was refluxed for an additional 6 h and the solid was filtered and dried to give BENSpm (HCl salt, 390 g/mol, 11.47g, yield 91.9%): NMR (400 MHz, $D_2O$) $\delta$ 1.28 (t, 6H), 2.07-2.18 (m, 6H), 3.09-3.21 (m, 16H).

### 2.2.3 Cell culture

MCF-7 human breast adenocarcinoma cells were cultured in RPMI medium with 10% FBS. MDA-MB-231 human breast cancer cells were cultured in RPMI with 10% FBS and 1% penicillin/streptomycin. All cells were cultured at 37 °C in incubator with 5% $CO_2$.

### 2.2.4 Transfection of siRNAs and Western blotting analysis

Transfection was done using Lipofectamine™ RNAiMAX following manufacturer's instructions. Briefly, MDA-MB-231 cells were seeded in 6-well plate at a density of 300,000 cells/well, and were allowed to attach overnight. For each well, appropriate amount of siRNA (36 pmol, final concentration 10 nM) was diluted in 300 µL RPMI (without FBS), and in another tube, 6 µL of Lipofectamine™ RNAiMAX was diluted in 300 µL RPMI (without FBS). The two solutions were then mixed and incubated at room temperature for 20 min to allow lipoplexes formation. The lipoplexes were added dropwise onto the cells (600 µL lipoplexes solution to 3 mL medium per well).

After 48 h incubation, cells were lysed and diluted with 4× NuPAGE® LDS sample buffer (Invitrogen). Collected cell lysates were then homogenized by sonication and the supernatants were loaded for polyacrylamide gel electrophoresis (PAGE) and electroblotted to nitrocellulose using the Mini Trans-Blot® system (Bio-Rad), as previously described [262]. Blots were developed using Immobilon Western Chemiluminescent HRP Substrate (Millipore) and were imaged using FUJIFILM Luminescence Image Analyzer LAS-1000plus.

### 2.2.5 Cytotoxicity assay

MDA-MB-231 cells were treated with increasing concentration of TRAIL, BENSpm, or BENSpm in combinations with Akt-2, survivin and PARP siRNAs for a required time length for the drug action. Concentrations of siRNAs were 10 nM in each well, which was delivered with Lipofectamine™ RNAiMAX using the same formulation as for the Western blot assay. For the combination of BENSpm and TRAIL, MDA-MB-231 and MCF-7 cells were incubated in 200 µL medium per well in 96-well plate with increasing concentration of BENSpm, TRAIL or their combinations. Medium was replaced once at 48 h with fresh medium containing the same concentration of the respective agents.

At the end of the treatment, drug-containing medium was aspirated and replaced by a mixture of 100 µL serum-free media and 20 µL of MTS reagent (CellTiter 96® AQueous Non-Radioactive Cell Proliferation Assay, Promega). After 2 h incubation, the absorbance was measured at a wavelength of 490 nm using Synergy 2 Microplate Reader (BioTek). The relative cell viability (%) was calculated as $[A]_{sample}/[A]_{untreated}$ ×

100%. The $IC_{50}$ were calculated as the drug concentration that inhibits growth of 50% of cells relative to untreated cells using GraphPad Prism [263].

### 2.2.6 Analysis of synergistic effect of BENSpm and TRAIL combination

The median effect/CI model was used to determine synergy of the combination treatment of BENSpm with TRAIL. The fraction of killed cells ($f_a$) was determined by MTS assay described above ($f_a$= 1- cell viability%). Results were analyzed by CompuSyn software (ComboSyn, Inc. Paramus, NJ) for the CI and DRI values to quantitatively determine the synergism of BENSpm and TRAIL combination [261].

## 2.3 Results and Discussion

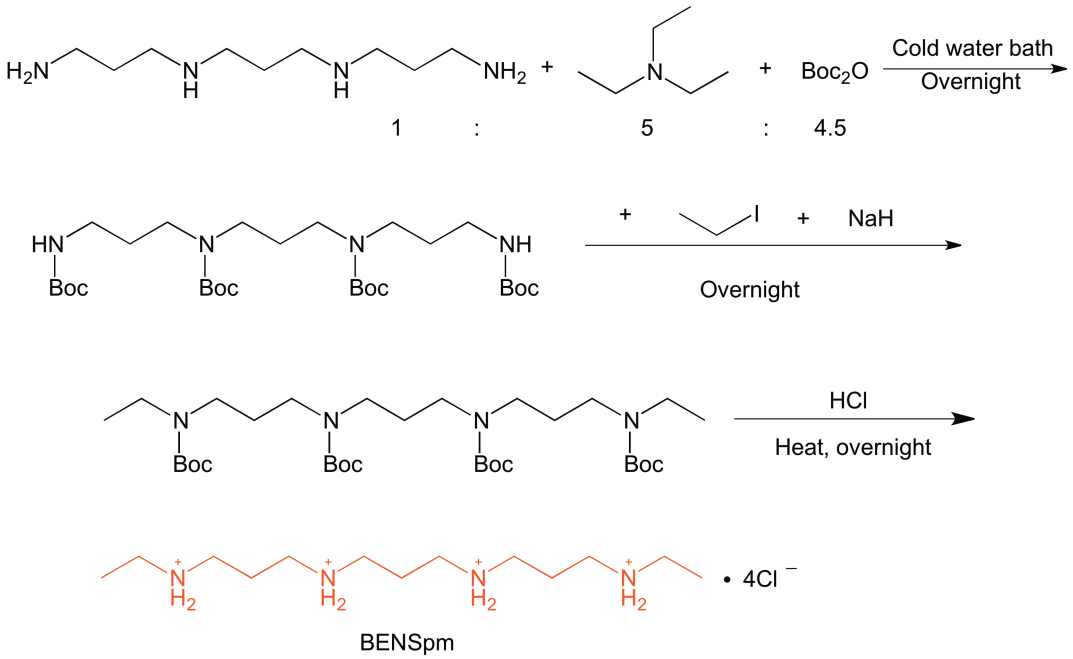


**Scheme 2.** The synthesis route of BENSpm.

### 2.3.1 Synthesis of BENSpm

BENSpm was synthesized by selective alkylation of Boc-protected norspermine at the primary amine ends (Scheme 2). The structure of BENSpm and complete deprotection of Boc were confirmed by $^{1}$H NMR (Figure 7). Compared with the parent norspermine, the primary amines are alkylated with ethyl groups in BENSpm. This prevents oxidation by multiple amine oxidases in the cells and prolongs the duration of BENSpm activity in targeting the polyamine pathway in cells [103]. The synthesized BENSpm (HCl salt) was used for the following studies.

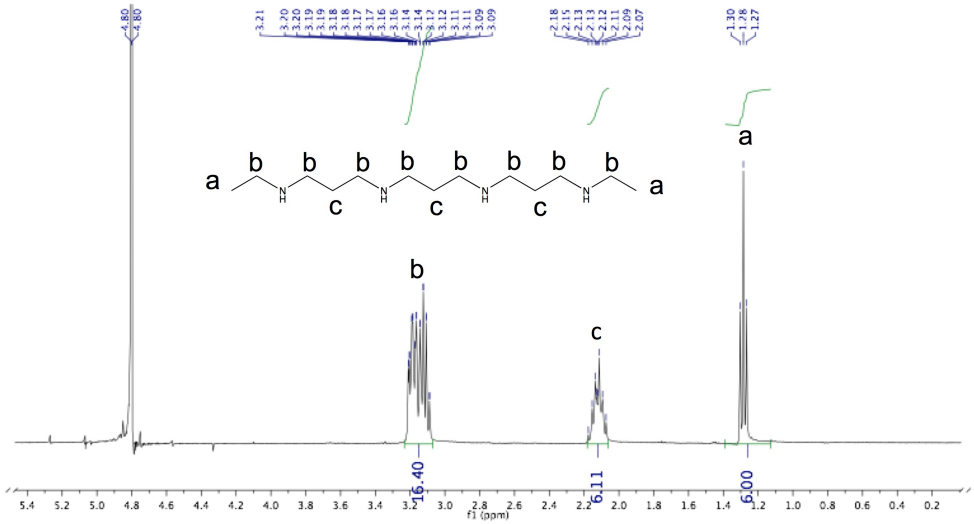


**Figure 7.** $^{1}$H-NMR spectra of BENSpm (HCl salt).

### 2.3.2 Combination effect of BENSpm and TRAIL with siRNAs

Western blot analysis verified that transfection of Akt-2, survivin and PARP siRNAs all resulted in significant knockdown of the corresponding proteins in MDA-MB-231 cells after 48 h incubation (Figure 8a). Since the required time length for BENSpm drug action is 120 h [199], cytotoxicity of BENSpm in combination with siRNAs was tested in the 120 h time frame. As shown in Figure 8b, where the points on y-axis

indicated the cell viability followed siRNAs treatment alone (as concentration of BENSpm equals zero), 120 h transfection with siRNAs resulted in significant cell killing. However, the cytotoxicity was predominantly associated with the delivery system, since significant cytotoxicity was observed not only in functional siRNAs treat cells, but also in control siRNA (ctrl siRNA) group (cell viability of 52% in ctrl siRNA group vs. ~33-36% in functional siRNAs groups). Cytotoxicity of combination of BENSpm with the functional siRNAs was not significantly different from BENSpm and ctrl siRNA co-treatment. It could be concluded that, although the pro-survival proteins Akt-2, survivin and PARP can be efficiently depleted by siRNA transfection, it did not necessarily sensitize the breast cancer cells towards BENSpm-related growth inhibition. The somewhat disappointing result from siRNA combinations demonstrated the complexity of drug-combination effect, and synergism need to be experimentally identified on a case-by-case basis.

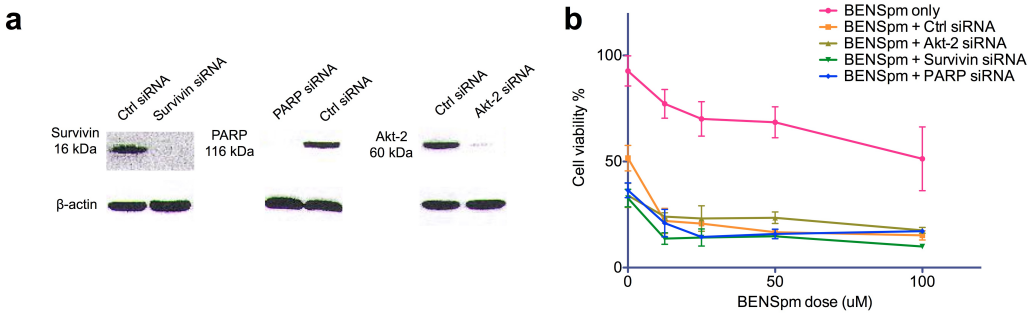


**Figure 8.** Combination of Akt-2, survivin and PARP siRNAs with BENSpm in MDA-MB-231 cells. (a) Western blot analysis of MDA-MB-231 cells treated with 10 nM survivin, PARP or Akt-2 siRNAs. β-actin is used as a loading control.(b) Combination of siRNAs with BENSpm for 120 h in MDA-MB-231 cells. Results were expressed as mean cell viability% ± SD (n=4).

### 2.3.3 Combination effect of BENSpm with TRAIL

In order to determine the combination effect of BENSpm and TRAIL, a constant molar ratio of BENSpm and TRAIL which equals to the ratio of their $IC_{50}$ (BENSpm:TRAIL 14,700:1) was used in combination for MDA-MB-231 cells. For MCF-7 cell line, which is more resistant to TRAIL treatment, a constant concentration of TRAIL (35 ng/mL) was used in combination. Four to six doses were used in serial dilutions covering the activity range of BENSpm and TRAIL. The CI value and DRI value were calculated by the Chou-Talalay method using CompuSyn software [264]. As shown in Figure 9, we first tested whether the parent BENSpm enhances activity of the TRAIL protein in triple-negative breast cancer cells MDA-MB-231. The observed CI values were <0.04 across the entire studied $f_a$ range, indicating a very strong synergy between BENSpm and TRAIL. We then expand the combination to another type of breast cancer cell, the estrogen-dependent MCF-7 cell line. As shown in Figure 10, less potent but still strong synergy between BENSpm and TRAIL was found also in the MCF-7 cell.

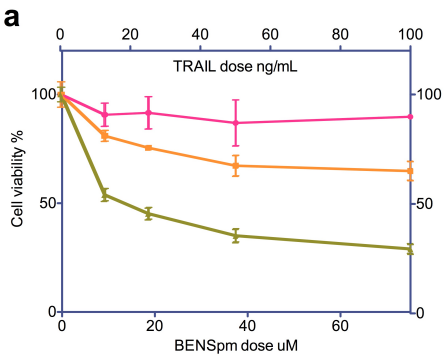


b

BENSpm only
BENSpm and TRAIL
TRAIL only

| MDA-MB-231 cell line | | | |
|---|---|---|---|
| Doses in combination | | CI value | DRI (TRAIL) |
| BENSpm (μM) | TRAIL (ng/mL) | | |
| 9.375 | 12.5 | 0.035 | 59 |
| 18.75 | 25 | 0.031 | 98 |
| 37.5 | 50 | 0.027 | 214 |
| 75 | 100 | 0.032 | 283 |

**Figure 9.** Synergistic activity of BENSpm and TRAIL in MDA-MB-231 cells. (a) Cytotoxicity of increasing concentration of TRAIL, BENSpm or their combination for 120 h. Cell viability was measured by MTS assay (n=3-4). (b) CI value and DRI calculated for each dose of BENSpm and TRAIL in combination using CalcuSyn software.

In addition, the calculated DRIs range for TRAIL treatment were 59-283 and 2.5-6.3 respectively, in MDA-MB-231 cells and MCF-7 cells. The result that ~280-fold dose reduction for TRAIL protein could be achieved when combined with BENSpm in MDA-MB-231 cells is especially promising for the application of nonviral gene delivery. As gene delivery is hampered by the low transfection efficiency, this finding provides the rationale for designing BENSpm based gene delivery system to deliver therapeutic genes (e.g., TRAIL), and enhanced treatment outcome is expected through the combination.

**a**

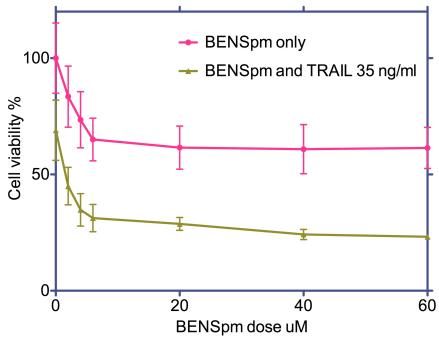


**b**

| MCF-7 cell line | | | |
|---|---|---|---|
| Doses in combination | | CI value | DRI (TRAIL) |
| BENSpm (μM) | TRAIL (ng/mL) | | |
| 2 | 35 | 0.401 | 2.5 |
| 4 | 35 | 0.269 | 3.7 |
| 6 | 35 | 0.232 | 4.3 |
| 20 | 35 | 0.209 | 4.8 |
| 40 | 35 | 0.169 | 6.0 |
| 60 | 35 | 0.161 | 6.3 |

**Figure 10.** Synergistic activity of BENSpm and TRAIL in MCF-7 cells. (a) Cytotoxicity of increasing concentration of BENSpm alone or in combination with TRAIL (35 ng/ml) was measured by MTS assay (n=3-4). (b) CI value and DRI calculated for each dose of BENSpm and TRAIL in combination using CalcuSyn software.

## 2.4 Conclusions

As a proof-of-concept, we test the combination effect of BENSpm with several therapeutic agents. Firstly, combination of BENSpm with functional siRNAs did not show beneficial outcome over the BENSpm combination with negative control siRNA, indicating no synergistic effect of BENSpm combined siRNA treatment in breast cancer MDA-MB-231 cells. However, we later identified strong synergistic combination of

BENSpm with potential therapeutic gene product TRAIL. For both cell lines tested, which are representative estrogen-dependent and triple-negative breast cancers, BENSpm and TRAIL combination demonstrated strong synergism and offers potential advantages to reduce the required treatment dose. Because the synergism is obtained regardless of the cell line sensitivity to TRAIL, this combination strategy offers additional benefits to overcome drug resistance in chemotherapy. In all, this finding inspired us for the attempt to develop BENSpm-based delivery system for the co-delivery of genes and BENSpm drug, which may further boost the therapeutic effect of the cargo genes. Design of the dual delivery systems will be further discussed in the following chapters.

# CHAPTER 3

# SYNTHESIS OF BISETHYLNORSPERMINE LIPID PRODRUG AS GENE DELIVERY VECTOR TARGETING POLYAMINE METABOLISM IN BREAST CANCER

Please note that the content of this chapter was published in *Molecular Pharmaceutics* [265]. As the second author of the study, I performed particle size and zeta potential measurements, cytotoxicity assays in MDA-MB-231 cells (cytotoxicity in MCF-7 cells were measured by Dr. C. Wu, the fifth author), luciferase transfection in MDA-MB-231 cells (transfection in B16F10 cells and MCF-7 cells were performed by Dr. Q. Zhou, the fourth author), SSAT assay and analysis of the combination treatment. The first author Dr. Y. Dong performed the synthesis and chemical characterization of the lipids. Dr. J. Li, the third author, performed agarose gel retardation assay and ethidium bromide exclusion assay. All the authors agreed with including their work in this dissertation.

## 3.1 Introduction

Successful implementation of novel gene therapy protocols requires the development of strategies to effectively deliver nucleic acids to disease targets. Cationic lipids and polymers continue to gain strength as viable alternatives to viral delivery vectors. However, progress in the development of these vectors continues to be hampered by their low transfection activity and toxicity of the cationic molecules. The classical biomaterial design paradigm: “preparing vectors that are biodegradable into

nontoxic low-molecular weight byproducts" yielded many cationic lipids and polymers with acceptable toxicity. Although the toxicity can be decreased to some extent by using biodegradable molecules, amplifying transfection activity is the more difficult problem to solve because it involves complex delivery across multiple barriers. One way to overcome the low transfection is to combine a therapeutic gene with traditional small-molecule drugs that enhance the gene's therapeutic activity [266, 267]. Such drug/gene combination therapies can be accomplished by a simple combination of gene therapy protocols with existing drugs. Alternatively, synthetic gene delivery vectors can be designed that not only deliver a gene but also augment the activity of the gene by exerting their own pharmacologic effect.

There are a growing number of successful examples of drug and gene delivery vectors that combine the delivery function with a pharmacologic activity. For example, Prof. Huang's group developed a novel cationic lipid capable of delivering siRNA while simultaneously enhancing siRNA antitumor effect by down-regulating pERK [71]. Pluronic copolymers have been shown to chemosensitize multidrug resistant cancers by inhibiting P-glycoprotein and decreasing cellular ATP pools [88]. Peptides with intrinsic proteasome inhibitory function have been shown to deliver and enhance transfection activity of plasmid DNA [90]. Cyclodextrins, widely used as excipients and as parts of drug delivery vectors, have been shown to have activity in the treatment of a lysosomal storage disorder [268].

Natural polyamines SPD, SPM, and their diamine precursor PUT are essential factors for growth of eukaryotic cells. We have recently proposed dually functioning cationic gene delivery vectors based on polyamine analogues [269]. These agents

exploit the self-regulatory nature of the metabolism of cellular polyamines and have multiple targets in the polyamine pathway. Polyamine metabolism is frequently dysregulated in cancer and other hyper-proliferative diseases [101]. The polyamine pathway is a distal downstream target for a number of oncogenes, and inhibition of polyamine synthesis disrupts the action of those genes [101, 270, 271]. All these factors make polyamine analogues attractive building blocks in the design of delivery vectors that can not only deliver a therapeutic gene but also augment the activity of the gene by exerting their own pharmacologic effect. The goal of this study was to develop biodegradable lipid prodrug based on the polyamine analogue BENSpm that can function dually as gene delivery vector and, after intracellular degradation, as active pharmacologic agent that synergistically augments the activity of a therapeutic gene in cancer. We have also tested the hypothesis that the synthesized lipid BENSpm prodrug will enhance activity of TRAIL in breast cancer.

## 3.2 Materials and Methods

### 3.2.1. Materials

Dioctadecylamine, 4-mercaptobenzoic acid, lithium aluminium hydride, HOBt (1-hydroxybenzotriazole), 1-(3-*N*,*N*-dimethylaminopropyl)-3-ethylcarbodiimide hydrochloride (EDCI), 3,3'-dithiodipropionic acid, zinc powder, carbomethoxysulfenyl chloride, p-nitrophenyl chloroformate, trifluoroacetic acid (TFA), dithiothreitol (DTT), hydroxylamine monochloride, spermidine, and ethidium bromide (EtBr) were purchased from Sigma-Aldrich (St. Louis, MO). [$^{14}$C]-Acetyl-CoA was purchased from PerkinElmer (Waltham, MA). Biodegradable scintillation cocktails (Bio-Safe NA™ for non-aqueous

samples, Bio-Safe II™ for aqueous samples) were purchased from RPI Corp. (Mount Prospect, IL). Trypsin-like enzyme (TrypLE Express) was purchased from Invitrogen-Gibco (Carlsbad, CA). RPMI 1640 Medium, Dulbecco's Modified Eagle's Medium (DMEM), fetal bovine serum (FBS), and Dulbecco's phosphate buffered saline (PBS) were purchased from Thermo Scientific-Hyclone (Logan, UT). Plasmid DNA, gWiz$^{TM}$ high-expression luciferase, containing luciferase reporter gene was from Aldevron (Fargo, ND). Luciferase assay system with reporter lysis buffer was purchased from Promega (Madision, WI). Recombinant human TRAIL/Apo2L protein was purchased from PeproTech (Rocky Hill, NJ). LipoBEN was synthesized as described in our previous publication [269]. All other reagents and solvents were purchased from commercial suppliers and were used without further purification unless otherwise stated.

3.2.2. Synthesis

NMR spectra were recorded on a Varian FT-NMR Unity-300, Mercury-400 or Mercury-500 MHz spectrometer. Chemical shifts (δ) are expressed in ppm and are internally referenced (0.00 ppm for TMS for $^{1}H$ NMR and 77.0 ppm for $CDCl_3$ for $^{13}C$ NMR). Mass spectra were recorded on a Waters ZQ2000 single quadrupole mass spectrometer using an electrospray ionization source.

*Synthesis of **3**.* A suspension of 3,3′-dithiodipropionic acid **2** (105 mg, 0.5 mmol) and HOBt (203 mg, 1.5 mmol) in anhydrous $CHCl_3$ (30 mL) was added to the solution of EDCI (233 mg, 1.5 mmol) in anhydrous $CHCl_3$ (10 mL) at 0 °C, followed by addition of the mixture of TEA (152 g, 0.21 mL, 1.5 mmol) and dioctadecylamine **1** (522 mg, 1 mmol) in $CHCl_3$ (10 mL). The resulting mixture was stirred at room temperature for 12 h,

when it turned to a clear solution. The reaction mixture was then partitioned with water (15 mL) at 0 °C. The organic layer was separated, and the water layer was extracted with $CHCl_3$ (3 × 10 mL). Combined organic layers were washed with brine, dried over anhydrous $Na_2SO_4$, and evaporated under vacuum to give the crude product. The residue was dry-loaded to a silica gel column, and separation (eluent: $CHCl_3$/ethyl acetate 4:1) gave the product **3** (0.58 g, 95%) as a white solid. $R_f$ 0.85 ($CHCl_3$). Mp 38-39 °C. $^1$H NMR (400 MHz, $CDCl_3$): δ 3.29 (bt, J = 7.8 Hz, 4H), 3.22 (bt, J = 7.6 Hz, 4H), 2.96 (t, J = 7.0 Hz, 4H), 2.73 (t, J = 7.4 Hz, 4H), 1.55-1.50 (m, 8H), 1.26 (bs, 112H), 0.88 (t, J = 6.6 Hz, 12H). $^{13}$C NMR (100 MHz, $CDCl_3$): 170.2, 47.9, 46.0, 33.5, 32.7, 31.9, 29.65, 29.60 (m), 29.55, 29.51, 29.4, 29.3, 29.1, 27.7, 27.0, 26.9, 22.6, 14.0. ESI MS (m/z): calcd for $C_{78}H_{156}N_2O_2S_2$ $[M + H]^+$ 1218.16, found 1217.99; $[M + Li]^+$ 1224.17, found 1224.00; $[M + K]^+$ 1256.12, found 1255.96.

*Synthesis of **4**.* The synthesis of **4** followed previous publication [272]. To a solution of **3** (0.55 g, 0.79 mmol) in acetic acid (10 mL) was added zinc powder (0.51 g, 7.9 mmol) at 0 °C. The mixture was refluxed for 40 min and monitored by TLC (viewed by UV and stained by DTNB). The mixture was filtered over Celite and washed with $CHCl_3$. The obtained organic solution was evaporated under vacuum. The residue was flushed with nitrogen to remove excess acetic acid. The white solid was dissolved in $CHCl_3$ (10 mL) and washed with water to neutrality. The combined organic layers were then washed with brine, dried over anhydrous $Na_2SO_4$, and concentrated under vacuum. The residue was purified by silica gel column (eluent: $CHCl_3$/ethyl acetate 4:1) to give the product **4** (0.55 g, 100%) as a white solid. $R_f$ 0.52 ($CHCl_3$). Mp 44-45 °C. $^1$H NMR (400 MHz, $CDCl_3$): δ 3.30 (bt, J = 7.8Hz, 2H), 3.20 (bt, J = 7.8 Hz, 2H), 2.80 (bq,

$J_1$ = 7.6 Hz, 2H), 2.63 (t, J = 6.6 Hz, 4H), 1.72 (t, J = 8.4 Hz), 1.53 (m, 4H), 1.26 (bs, 56H), 0.88 (t, J = 7.0 Hz, 6H). $^{13}$C NMR (100 MHz, $CDCl_3$): 169.9, 47.7, 45.9, 37.0, 31.8, 29.60, 29.56 (m), 29.5, 29.4, 29.3, 29.2, 28.9, 27.7, 26.9, 26.8, 22.6, 20.2, 13.9. ESI MS (m/z): calcd for $C_{39}H_{79}NOS$ $[M + H]^+$ 610.59, found 610.51; $[M + Li]^+$ 616.60, found 616.52; $[M + K]^+$ 648.55, found 648.47.

*Synthesis of **5**.* The solution of **4** (0.53 g, 0.87 mmol) in methanol (5 mL) was added dropwise to a solution of carbomethoxysulfenyl chloride (0.11 g, 0.87 mmol) in methanol (10 mL) and $CHCl_3$ (20 mL) at 0 °C. The mixture was stirred for 30 min at 0 °C, then allowed to reach room temperature, and after 4 h evaporated under vacuum. The obtained residue was dissolved in $CHCl_3$ (10 mL) and purified on silica ($CHCl_3$/ethyl acetate 4:1). Pure product **5** was obtained as colorless oil, which turned to a white solid when kept in a freezer (0.55 g, 90%). $R_f$ 0.39 ($CHCl_3$). Mp 36-37 °C. $^1$H NMR (400 MHz, $CDCl_3$): δ 3.88 (s, 3H), 3.29 (bt, J = 7.8 Hz, 2H), 3.20 (bt, J = 7.8 Hz, 2H), 3.01 (t, J = 7.2 Hz, 2H), 2.72 (t, J = 7.0 Hz, 4H), 1.52 (m, 4H), 1.26 (bs, 56H), 0.88 (t, J = 7.0 Hz, 6H). $^{13}$C NMR (100 MHz, $CDCl_3$): 170.1, 169.7, 55.2, 47.8, 46.0, 35.1, 32.7, 31.9, 29.63, 29.59, 29.52 (m), 29.5, 29.3, 29.2, 29.0, 27.7, 26.9, 26.8, 22.6, 20.2, 14.0. ESI MS (m/z): calcd for $C_{41}H_{81}NO_3S_2$ $[M + H]^+$ 700.57, found 700.57; $[M + Na]^+$ 722.55, found 722.54; $[M + Li]^+$ 706.58, found 706.58; $[M + K]^+$ 738.52, found 738.51.

*Synthesis of **6**.* A solution of 4-mercaptobenzoic acid (0.77 g, 5 mmol) in dry THF (10 mL) was added dropwise to a suspension of lithium aluminum hydride (0.57 g, 15 mmol) in dry THF (10 mL) under nitrogen at 0 °C [273]. The mixture was stirred overnight at room temperature. Water (5 mL) was added, followed by aqueous HCl (1 N, 5 mL) at 0 °C, and the mixture was stirred for 5 min. The solution was extracted with

diethyl ether (3 × 10 mL). The organic layer was washed with $H_2O$ (20 mL) and brine (10 mL), dried over anhydrous $Na_2SO_4$, and then concentrated under vacuum at room temperature. The residue was purified by a short silica gel column to give the product as a white solid (0.56 g, 80%). $R_f$ 0.28 (hexane: EA 2: 1) Mp 49-51 °C. $^1$H NMR (400 MHz, $CDCl_3$): δ 7.26-7.20 (m, 4H), 4.60 (s, 2H), 3.45 (s, 1H), 2.00 (bs, 1H). $^{13}$C NMR (100 MHz, $CDCl_3$): 138.3, 129.9, 129.5, 127.8, 64.7.

*Synthesis of* ***7****.* A solution of **6** (0.32 g, 2.28 mmol) in $CH_3OH/CHCl_3$ (5 mL/10 mL) was added to a solution of **5** (0.53 g, 0.76 mmol) in $CH_3OH$ (5 mL) at 0 °C under nitrogen. The mixture was stirred for 1 h at 0 °C and then warmed to room temperature. After 3 days, the mixture was evaporated and the obtained residue was dissolved by $CHCl_3$ and purified by a short silica gel column (hexane/ethyl acetate 3:1). Compound **7** was obtained as colorless oil, which turned to a white solid in the freezer (0.42 g, 75%). $R_f$ 0.38 (hexane/ethyl acetate 3: 1). Mp 40-41 °C. $^1$H NMR (400 MHz, $CDCl_3$): δ 7.47 (d, J = 8.4 Hz, 2H), 7.28 (d, J = 8.4 Hz, 2H), 4.61 (s, 2H), 3.35 (bs, 1H), 3.24 (bt, J = 7.6 Hz, 2H), 3.10 (bt, J = 7.8 Hz, 2H), 2.96 (t, J = 7.0 Hz, 2H), 2.66 (t, J = 7.2 Hz, 2H), 1.47 (m, 4H), 1.26 (bs, 56H), 0.88 (t, J = 7.0 Hz, 6H). $^{13}$C NMR (100 MHz, $CDCl_3$): 170.1, 140.2, 135.9, 127.6, 127.4, 64.1, 47.8, 46.0, 34.0, 32.4, 31.8, 29.58, 29.54, 29.47 (m), 29.4, 29.3, 29.2 (m), 28.9, 27.6, 26.9, 26.7, 22.6, 14.0. ESI MS (m/z): calcd for $C_{46}H_{85}NO_2S_2$ $[M + H]^+$ 748.60, found 748.61; $[M + Na]^+$ 770.59, found 770.60; $[M + Li]^+$ 754.62, found 754.63; $[M + K]^+$ 786.57, found 786.59.

*Synthesis of* ***8****. p*-Nitrophenyl chloroformate (0.23 g, 1.12 mmol) was added to a solution of **7** (0.42 g, 0.56 mmol) in anhydrous $CHCl_3$ at 0 °C under nitrogen, followed by TEA (0.234 mL, 1.68 mmol). The mixture was stirred for 30 min and then warmed to

room temperature. After stirring for 24 h, the mixture was evaporated and the obtained residue was dissolved in $CHCl_3$ and purified by a short silica gel column (hexane/ethyl acetate 5:1). Recrystallization from ethyl acetate gave the pure product **8** as a white solid (0.36 g, 70%). $R_f$ 0.37 (hexane/ethyl acetate 5:1). Mp 52-53 °C. $^1$H NMR (400 MHz, $CDCl_3$): δ 8.27 (d, J = 8.8 Hz, 2H), 7.58 (d, J = 8.8 Hz, 2H), 7.41− 7.37 (m, 4H), 5.27 (s, 2H), 3.28 (bt, J = 7.8 Hz, 2H), 3.14 (bt, J = 7.8 Hz, 2H), 3.04 (t, J = 7.0 Hz, 2H), 2.71 (t, J = 6.8 Hz, 2H), 1.48 (m, 4H), 1.26 (bs, 56H), 0.88 (t, J = 6.6 Hz, 6H). $^{13}$C NMR (100 MHz, $CDCl_3$): 169.9, 155.4, 152.4, 145.4, 138.7, 132.6, 129.4, 127.2, 125.2, 121.7, 70.3, 47.8, 46.1, 34.2, 32.5, 31.9, 29.66, 29.62, 29.6 (m), 29.4, 29.3, 29.0, 27.7, 27.0, 26.8, 22.6, 14.1. ESI MS (m/z): calcd for $C_{53}H_{88}N_2O_6S_2$ $[M + H]^+$ 913.62, found 913.72; $[M + Na]^+$ 935.60, found 935.69; $[M + Li]^+$ 919.62, found 919.74.

*Synthesis of Lipo-SS-BEN.* BENSpm·4HBr (0.705 g, 1.25 mmol) was stirred with solid sodium hydroxide (1.0 g, 25 mmol) in anhydrous $CHCl_3$ (20 mL) for 3 h at room temperature. Anhydrous $Na_2SO_4$ (1.0 g) was added, and the mixture was stirred for another 30 min. Filtration and washing with $CHCl_3$ (10 mL) gave a solution that contained free base BENSpm (1.25 mmol). The obtained BENSpm solution in $CHCl_3$ was cooled downed to 0 °C, and a solution of **8** (0.23 g, 0.25 mmol) in anhydrous $CHCl_3$ (15 mL) was added dropwise under nitrogen. After addition, the reaction mixture was stirred at 0 °C for 2 h to reach completion based on TLC. The reaction mixture was purified by a short silica gel column (methanol/ethyl acetate 1: 1) to remove *p*-nitrophenol, followed by elution with $CH_2Cl_2$/$CH_3OH$/sat. $NH_3$ (25: 10: 0.5). The collected eluent containing product was neutralized with 5 M acetic acid to pH 7.4. Evaporation under reduced pressure at 25 °C gave a solid residue. Residual ammonium acetate was

removed under vacuum at room temperature to give the product as acetate salt (0.36 g, 70%, kept at -40 °C). $R_f$ 0.46 ($CH_2Cl_2$/$CH_3OH$/sat. NH3 25:10:1). Mp 36-40 °C. $^1$H NMR (400 MHz, $CDCl_3$/$CD_3OD$ 10:1): δ 7.54 (d, J = 8.0 Hz, 2H), 7.32 (d, J = 8.0 Hz, 2H), 5.09 (s, 2H), 3.36 (m, 6H), 3.22 (bt, 2H), 2.99 (t, J = 6.4 Hz, 2H), 2.85 (m, 4H), 2.76 (m, 6H), 1.95 (s, 3H), 1.79 (bm, 4H), 1.51 (bm, 4H), 1.26 (bs, 59H), 1.14 (t, J = 6.8 Hz, 3H), 0.88 (t, J = 6.6 Hz, 6H). $^{13}$C NMR (100 MHz, $CDCl_3$): 177.3, 170.0, 137.2, 135.2, 128.8, 127.4, 66.0, 47.9, 46.1, 34.1, 32.6, 31.9, 29.7, 29.6 (m), 29.4, 29.3, 29.0, 27.7, 27.0, 26.9, 25.2, 24.1, 23.2, 22.6, 14.1. ESI MS (m/z): calcd for $C_{60}H_{115}N_5O_3S_2$ $[M + H]^+$ 1018.85, found 1018.89; $[M + 2H]^{2+}$ 509.93, found 510.23; $[M+Li]^+$ 1024.86, found 1024.94.

*Synthesis of **9**.* $Boc_2O$ (0.2 g, 0.92 mmol) was added to a solution of Lipo-SS-BEN (0.11 g, 0.11 mmol) in anhydrous $CHCl_3$ (5 mL) at 0 °C under nitrogen. The mixture was stirred for 1 h at 0 °C and then warmed to room temperature. After stirring for 12 h, the mixture was purified by a short silica gel column to give pure product **9** as colorless oil (0.11 g, 75%). $R_f$ 0.30 (hexane/ethyl acetate 5: 1). $^1$H NMR (400 MHz, $CDCl_3$): δ 7.52 (d, J = 8.4 Hz, 2H), 7.30 (d, J = 8.0 Hz, 2H), 5.09 (s, 2H), 3.30-3.10 (m, 22H), 3.02 (t, J = 6.8 Hz, 2H), 2.72 (t, J = 6.8 Hz, 2H), 1.74 (m, 6H), 1.49-1.45 (muls, 31H), 1.26 (bs, 56H), 1.09 (t, J = 6.8 Hz, 2H), 0.88 (t, J = 7.0 Hz, 6H). $^{13}$C NMR (100 MHz, $CDCl_3$): 170.1, 155.8, 155.4, 152.4, 145.3, 138.6, 132.6, 129.4, 127.2, 125.2, 121.7, 70.3, 47.8, 46.1, 34.2, 32.5, 31.9, 29.66, 29.62, 29.6 (m), 29.4, 29.3, 29.0, 27.7, 27.0, 26.8, 22.6, 14.1. ESI MS (m/z): calcd for $C_{75}H_{139}N_5O_9S_2$ $[M + Na]^+$ 1340.99, found 1341.42; $[M + 2Na]^{2+}$ 681.99, found 682.54; $[M + K]^+$ 1356.96, found 1357.39.

3.2.3. EtBr exclusion assay

The ability of the cationic lipids to condense DNA was determined by measuring changes in EtBr/DNA fluorescence. DNA solution at a concentration of 20 μg/mL was mixed with EtBr (1 μg/mL), and fluorescence was measured and set to 100% using $\lambda_{exc}/\lambda_{em}$ 540/590 nm. Fluorescence readings were taken following a stepwise addition of the lipid solution prepared in 10 mM HEPES pH 7.4, and the condensation curve for each lipid was constructed.

3.2.4. Agarose gel retardation assay

The condensation ability of the lipids and the redox stability of the lipoplexes were examined by agarose gel electrophoresis. Lipid/DNA complexes were formed at specified N/P ratios and incubated with or without 20 mM GSH and with or without increasing concentration of heparin for 30 min. Samples were loaded onto a 0.8% agarose gel containing 0.5 μg/mL EtBr and run for 60 min at 120 V in 0.5× TBE running buffer. The gel was visualized under UV illumination on a Gel Logic 100 imaging system.

3.2.5. Particle size and zeta potential measurement

The hydrodynamic diameters and zeta potentials of lipid/DNA complexes prepared in 10 mM HEPES (pH 7.4) were determined using ZetaPlus Particle Size and Zeta Potential analyzer (Brookhaven Instruments) (Table 4). Lipid/DNA complexes were formed at specified N/P ratios and incubated for 30 min. Scattered light was detected at 90° angle and 25 °C.

### 3.2.6. Cell lines

B16F10 mouse melanoma cells were cultured in DMEM supplemented with 10% FBS. MCF-7 human breast adenocarcinoma cells were cultured in RPMI medium with 10% FBS. MDA-MB-231 breast cancer cells were cultured in RPMI with 10% FBS and 1% penicillin/streptomycin. All cells were cultured at 37 °C in incubator with 5% $CO_2$.

### 3.2.7. Cell viability assay

Cytotoxicity of the cationic lipids in human breast cancer cell lines MCF-7 and MDA-MB-231 was determined by MTS assay using CellTiter 96® Aqueous Cell Proliferation Assay Kit (Promega). 4,000 cells were seeded in a 96-well plate and allowed to attach overnight, culturing medium was then removed and replaced with 200 µL of medium with increasing concentration of the relative drug. Medium was replaced every 48 h with fresh medium containing the same concentration of the respective drug. After 120 h treatment, cell viability was determined by MTS assay according to manufacturer's protocol. The results are expressed as mean percentage cell viability relative to untreated cells ± SEM (n = 4-8). $IC_{50}$ values were calculated using Prism 5 (Graphpad Software, Inc.) using sigmoidal nonlinear regression.

### 3.2.8. Luciferase transfection

Complexes were prepared by adding a predetermined amount of cationic lipids to the solution of plasmid DNA in 10 mM HEPES pH 7.4 to achieve a final DNA concentration of 32 µg/mL and N: P ratios of 2, 4, 8, 16, 32. Mass of 325 per one

phosphate group of DNA was assumed in the calculations. All transfection studies were performed in 96-well plates or 48-well plates with cells plated 24 h before transfection at the seeding density of 12,000 cells/well (for 96-well plate) and 50,000 cells/well (for 48-well plate). The cells were incubated with DNA complexes for 3 h in 150 µL of medium without FBS at 2 µg DNA/mL. Luciferase expression was measured after 24 h and expressed as mean relative light units (RLU) per mg of cellular protein measured by the bicinchoninic acid (BCA) assay ± SD of quadruplicate samples.

### 3.2.9. SSAT assay

Enzymatic activity of SSAT in MDA-MB-231 cells was determined using [$^{14}$C]-Acetyl-CoA substrate as previously described [274, 275]. In brief, cells were harvested after the treatment with BENSpm, LipoBEN and Lipo-SS-BEN at the doses of the relative $IC_{50}$ values, and resuspended in SSAT breaking buffer (5 M HEPES, 1 M DTT, PH 7.2) at $2\times10^7$ cells/mL and centrifuged at 14,000 rpm for 15 min at 4 °C. 25 µL of the supernatant was used to obtain total cellular protein concentration using BCA protein assay reagent (Pierce, Thermo Scientific). Another 20 µL of each sample was mixed with reaction mixture (10 µL 0.5 M HEPES, pH 7.8, 5 µL 30 mM spermidine, 0.5 µL [$^{14}$C]-Acetyl-CoA, 14.5 µL dd$H_2O$) and incubated in 37 °C water bath for 5 min. 20 µL 0.5 M hydroxylamine was then added to each sample. Reaction was stopped by boiling the samples for 3 min. 50 µL of each sample was then pipetted to p81 Whatman filter, and put into wash system with continuous water flow for 30 min and suspended in Biosafe counting fluid. Each sample was counted for 1 min using 1209 Rackbeta liquid scintillation counter (PerkinElmer).

### 3.2.10. Analysis of the combination treatment with TRAIL

The median effect/combination index model was used to determine synergy of the combination treatments of the cationic lipids with TRAIL. Cells were treated for 120 h with increasing concentration of TRAIL, LipoBEN, Lipo-SS-BEN, or their combinations at a constant molar ratio equal to the ratio of their $IC_{50}$. The following molar ratios were used: Lipo-SS-BEN: TRAIL 1,372: 1; and Lipo-SS-BEN: TRAIL 19,600: 1. Cell viability was measured by MTS assay as described above. Results were analyzed by CompuSyn software (ComboSyn, Inc. Paramus, NJ) to quantitatively determine whether the combination treatment was synergistic [261].

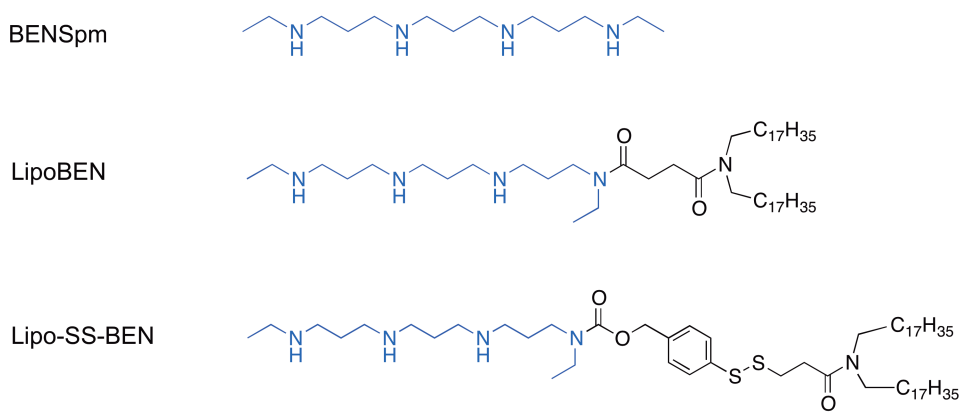


**Figure 11.** Structure of BENSpm and its lipid derivatives.

## 3.3 Results and Discussion

We have previously proposed that BENSpm can serve as a suitable building block of cationic lipids and polymers that can function dually as gene delivery vectors and active pharmacologic agents targeting dysregulated polyamine metabolism in cancer. To that end, we reported synthesis of a lipid derivative of BENSpm (LipoBEN,

Figure 11) and demonstrated its ability to deliver genes in vitro [269]. The cytotoxic effects of BENSpm result, in part, from inducing polyamine catabolic enzymes such as SSAT. Here we measured whether the SSAT inducing capability is preserved in LipoBEN by measuring SSAT activity in human breast cancer cells MDA-MB-231 (Figure 12). The results show that modification of BENSpm with the lipid moiety results in the loss of its SSAT-inducing activity. This result motivated the present study and provided a strong rationale for adopting a prodrug approach to the synthesis of BENSpm-based gene delivery vectors.

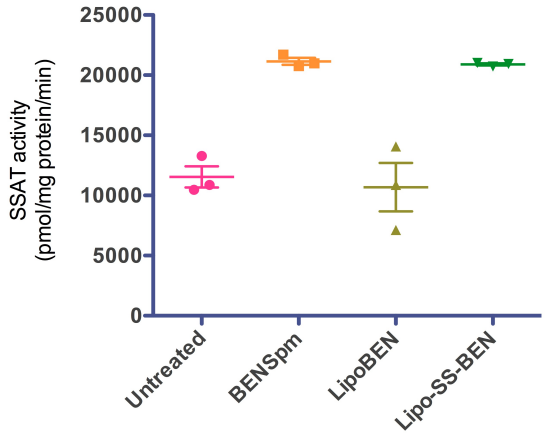


**Figure 12.** SSAT induction by BENSpm and its lipid derivatives. MDA-MB-231 cells were treated with $IC_{50}$ dose of indicated sample for 72 h. Results are shown as mean pmol of $N^1$-acetylspermidine/mg of protein/min ± SD, n=3. One-way ANOVA with Tukey's multiple comparison test ($p < 0.05$ untreated vs BENSpm, untreated vs Lipo-SS-BEN, and LipoBEN vs Lipo-SS-BEN).

### 3.3.1. Synthesis of Lipo-SS-BEN prodrug

We have considered multiple prodrug strategies in our approach. Ester prodrugs are widely used in drug design because of easy degradation by ubiquitous plasma

esterases or chemical hydrolysis. Prodrug strategies for amine drugs like BENSpm, however, are limited by the high stability of amide bonds. For dual-functioning BENSpm-based gene delivery vectors, spatiotemporal considerations of the prodrug activation were crucial. Successful gene delivery requires the delivery vector to remain intact until the DNA is transported into the target cell. Therefore, enzymatically activated amine prodrug approaches, such as carbamates and N-acyloxyalkyl derivatives, in which activation typically occurs in the plasma, were not considered suitable. Other strategies that limit prodrug activation to intracellular enzymes, such as peptide spacers activated by lysosomal cathepsins [276], were excluded because of the unfavorable intracellular location of the activation (lysosomal activation and release of DNA is considered premature). Functional groups like β-aminoketones, N-Mannich bases, and enaminones offer easy nonenzymatic hydrolytic transformation of amine drugs from their prodrug forms [277-279]. The possible ways to control spatiotemporal localization of the activation in these approaches are limited. However, it is well established that disulfide reduction is localized predominantly to the cytoplasm and nucleus, which is highly beneficial for gene delivery [262, 280-284]. Based on these considerations, we selected reducible dithiobenzyl carbamate linker [285, 286] to synthesize Lipo-SS-BEN prodrug that can be activated by intracellular thiolysis of the disulfide bond (Scheme 3).

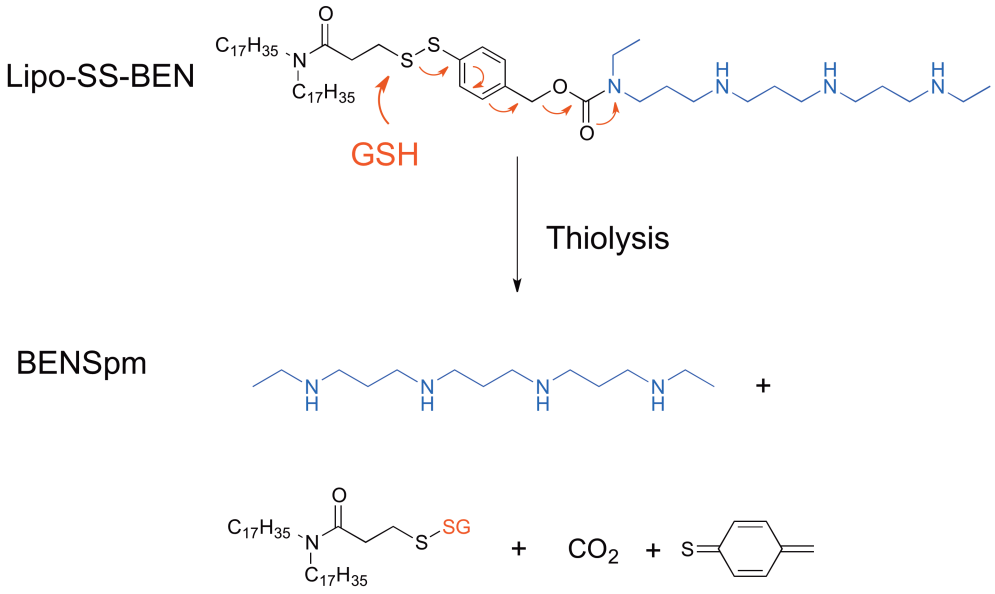


**Scheme 3.** Mechanism of thiolytic activation of Lipo-SS-BEN.

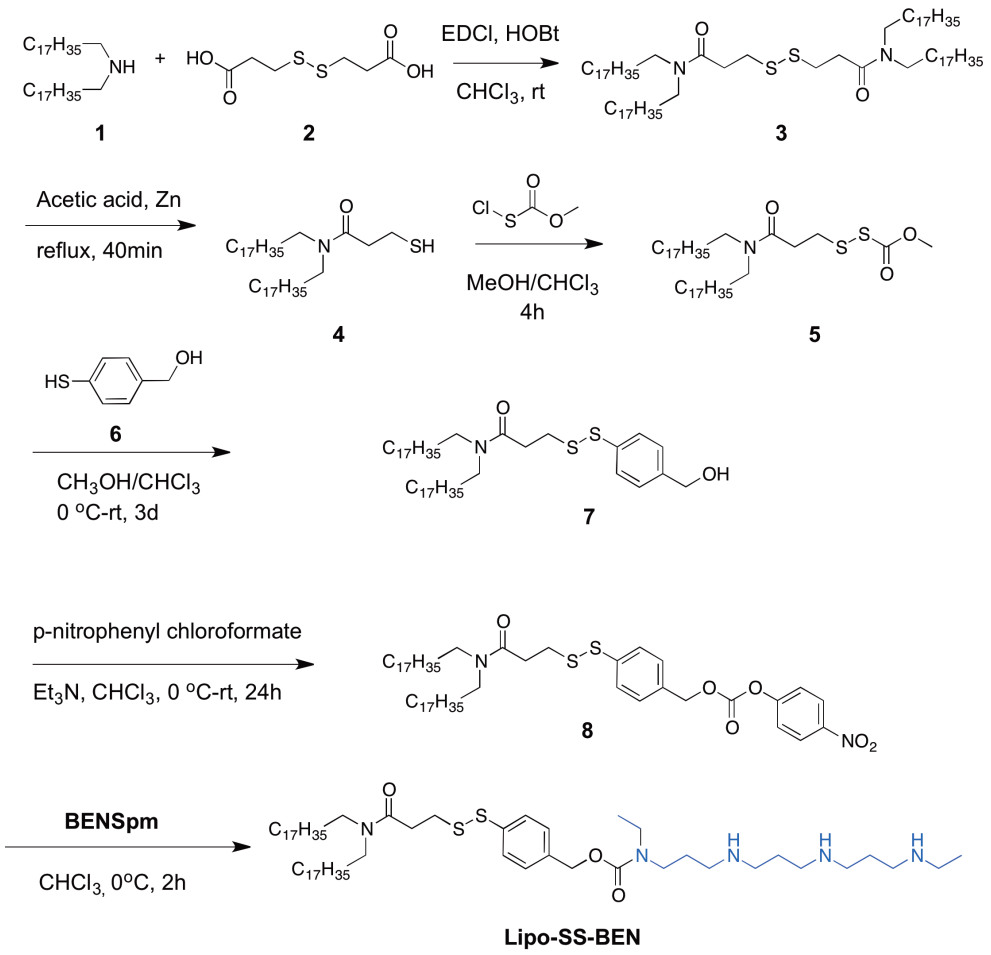


**Scheme 4.** Synthesis of Lipo-SS-BEN prodrug.

The target compound Lipo-SS-BEN was synthesized using a six step synthesis, depicted in Scheme 4. Despite the four amines in BENSpm, a single product Lipo-SS-BEN was detected by ESI-MS and TLC. ESI-MS of the reaction mixture gave the expected m/z 1018.97 and 510.26 peaks, corresponding to m/z $(M + H)^+$ and $(M + 2H)^{2+}$ of Lipo-SS-BEN (Figure 13a). Excess BENSpm (MW 244.26) was seen at m/z $(M + H)^+$ and $(M + 2H)^{2+}$ 245.47 and 123.33 in Figure 13a. Purification of Lipo-SS-BEN was confronted with difficulties caused by easy decomposition during drying due to

susceptibility to disulfide-disulfide exchange reactions. Purification of the reaction mixture by silica gel chromatography gave the expected Lipo-SS-BEN in the eluent. Isolated Lipo-SS-BEN was neutralized with 5 M acetic acid and the solvent was removed to give the desired compound as acetate salt mixed with ammonium acetate. The ammonium acetate could be removed slowly under reduced pressure but some decomposition was still observed (Figure 13b, c).

Finally, we confirmed that, due to steric effects, it was the terminal and not the internal amine of BENSpm that was substituted in Lipo-SS-BEN. The purified Lipo-SS-BEN was reacted with $Boc_2O$ to give fully Boc-protected compound **9** (Scheme 5). Reductive degradation of **9** with DTT gave tri-Boc-protected BENSpm **10**. The $^{1}H$ NMR and $^{13}C$ NMR of compound **10** were found to agree with the known NMR spectra of 3,7,11-tri-Boc BENSpm reported in our previous study [269]. This result confirmed that the location of BENSpm substitution in Lipo-SS-BEN shown in Figure 11 and Scheme 4 is correct. We have also attempted synthesis of Lipo-SS-BEN by reaction of **8** with **10**, but this approach failed due to decomposition of compound **9** during Boc deprotection with TFA.

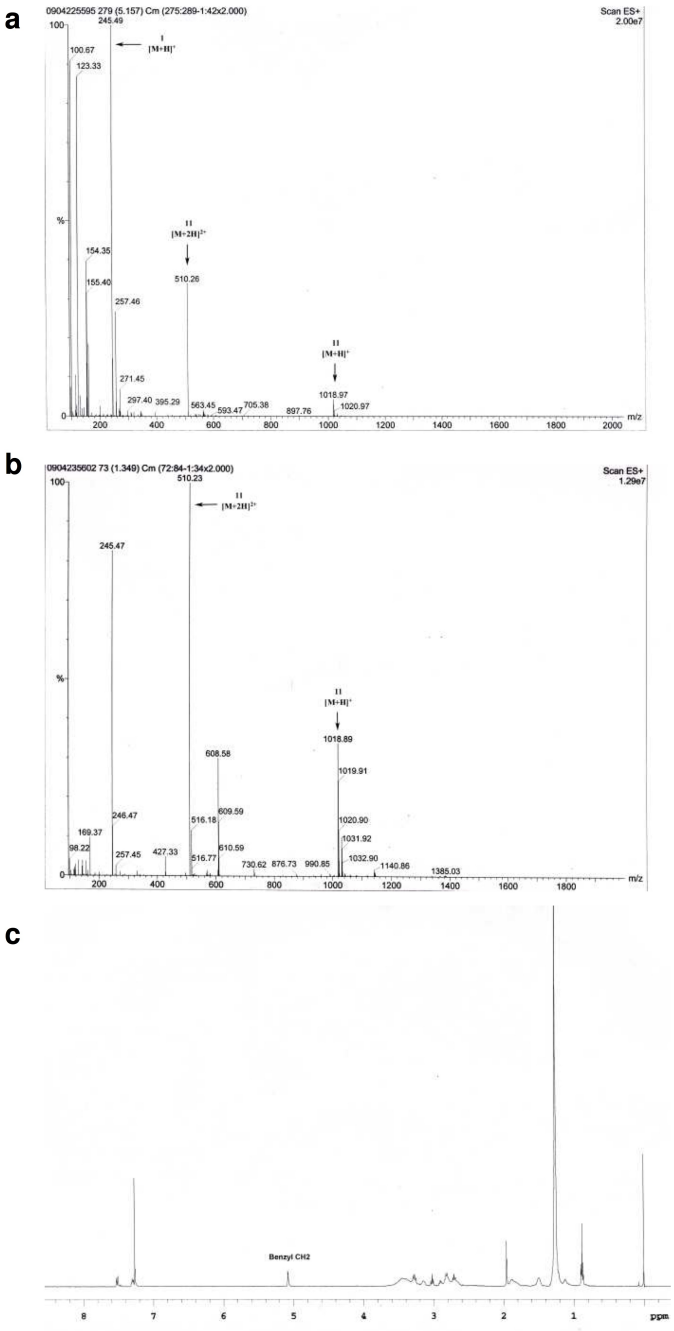


**Figure 13.** ESI-MS and $^{1}H$ NMR spectra of Lipo-SS-BEN prodrug. (a) ESI-MS of unpurified Lipo-SS-BEN after reaction of **8** with BENSpm. (b) ESI-MS of Lipo-SS-BEN after purification. (c) $^{1}H$ NMR of Lipo-SS-BEN in $CDCl_3$.

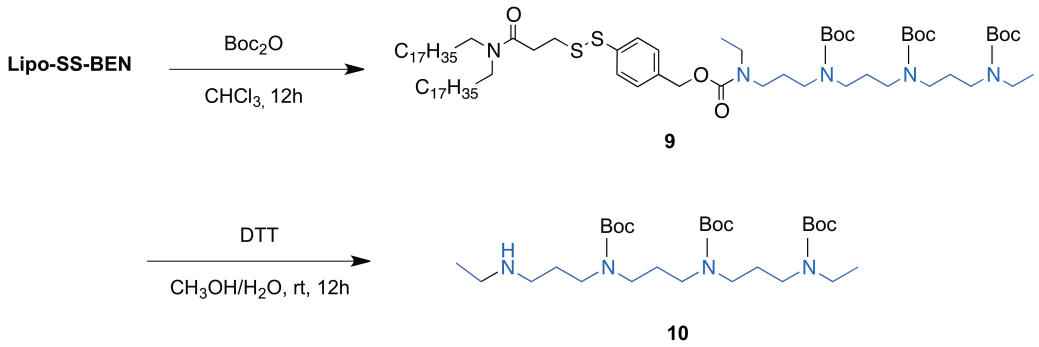


**Scheme 5.** Synthesis and degradation of compound **9**.

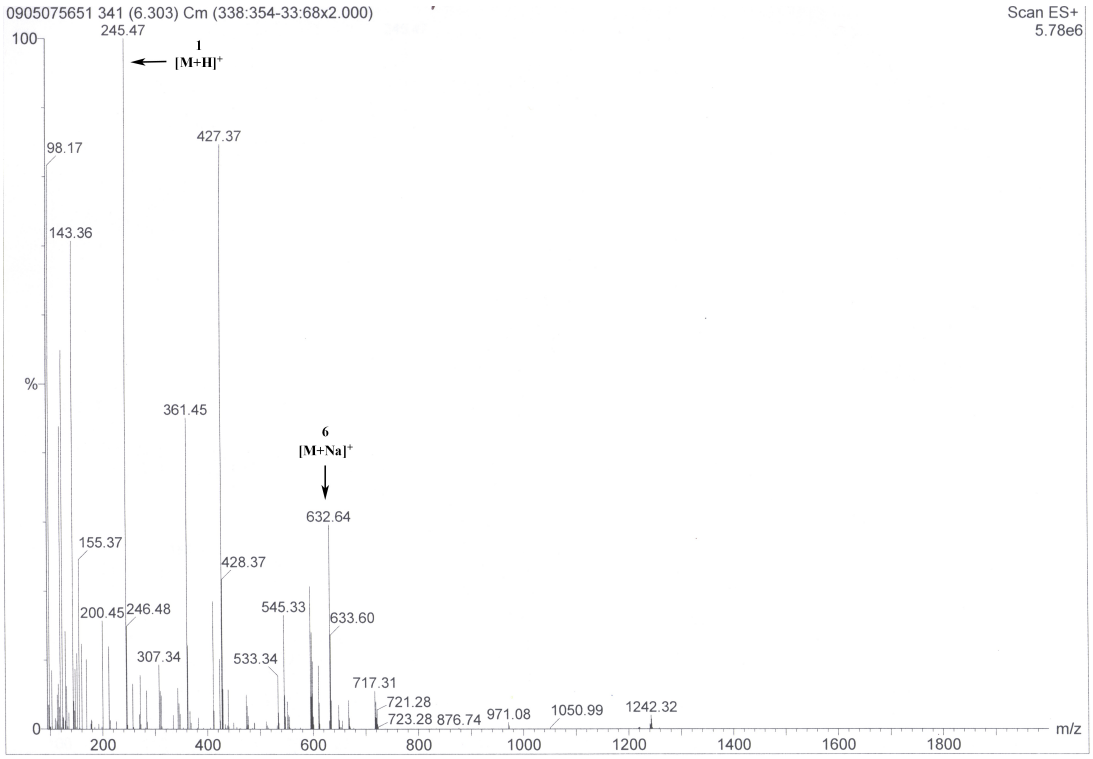


**Figure 14.** ESI-MS after reductive degradation of Lipo-SS-BEN.

3.3.2. Reductive release of BENSpm from Lipo-SS-BEN and restoration of SSAT inducing activity

Intracellular reduction or thiolytic breakage of the disulfide in Lipo-SS-BEN by GSH is expected to lead to an unstable p-mercaptobenzyl urethane intermediate,

followed by a breakdown via 1,6-elimination and decarboxylation, and ultimately result in the regeneration of the original BENSpm molecule and a GSH-conjugated lipid [287, 288]. For success of our approach, it was necessary to verify that Lipo-SS-BEN is transformed to free BENSpm following cleavage of the disulfide bond. Lipo-SS-BEN was therefore treated with excess of a strong reducing agent (100 mM DTT) in PBS at 37 °C, and progress of the reaction was monitored by TLC and ESI-MS for 24 h. The TLC showed complete disappearance of Lipo-SS-BEN after 10 min of treatment with DTT and appearance of a mixture of intermediates that disappeared after 4 h (not shown). ESI-MS analysis shown in Figure 14 confirmed the TLC results by showing complete decomposition of Lipo-SS-BEN and release of BENSpm as indicated by the disappearance of the peak at 1018 and appearance of the peak at 632.64, corresponding to m/z $[M + Na]^+$ of regenerated compound **4** (MW 609.58) and the peaks of free BENSpm shown at m/z $(M + H)^+$ and $(M + 2H)^{2+}$ at 245.47 and 123.33. The activation of the Lipo-SS-BEN prodrug and release of functional BENSpm was subsequently confirmed in MDA-MB-231 cells by demonstrating restored SSAT-inducing activity when compared with nondegradable LipoBEN (Figure 12). This result clearly suggests that the dithiobenzyl carbamate linker is cleaved in the intracellular environment and that BENSpm is released in its active form.

**Table 3.** Cytotoxicity of TRAIL, BENSpm and its derivatives in MDA-MB-231.

| Sample | $IC_{50}$ [a] μM |
|---|---|
| BENSpm | 91.4 ± 37.6 |
| Lipo-SS-BEN | 21.4 ± 2.9 |
| LipoBEN | 6.84 ± 0.69 |
| TRAIL | 0.0051 ± 0.2 |

[a] $IC_{50}$ values were determined by MTS assay after 120 h treatment

3.3.3. Decreased toxicity of Lipo-SS-BEN and synergistic enhancement of TRAIL activity

Toxicity of cationic vectors is a major concern in their use in gene delivery. We expected that degradability of Lipo-SS-BEN will not only restore BENSpm activity as shown above but also will result in decreased toxicity of the lipid. We measured the toxicity using MTS assay in MDA-MB-231 cells (Table 3). The results confirmed that Lipo-SS-BEN is significantly less toxic than the nondegradable LipoBEN. Similar results were observed also in MCF-7 cells, where LipoBEN showed $IC_{50}$ = 1.40 ± 0.40 μM while Lipo-SS-BEN showed decreased toxicity with $IC_{50}$ = 17.2 ± 1.9 μM. Our results confirm previous studies that cationic lipids and polymers degradable by intracellular disulfide reduction exhibit reduced toxicity compared to nondegradable analogues [289-291]. The fact that Lipo-SS-BEN had lower $IC_{50}$ than the parent BENSpm is a reflection of the general toxicity of cationic lipids and not a result of enhanced antiproliferative activity of

BENSpm as suggested by similar SSAT-inducing activity of Lipo-SS-BEN and BENSpm (Figure 12).

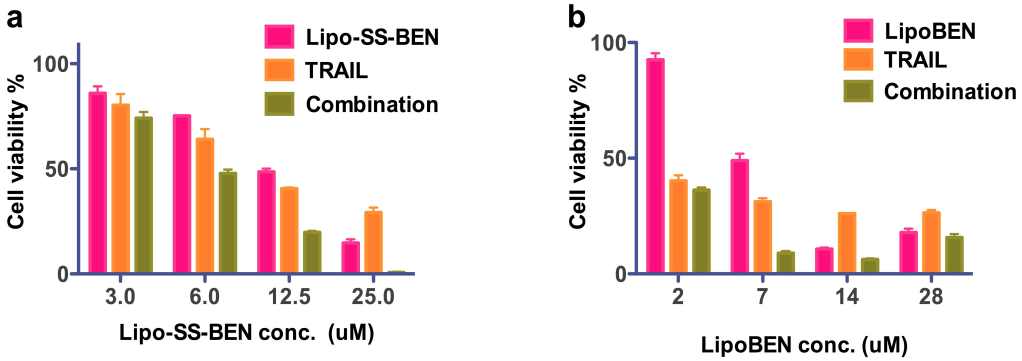


c

| Doses in combination | | CI value |
|---|---|---|
| Lipo-SS-BEN (μM) | TRAIL (ng/mL) | |
| 3 | 3 | 1.32 |
| 6 | 6 | 1.13 |
| 12.5 | 12.5 | 0.88 |
| 25 | 25 | 0.15 |

d

| Doses in combination | | CI value |
|---|---|---|
| LipoBEN (μM) | TRAIL (ng/mL) | |
| 2 | 12.5 | 0.68 |
| 7 | 25 | 0.23 |
| 14 | 50 | 0.35 |
| 28 | 100 | 1.53 |

**Figure 15.** Effect of (a) Lipo-SS-BEN or (b) LipoBEN on antiproliferative activity of TRAIL in MDA-MB-231 cells and the calculated CI value for combination of TRAIL with (c) Lipo-SS-BEN or (d) LipoBEN.

The main objective of this study was to design BENSpm-based lipids capable of functioning dually as (i) gene delivery vectors and (ii) active anticancer agents targeting dysregulated polyamine metabolism in cancer. As described in Chapter 2, BENSpm showed strong synergistic effect with TRAIL in MDA-MB-231 cells. Thus it was important to investigate if the Lipo-SS-BEN prodrug retained the synergism with TRAIL. To allow determination of synergy using the Chou-Talalay method, all TRAIL combination experiments were performed at constant BENSpm lipid: TRAIL ratios (Figure 15) determined from the ratios of the $IC_{50}$ values of the individual agents. Four

doses were used in serial dilutions covering the activity range of LipoBEN, Lipo-SS-BEN, and TRAIL, and the fraction of killed cells ($f_a$) was determined by MTS assay. CI value was calculated by the Chou-Talalay method using CompuSyn software [264]. As described in Chapter 2, the parent BENSpm enhances activity of the TRAIL protein in triple-negative breast cancer cells MDA-MB-231, with CI values less than 0.04 across the entire studied $f_a$ range. We then evaluated whether the enhancing effect of BENSpm on TRAIL activity is preserved in Lipo-SS-BEN (Figure 15a and c). Combination treatment with Lipo-SS-BEN and TRAIL was indeed more effective than either of the agents alone, but the calculated CI values were higher than in the case of BENSpm/TRAIL combination, indicating a weaker synergism and a simple additive effect at lower $f_a$ range. A similar outcome was obtained when the cells were treated with LipoBEN/TRAIL combination (Figure 15b and d). We hypothesize that the transition from a strong synergism in BENSpm/TRAIL treatment to a weaker synergism and even more additive effect of the BENSpm lipids is the result of nonspecific toxicity associated with the cationic lipids and not a specific effect of BENSpm on polyamine metabolism. The effect of the nonspecific lipid toxicity is prominent even in Lipo-SS-BEN despite its degradability. We propose that, in order to take full advantage of the BENSpm/TRAIL synergism that is based on a specific mechanism of action of BENSpm on the polyamine metabolism, toxicity of the BENSpm-based delivery vectors will have to be decreased even beyond the decrease achieved with Lipo-SS-BEN.

**Table 4.** Hydrodynamic diameter and zeta potential of Lipo-SS-BEN/DNA (N/P 20) and LipoBEN/DNA (N/P 8) complexes.

| Sample | Size (nm) | Zeta (mV) |
|---|---|---|
| Lipo-SS-BEN | 98.6 ± 0.9 | 30.9 ± 3.1 |
| LipoBEN | 86.2 ± 0.8 | 41.0 ± 1.1 |

3.3.4. Evaluation of DNA complexes of Lipo-SS-BEN.

The ability to efficiently deliver genes is an important requirement for the dually functioning BENSpm-based delivery vectors. We have therefore conducted preliminary studies to determine their ability to deliver reporter gene *in vitro*. We first confirmed the ability of LipoBEN and Lipo-SS-BEN to condense DNA using EtBr exclusion assay (Figure 16a). Both Lipo-SS-BEN and LipoBEN efficiently condensed DNA, while the parent BENSpm showed poor condensation ability with only 20% decrease in fluorescence intensity at N/P 8. LipoBEN showed a more efficient DNA condensing ability as indicated by the fact that full DNA condensation was achieved at N/P < 2, while N/P 5 was required in the case of Lipo-SS-BEN.

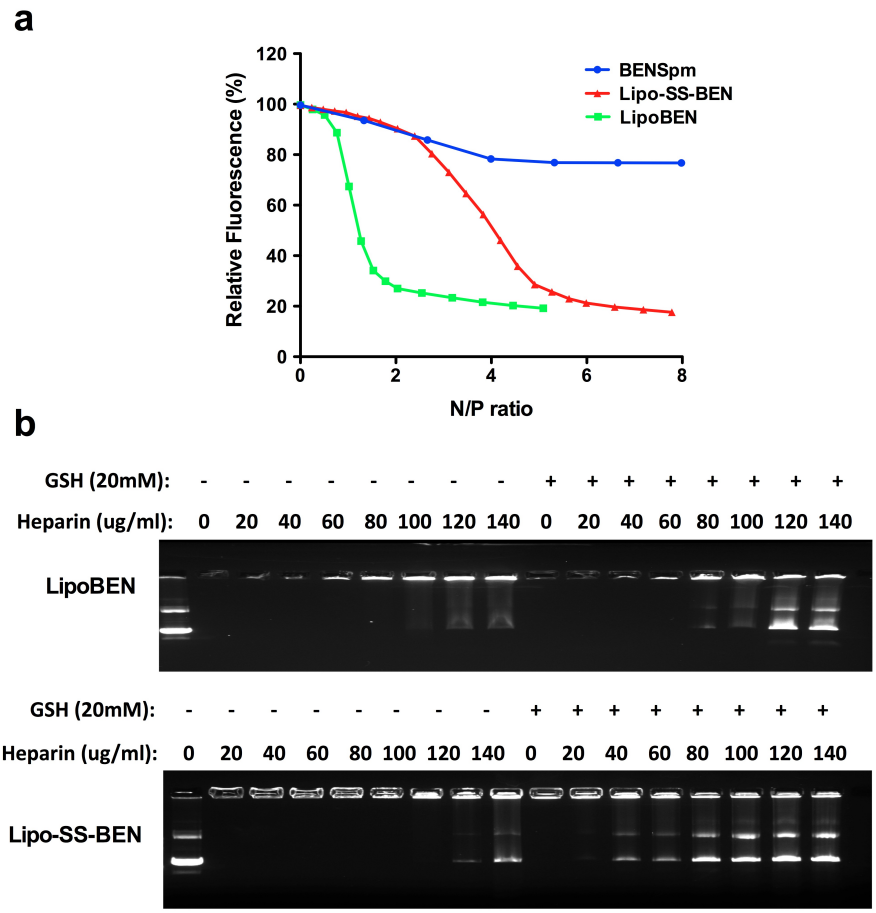


**Figure 16.** DNA condensation and reduction-triggered DNA release from Lipo-SS-BEN complexes. (a) DNA condensation by BENSpm, LipoBEN and Lipo-SS-BEN assessed by EtBr exclusion assay. (b) Effect of disulfide reduction on susceptibility of Lipo-SS-BEN/DNA complexes to polyelectrolyte exchange reactions with heparin. LipoBEN/DNA (N/P 8) and Lipo-SS-BEN (N/P 20) were treated with increasing concentration of heparin either alone or in combination with 20 mM GSH.

We expect that the intracellular cleavage of the disulfide bond in Lipo-SS-BEN should be mediated by thiol/disulfide exchange reactions with small redox molecules like GSH. The reduction is expected not only to release the active form of BENSpm but also to facilitate release of the DNA from Lipo-SS-BEN/DNA complexes. Cellular GSH is predominantly present in the cytoplasm (1-11 mM), which is also the principal site of

GSH biosynthesis [292-294]. However, nuclear GSH concentrations are typically even higher and can reach up to 20 mM [295-297]. As shown above, the reduction of the disulfide bond in Lipo-SS-BEN resulted in the release of BENSpm. The effect of disulfide reduction on the DNA release was investigated by incubating Lipo-SS-BEN/DNA and control LipoBEN/DNA complexes with 20 mM GSH and by analyzing the concentration of heparin required to destabilize the complexes and release free DNA (Figure 16b). The control nonreducible LipoBEN/DNA complexes were stable in the absence of GSH up to 100 μg/mL heparin. At heparin concentrations 100 μg/mL and above, signs of free DNA were observed but most of the DNA was confined to the start of the gel. In the reducing environment of 20 mM GSH, first signs of DNA release from the LipoBEN/DNA complexes were observed at 80 μg/mL heparin. Strong responsiveness to reducing conditions was observed for Lipo-SS-BEN/DNA complexes, suggesting that the employed prodrug strategy not only results in the release of an active form of BENSpm but also facilitates DNA release from the complexes. We predict that the fact that cancer cells often exhibit elevated levels of GSH will further increase the effectiveness of the thiolytically activated gene delivery vector [282]. No DNA release was observed in oxidizing conditions up to 120 μg/mL heparin, while only 40 μg/mL heparin was required to cause DNA release in the reducing conditions of 20 mM GSH.

Initial transfection activity of the BENSpm-based DNA complexes was determined in a panel of three cell lines using luciferase reporter plasmid (Figure 17). DOTAP/DNA complexes were used as controls. DNA complexes of the nondegradable LipoBEN showed consistently higher transfection activity than bioreducible Lipo-SS-

BEN/DNA complexes in all three cell lines. As expected, transfection of BENSpm/DNA complexes was several orders magnitude lower than transfection of any of the BENSpm lipid complexes across all tested N/P ratios. Overall, transfection of the Lipo-SS-BEN complexes showed a stronger dependence on the N/P ratio, in particular in the B16F10 and MDA-MB-231 cells. Between the lowest and highest tested N/P ratio, the transfection of Lipo-SS-BEN complexes increased 192-, 15-, and 6,760-fold in the B16F10, MCF-7, and MDA-MB-231 cells, respectively. For comparison, the corresponding increases for LipoBEN complexes were 4-, 6-, and 270-fold. The strong N/P dependence is likely the result of premature disulfide breakage in Lipo-SS-BEN. It suggests that Lipo-SS-BEN may be partly degraded already before cell uptake by extracellular thiols, thus requiring larger lipid excess to achieve comparable transfection as LipoBEN complexes. Differences among the three cell lines are likely the result of different amounts of secreted thiols from different cells as suggested previously [298].

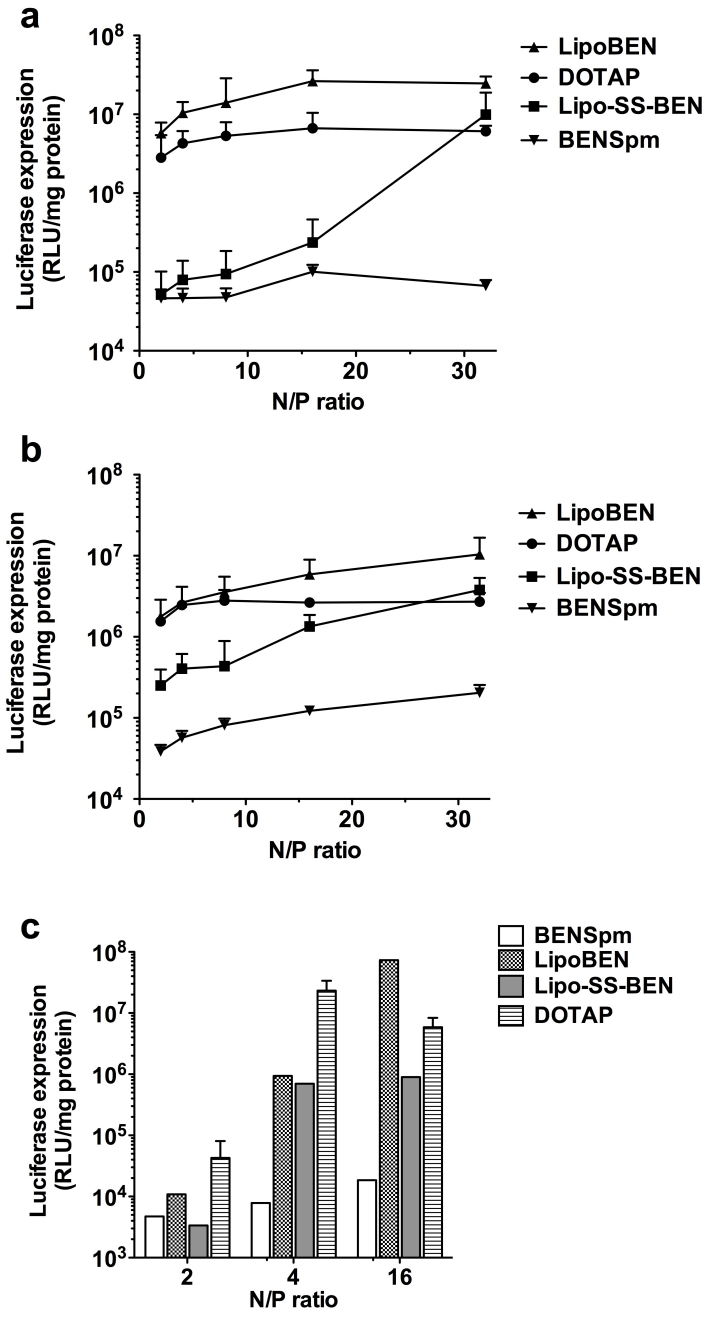


**Figure 17.** Transfection activity of BENSpm and its lipid derivatives in (a) B16F10 cells, (b) MCF-7 cells, and (c) MDA-MB-231 cells. Results are expressed as luciferase expression in RLU/mg of protein (mean ± SD, n=4).

## 3.4 Conclusions

We described synthesis of degradable BENSpm prodrug capable of functioning dually as a gene delivery vector and an active anticancer agent targeting dysregulated polyamine metabolism in cancer. The used dithiobenzyl carbamate linker in the Lipo-SS-BEN prodrug is cleavable by thiolysis, which leads to the release of free BENSpm and restoration of SSAT-inducing activity of BENSpm. BENSpm demonstrated a strong synergy with TRAIL in triple negative breast cancer cells MDA-MB-231. Although Lipo-SS-BEN also enhanced TRAIL activity, the results were confounded by nonspecific lipid-related toxicity that diminished the synergistic enhancement that originated in the specific mechanism of action of BENSpm on the polyamine pathway.

In conclusion, we demonstrated that BENSpm could serve as a suitable building block for the design of gene delivery vectors with dual functionality. However, in order to take full advantage of the synergism based on BENSpm, general toxicity associated with the lipid delivery vector will have to be further decreased, even beyond the reduction achieved with Lipo-SS-BEN. Another drawback of the Lipo-SS-BEN is the instability of the lipid vector in extracellular environment, as demonstrated by decreased transfection efficiency compared with LipoBEN. In all, this approach shines light on our future endeavor towards reduced vector toxicity and more stable linker system of the prodrug design.

# CHAPTER 4

# DENDRITIC POLYGLYCEROL WITH POLYAMINE SHELL AS A POTENTIAL MACROMOLECULAR PRODRUG AND GENE DELIVERY VECTOR

## 4.1 Introduction

In Chapter 3, we have synthesized biodegradable lipid prodrug (Lipo-SS-BEN) based on BENSpm using thiolytically sensitive dithiobenzyl carbamate linker [265, 269]. We have demonstrated that Lipo-SS-BEN can fulfill its function as a gene delivery vector while at the same time exhibit anticancer effect after intracellular cleavage of the dithiobenzyl carbamate linker and release of BENSpm. However, toxicity caused by the cationic lipid combined with extracellular instability of the linker hindered further development of the system.

In order to address the problems with toxicity and linker stability, we have chosen dendritic polyglycerol (PG) as a safe component onto which to conjugate BENSpm. PG is a dendritic polyol that exhibits thermal and oxidative stability, high water solubility and negligible toxicity at cellular level [299, 300]. It can be synthesized by a simple one-step ring-opening polymerization, which allows for large-scale production. The presence of a large number of surface functional groups (64 surface hydroxyls for PG with molecular weight 5 kDa) renders PG ideal for surface functionalization [301, 302]. Our previous studies with BENSpm-based gene delivery vectors suggested that BENSpm has to be released from the vector in order to exert its full therapeutic effect via modulation of the polyamine pathway in cancer cells [265]. Selection of a biodegradable linker therefore

became critical for the success of BENSpm-based gene delivery vectors with dual functionality. Instead of the dithiobenzyl carbamate linker cleavable by disulfide reduction with glutathione described in Chapter 3, we have chosen a carbamate linker cleavable by hydrolysis to conjugate BENSpm to PG. Carbamates are widely used in the design of amine-containing prodrugs because of an easy enzymatic cleavage or hydrolysis of the bond [210, 302-304]. Moreover, a recent report suggested that conjugates of PG with oligoamines similar to BENSpm could be enzymatically cleaved by the action of lipases [302]. Thus, we proposed to design BENSpm-conjugated PG prodrug via carbamate linkage (PG-BEN), which we expected to be beneficial for both BENSpm release and gene delivery functions.

## 4.2 Materials and Methods

### 4.2.1. Materials

Plasmid DNA containing luciferase reporter gene (gWiz-Luc) was from Aldevron (Fargo, ND). Dulbecco's Modified Eagle Medium (DMEM), Dulbecco's Phosphate Buffered Saline (PBS), RPMI 1640 Medium, Fetal Bovine Serum (FBS) and RNase A (10 mg/mL) were from Thermo Scientific (Waltham, MA). Eagle's Minimum Essential Medium (EMEM) was from Corning (Manassas, VA). MDA-MB-231-luc2 cells and B16F10-luc2 cells stably transfected with firefly luciferase gene (luc2) were purchased from Caliper (Hopkinton, MA). HepG2 cell line and B16F10 cell line were purchased from American Type Culture Collection (ATCC; Manassas, VA). MDA-MB-231 cell line was a kind gift from Dr. Jing Li, Karmanos Cancer Institute (Detroit, MI). Anti-luciferase siRNA (pGL4) (antisense sequence 5′-GAAGUGCUCGUCCUCGUCCUU-3′) and

negative control siRNA (ON-TARGET plus Non-targeting siRNA #1) were purchased from Dharmacon (Lafayette, CO). Dendritic PG (5 kDa) was purchased from Johannes Gutenberg-Universität Mainz, Germany. Lipofectamine™ RNAiMAX transfection reagent was purchased from Invitrogen (Grand Island, NY). Norspermine, phenyl chloroformate (99%), and heptafluorobutyric acid (HFBA) were from Alfa Aesar (Ward Hill, MA). Pyridine (DriSolv®, anhydrous) was from EMD Millipore (Billerica, MA). 4-(Dimethylamino)-pyridine (DMAP) and benzoylated dialysis tubing (nominal molecular weight cut-off 2,000 Da) were from Sigma-Aldrich (St. Louis, MO). Hydrogen chloride (5-6 N solution in 2-propanol) was from Acros Organics (Fair Lawn, NJ). All other reagents and chemicals were obtained from Fisher Scientific or VWR International unless otherwise noted.

### 4.2.2. Cell culture

B16F10 mouse melanoma cells were cultured in DMEM supplemented with 10% FBS. MDA-MB-231 human breast cancer cells and B16F10-luc2 cells were cultured in RPMI supplemented with 10% FBS. HepG2 cells and MDA-MB-231-luc2 cells were cultured in EMEM supplemented with 10% FBS. All cells were kept at 37 °C in incubator with 5% $CO_2$.

### 4.2.3. Polymer analysis

NMR spectra were recorded on Mercury-400 MHz Spectrometer and chemical shifts ($\delta$) were expressed in ppm. IR spectra were recorded using JASCO FT/IR 4200 spectrometer (Easton, MD). Weight-average molecular weight ($M_w$) and polydispersity

index (PDI) of polymers were determined by Size Exclusion Chromatography (SEC) using Viscotek GPCmax chromatography system equipped with a refractive index detector and a light scattering detector. The columns used were single-pore AquaGel$^{TM}$ columns (cat# PAA-202 and PAA-203, PolyAnalytik, London, ON, Canada). OmniSEC software was used for chromatographic data processing. Sodium acetate buffer (0.3 M, pH 5) was used as the mobile phase at a flow rate of 0.3 mL/min. Amine content in the PG derivatives was determined by elemental analysis of C, H, N, Cl (Atlantic Microlabs Inc., Norcross, GA). The chemical formula of PG was assumed to be $(C_3H_5O_2)_n$-$(OH)_{64}$ for the calculation of amine content in PG-BEN, norspermine-conjugated PG (PG-Nor) and amine-terminated PG (PG-$NH_2$) using the results of elemental analysis.

4.2.4. Synthesis of PG derivatives

*Synthesis of PG phenyl carbonate and PG-$NH_2$.* PG phenyl carbonate and PG-$NH_2$ were synthesized following published procedures [302, 305]. PG (5 kDa, 1 g, 13.5 mmol OH-groups) was dissolved in 8 mL anhydrous pyridine and added dropwise into phenyl chloroformate (2.44 g, 15.6 mmol) solution in 20 mL pyridine. The reaction mixture was stirred for 16 h in ice bath. Additional chloroform and water were added at the end of the reaction until the formed solid product was dissolved. The organic layer was extracted three times with chloroform and then dried with $MgSO_4$. The solution was then concentrated and dialyzed against chloroform to give the PG phenyl carbonate (2.71 g, yield 93.1%).

PG-$NH_2$ was synthesized by a conversion of hydroxyl groups to amine groups following published procedure [302, 305]. Briefly, PG (5.2 g, 70.72 mmol OH-groups)

was dissolved in pyridine (40 mL), and a solution of methanesulfonyl chloride (9.3 g, 81.3 mmol) in pyridine (7 mL) was added dropwise. The reaction mixture was kept in ice bath and stirred for 16 h. Excess amount of ice was then added to the reaction mixture until a yellow solid precipitated. The solid product was washed with water three times, dissolved and dialyzed against acetone to give a brown product of PG methanesulfonate ester (8.94 g, yield = 83.5%). PG methanesulfonate ester (8.94 g, 59.05 mmol methanesulfonate groups) was dissolved in DMF (100 mL) and $NaN_3$ (17.93 g, 275.84 mmol) was added. The suspension was then kept at 60 °C for 3 days. The reaction mixture was filtered and the yellowish filtrate was concentrated by rotary evaporator. The raw product was then dissolved and dialyzed against $CHCl_3$ to give the final product of PG-$N_3$ (5.75 g, yield = 99%).

PG-$N_3$ (5.75 g, 58.54 mmol $N_3$-group) was dissolved in THF (60 mL) and triphenylphosphine ($PPh_3$, 15.34 g, 58.54 mmol) and $H_2O$ (5 mL) were added. The reaction mixture was kept stirring for 16 h while 50 mL of water was added dropwise during the reaction. The mixture was then concentrated by rotary evaporation, followed by extraction with $CHCl_3$. The aqueous layer was concentrated to dryness by rotary evaporator, then dissolved and dialyzed against methanol to give a brown viscous PG-$NH_2$ (3.94 g, 93%). $^1$H-NMR (400 MHz, MeOD): $\delta$ = 3.3-3.8 (m, CH and $CH_2$ of PG), 2.52-3.18 (m, -$CH_2$-$NH_2$ of PG).

*Synthesis of PG-BEN and PG-Nor.* Solution of 200 mg PG phenyl carbonate (0.93 mmol phenyl carbonate group) in pyridine (15 mL) was added dropwise to a mixture of BENSpm (1.5 g, 6.14 mmol) or norspermine (1.75 g, 9.3 mmol) and DMAP

(1.1 mg, 0.009 mmol) in pyridine (10 mL) at 0 °C. The reaction mixture was then kept under reflux for 2 days. Solvent was removed by rotary evaporator and the concentrate was dialyzed against methanol to give the final product PG-BEN (230 mg, yield 67.6%) or PG-Nor (130 mg, yield 50.3 %). Free amine groups on PG-BEN and PG-Nor were then converted into HCl salt by first dissolving PG-BEN or PG-Nor in ethanol and then precipitating out the corresponding salt by adding HCl (1.2 eq., 5-6 N HCl in 2-propanol). The precipitate was then washed three times with ethanol and dried in vacuum to afford the final product PG-BEN.HCl and PG-Nor.HCl. $^{1}$H-NMR (400 MHz, $D_2O$) of PG-BEN: $\delta$ = 1.17 (**a1**, $CH_3$-$CH_2$-NH-), 1.29 (**a2**, $CH_3$-$CH_2$-N-(COO-PG)-), 1.60-2.22 (**c1**,**c2**, -$CH_2$-$CH_2$-NH-), 2.90-3.47 (**b1**,**b2**, -$CH_2$-NH-), 2.89-4.03(PG). $^{1}$H-NMR (400 MHz, $D_2O$) of PG-Nor: $\delta$ = 1.91 (**a1**, -$CH_2$-$CH_2$-NH-COO-), 2.11 (**a2**, -$CH_2$-$CH_2$-NH-), 2.94-3.70 (**b1**, **b2**, -$CH_2$-NH-), 2.94-4.33 (m, CH and $CH_2$ of PG).

4.2.5. Buffering capacity

Buffering capacity of the synthesized PG derivatives was determined by acid-base titration as previously described (Chen et al., 2009). Briefly, 6 mL solution of each PG derivatives (10 mM total amine concentration) was adjusted to pH 4.0 by 1M HCl, and then the solution was titrated to pH 11.0 using 0.1 M NaOH and 1M NaOH. The pH after each addition of NaOH was recorded by pH meter (Fisher Science Education$^{TM}$, Fisher Scientific, Pittsburgh, PA).

4.2.6. EtBr exclusion assay

The ability of the polycations to condense gWiz-Luc DNA or negative control siRNA into polyplexes was determined by EtBr exclusion assay by measuring the changes in EtBr/DNA or EtBr/siRNA fluorescence. DNA and siRNA solutions at a concentration of 20 μg/mL in 10 mM HEPES buffer (pH 7.4) were mixed with EtBr (1 μg/mL) and fluorescence was measured and set to 100% using an excitation wavelength of 540 nm and an emission wavelength of 590 nm. Fluorescence readings were taken following a stepwise addition of PG derivatives solution, and the condensation curve for each PG derivative was constructed. PEI (25 kDa, branched) was used as positive control.

4.2.7. Agarose gel retardation assay

Twenty μL polyplexes of PG derivatives or PEI with 20 μg/mL gWiz-Luc DNA at different N/P ratios (0.5, 1, 2, 4, 8, 16) were loaded onto 0.8% agarose gel containing 0.5 μg/mL EtBr. Samples were run for 60 min at 120V in 0.5× TBE running buffer. For siRNA polyplexes, 20 μL polyplexes of PG derivatives or PEI with 20 μg/mL negative control siRNA at different N/P ratios (0.25, 0.5, 1, 2, 4, 8) were loaded onto 2% agarose gel containing 0.5 μg/mL EtBr and run for 30 min at 75V. The gels were visualized under UV illumination on a KODAK Gel Logic 100 Imaging System.

4.2.8. Particle size and zeta potential of polyplexes

Hydrodynamic diameters and zeta potentials of PG derivatives/DNA polyplexes were determined using ZetaPlus Particle Size and Zeta Potential analyzer (Brookhaven Instruments). Scattered light was detected at 90° angle and 25 °C. Polyplexes were

prepared at desired N/P ratios (4, 8, 16, 32) by adding a pre-determined amount of polycation to the solution of plasmid DNA in 10 mM HEPES (pH 7.4) to achieve a final DNA concentration of 20 μg/mL (300 μL). For PG derivatives/siRNA polyplexes, optimized N/P ratio in transfection experiment was used (N/P ratios: PG-BEN/siRNA 7, PG-Nor/siRNA 10, PG-$NH_2$/siRNA 24). The polyplexes were incubated for 30 min at room temperature and then diluted to 1.5 mL for size and zeta potential measurement. Mass of 325 per one phosphate group of nucleic acid was used in the calculations.

### 4.2.9. Atomic force microscopy

For atomic force microscopy (AFM), DNA polyplexes of PG derivatives and PEI were prepared at N/P ratio of 16 with DNA concentration of 20 μg/mL in 10 mM HEPES buffer (pH 7.4). AFM images were acquired by Nanoimaging Core Facility (College of Pharmacy, University of Nebraska Medical Center).

### 4.2.10. Heparin displacement assay for siRNA polyplexes

The relative stability of PG derivatives/siRNA polyplexes was tested by measuring siRNA release from the polyplexes in the presence of heparin. All siRNA polyplexes were prepared at w/w ratio of 7 at siRNA concentration of 20 μg/mL. Polyplexes were allowed to stabilize for 25 min and then the polyplex solutions were incubated with heparin for 10 min at different concentrations (0, 10, 20, 40, 80, 160, 240 μg/mL). Samples were then loaded onto 2% agarose gel and run for 45 min at 75 V. The gel was visualized by a KODAK Gel Logic 100 Imaging System.

4.2.11. RNase digestion assay for siRNA polyplexes

siRNA polyplexes of PG derivatives were incubated with increasing amount of RNase A for 30 min at 37 °C. Polyplexes were prepared as described in heparin displacement assay. To inactivate the RNase, samples were further incubated for 30 min at 70 °C. Heparin (240 μg/mL) was then added to each sample for complete release of intact siRNA from the polyplexes. Twenty μL sample was loaded onto 2% agarose gel containing 0.5 μg/mL EtBr and run for 30 min at 75 V. The gel was visualized using a KODAK Gel Logic 100 Imaging System.

4.2.12. Transfection

All DNA transfections were conducted in 48-well plates. Cells were seeded at a density of 40,000 cells/well 24 h prior to transfection. On the day of transfection, cells were incubated with the polyplexes (2.35 μg/mL DNA) in media containing 10% FBS. After 4 h incubation, polyplexes were completely removed and the cells were maintained in complete culture medium for 24 h prior to measuring luciferase expression. The medium was discarded and the cells were lysed in 100 μL of 0.5× cell culture lysis reagent buffer (Promega, Madison, WI) for 30 min. To measure the luciferase content, 100 μL of 0.5 mM luciferin solution was automatically injected into each well of 20 μL of cell lysate and the luminescence was integrated over 10 s using Synergy 2 Microplate Reader (BioTek). Total cellular protein in the cell lysate was determined by the bicinchoninic acid (BCA) protein assay using calibration curve constructed with standard bovine serum albumin solutions (Pierce, Rockford, IL).

Transfection activity was expressed as relative light units (RLU)/mg cellular protein ± SD of triplicate samples.

For siRNA transfection, B16F10-luc2 cells and MDA-MB-231-luc2 cells were seeded at a density of 40,000 cells/well or 50,000 cells/well, respectively, in 48-well plates one day before transfection. Polyplexes and positive control Lipofectamine RNAiMAX lipoplexes were formed in serum-free Eagle's Minimum Essential Medium (EMEM) medium (for MDA-MB-231-luc2 cells) and RPMI medium (for B16F10-luc2 cells). PG derivatives and siRNA were mixed at w/w 7 and incubated at room temperature for 20 min before use. Transfections were conducted with 100 nM siRNA for the polyplexes and 10 nM siRNA for the control RNAiMAX lipoplexes. The cells were incubated at 37 °C for 48 h and lysed for assaying luciferase activity. Transfection activity was expressed as the percentage of luciferase expression of untreated cells.

### 4.2.13. Cytotoxicity

Toxicity of polycations was evaluated by MTS assay. The cells were seeded in 96-well microplates at a density of 10,000 cells/well. After 24 h, culture medium was replaced by 200 µL of serial dilutions of a polymer in medium with 10% FBS and the cells were incubated for 24 h. Polymer solutions were aspirated and replaced by a mixture of 100 µL serum-free media and 20 µL of MTS reagent (CellTiter 96® AQueous Non-Radioactive Cell Proliferation Assay, Promega). After 2 h incubation (MDA-MB-231 cells) or 1.5 h incubation (B16F10 and HepG2 cells), the absorbance was measured at a wavelength of 490 nm. The relative cell viability (%) was calculated as

$[A]_{sample}/[A]_{untreated}$ × 100%. The $IC_{50}$ were calculated as the polymer concentration that inhibits growth of 50% of cells relative to untreated cells using GraphPad Prism [263].

### 4.2.14. Polyamine analysis by LC-MS/MS

Intracellular levels of polyamines were quantified using AQUITY UPLC TQD system (Waters, MA) with IntelliStart program built in Masslynx 4.1 software. Ten µg/mL of BENSpm, SPM, SPD, and PUT were dissolved in water: acetonitrile (1: 1) and detected in MRM mode using positive electrospray ionization (ESI+): m/z (parent > daughter) 245.24 > 143.10 for BENSpm; 203.14 > 129.14 for SPM; 146.10 > 112.05 for SPD and 89.09 > 71.95 for PUT. Chromatographic separation was performed using ACQUITY UPLC BEH C18 Column (2.1 x 50 mm, 1.7 µm). A gradient solvent system consisting of 0.2% HFBA in water (solution A) and 0.2% HFBA in acetonitrile (solution B) was used and the gradient was increased from 5 to 95% of B over 5 min at a flow rate of 0.2 mL/min [306]. The polyamines eluted at the following elution times: 2.55 min (BENSpm), 2.44 min (SPM), 2.29 min (SPD) and 1.98 min (PUT). Standard curve for each polyamine was linear within the concentration range from 16 ng/mL to 2 µg/mL (correlation coefficient $r^2$ > 0.96 for all). MDA-MB-231 cells were treated with 2.5 µg/mL BENSpm, 6 µg/mL PG-BEN (equiv. amount of 2.5 µg/mL BENSpm) for 72 h and then lysed in 5% perchloric acid at a concentration of $5\times10^6$ cells/mL. The supernatant of the cell lysate was then used for LC-MS/MS detection of polyamine levels.

### 4.2.15. PG-BEN degradation

BENSpm release from PG-BEN was monitored by both LC-MS/MS and SEC. LC-MS/MS analysis for BENSpm content in cell lysate was conducted following 72 h treatment of MDA-MB-231 with 2.5 µg/mL BENSpm or 6 µg/mL PG-BEN. PG-BEN degradation was also evaluated at extreme conditions following incubation for 48 h at 90 °C in 0.1 M HCl or 0.1 M NaOH solution. Changes in SEC chromatograms of BENSpm and PG-BEN were monitored using conditions described in earlier section (4.2.2).

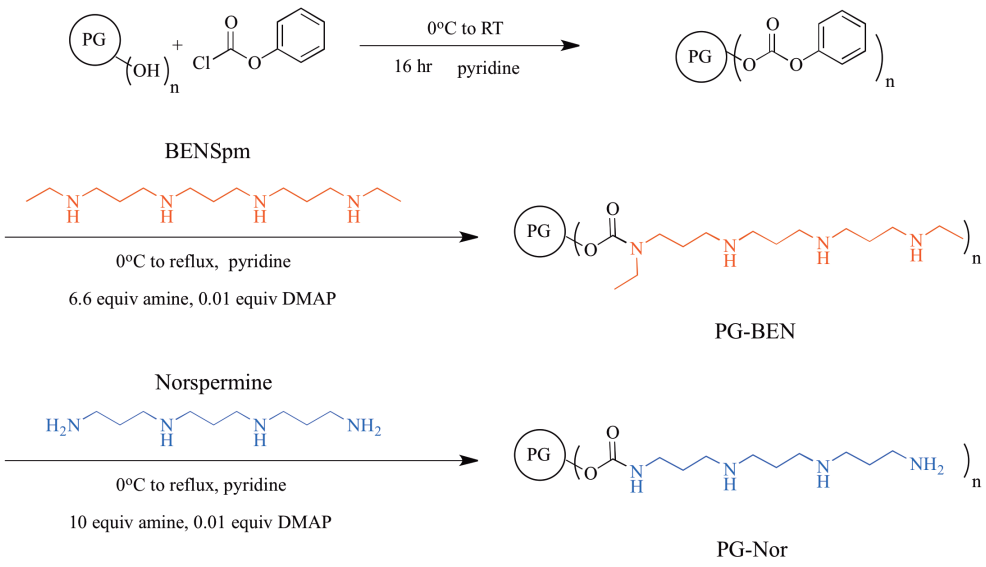


**Scheme 6.** Synthesis of PG-BEN, PG-Nor

## 4.3 Results and Discussion

### 4.3.1 Synthesis and characterization of PG derivatives

PG-BEN and PG-Nor were synthesized following a modified published procedure for the synthesis of PG-oligoamine conjugates (Scheme 6) [302]. Surface hydroxyl groups of PG were first activated using phenyl chloroformate to form PG phenyl

carbonate. This activated form of PG was then reacted with amine groups of BENSpm and norspermine to form PG-BEN and PG-Nor. Because both BENSpm and norspermine have four reactive amines in their structure, there was a possibility of intermolecular cross-linking between multiple PG molecules. Our goal was to minimize the extent of any cross-linking reactions. We have thus used a large excess of BENSpm and norspermine in the reaction. The use of excess polyamine also allowed us to maximize the content of polyamines per PG molecule because of the decreased likelihood that one BENSpm or norspermine molecule would react with multiple hydroxyls in a single PG molecule. PG-$NH_2$ was synthesized as a control polymer for this study, by conversion of the PG surface hydroxyl groups to primary amines (Scheme 7).

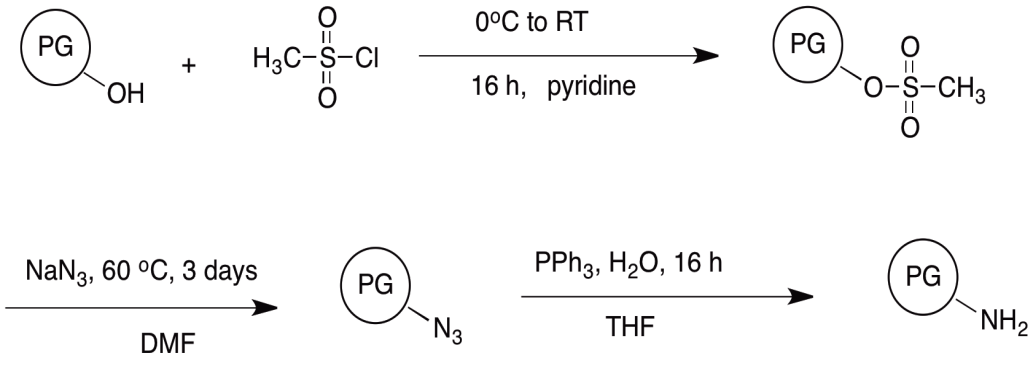


**Scheme 7.** Synthesis of PG-$NH_2$

The FT-IR analysis qualitatively verified successful conjugation of the polyamines to PG (Figure 18a and b). The signal in the IR spectrum of PG-BEN and PG-Nor at 1730-1690 $cm^{-1}$ (C=O stretch) indicated the presence of carbonyl bonds. The signal of PG-BEN, PG-Nor and PG-$NH_2$ at 1650-1515 $cm^{-1}$ (N-H bend) confirmed the presence of amine groups. These results confirmed that BENSpm and norspermine were

successfully conjugated to the surface of PG via carbamate linkage.

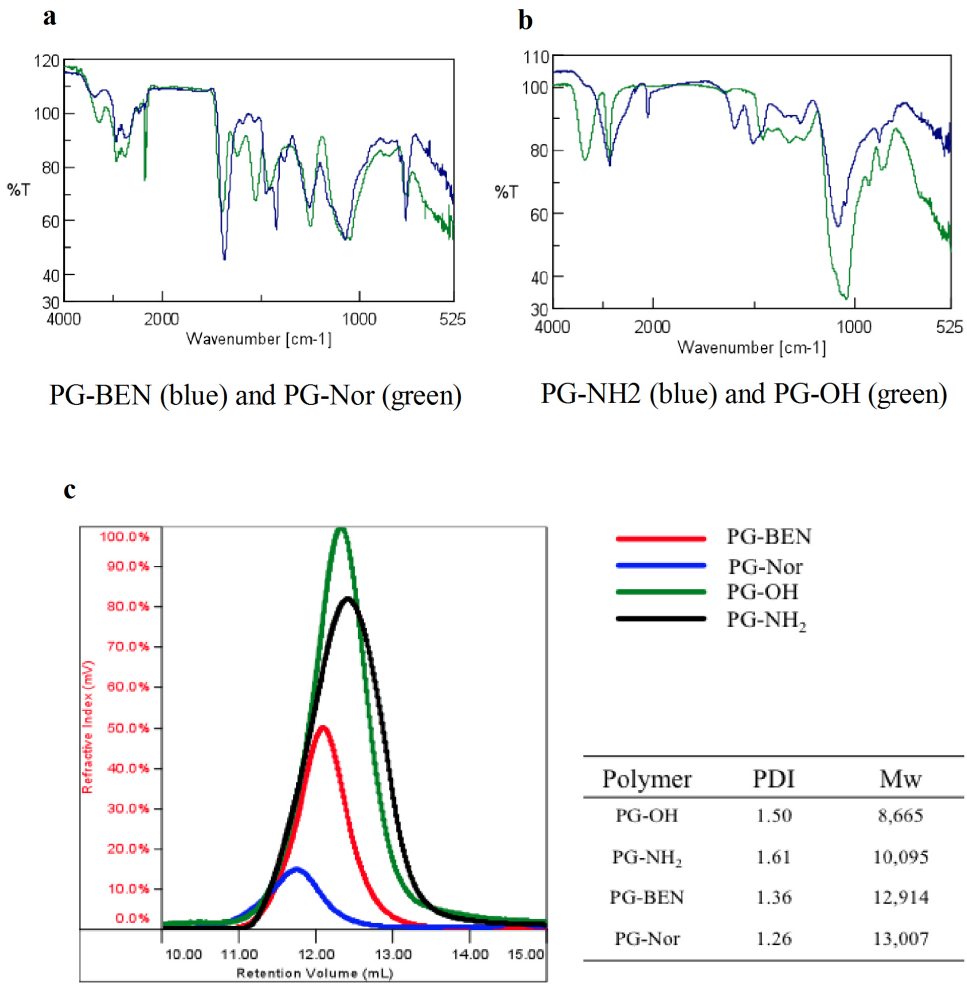


| Polymer | PDI | Mw |
|---|---|---|
| PG-OH | 1.50 | 8,665 |
| $PG-NH_2$ | 1.61 | 10,095 |
| PG-BEN | 1.36 | 12,914 |
| PG-Nor | 1.26 | 13,007 |

**Figure 18.** Characterization of PG derivatives. (a) FT-IR spectra of PG-BEN (blue) and PG-Nor (green). (b) FT-IR spectra of PG-NH2 (blue) and PG (green). (**c**) Size exclusion chromatographs.

SEC was used to confirm that no crosslinking occurred during conjugation of BENSpm and norspermine to PG (Figure 18c). The determined molecular weights were nearly identical for PG-BEN (12.9 kDa) and PG-Nor (13.0 kDa) and represented an almost 4 kDa increase over the parent PG. Narrow PDI and absence of a peak or a

shoulder at lower retention volumes indicated that no significant crosslinking occurred in either of the conjugation reactions.

**Table 5.** Characterization of the synthesized PG derivatives.

| Polymer | Number of Nor or BEN per PG | % of modified PG hydroxyls |
|---|---|---|
| PG-$NH_2$ | -- | 92% |
| PG-Nor | 27 | 42% |
| PG-BEN | 23 | 36% |

We then used elemental analysis (C, H, N, Cl) to determine the amine content in the synthesized PG derivatives. Based on the elemental analysis, we calculated that on average, there were 23 BENSpm molecules and 27 norspermine molecules attached to a single PG molecule (Table 5). These results correspond to 36% and 42% modified PG hydroxyls, respectively. In comparison, direct conversion of the hydroxyls to primary amines in PG-$NH_2$ resulted in 92% hydroxyl conversion (Table 5). Steric hindrance is the most likely explanation for the lower conjugation efficiency in case of BENSpm and norspermine. We then used NMR to analyze whether BENSpm and norspermine were attached to PG via a single amine or via multiple amines on a single polyamine molecule (Figure 19). Taking advantage of the differences in NMR shifts of the terminal methyl in BENSpm after conjugation to PG, we observed that the integral intensities of a1 and a2 were nearly equal (a1: a2 1.00: 1.03). Based on the assumption that BENSpm conjugation to PG mainly occurred at the terminal amine groups, the ratio of a1: a2 suggests that on average, only one terminal amine of BENSpm was attached to

PG. Because of insufficient NMR signal separation, our analysis could not determine whether any non-terminal secondary amines in BENSpm participated in the conjugation to PG. Similar analysis for PG-Nor using signals of the methylenes in β position to the terminal primary amines, led to similar conclusion as suggested by the ratio of the a1: a2 = 1.95: 1.00 (Figure 19).

Strong buffering capacity of polyamine gene delivery vectors has been recognized as an important factor for intracellular trafficking of polyplexes, such as to enhance endosomal escape and to avoid the trafficking to degradative lysosomes[307, 308]. Although the correlation between buffering capacity and enhanced transgene activity is under debate [309, 310], buffering capacity of polyamine vector remains an important property for gene delivery. Here, we measured the buffering capacities of PG derivatives in comparison with PEI (Figure 20). The results of titration curves showed that, at the pH range between 5.0 to 7.4 that corresponds to the extracellular environment and endosomal environment, the buffering capacity of PG-BEN and PG-Nor is stronger than PG-$NH_2$ and PEI. One explanation is that there are different types of amines in the different PG derivatives and PEI ($pK_a$ secondary amine < primary amine), and the protonation of an amine group electrostatically suppresses the protonation of neighboring amines [311], thus leads to the different pattern of titration curves between each PG derivatives and PEI.

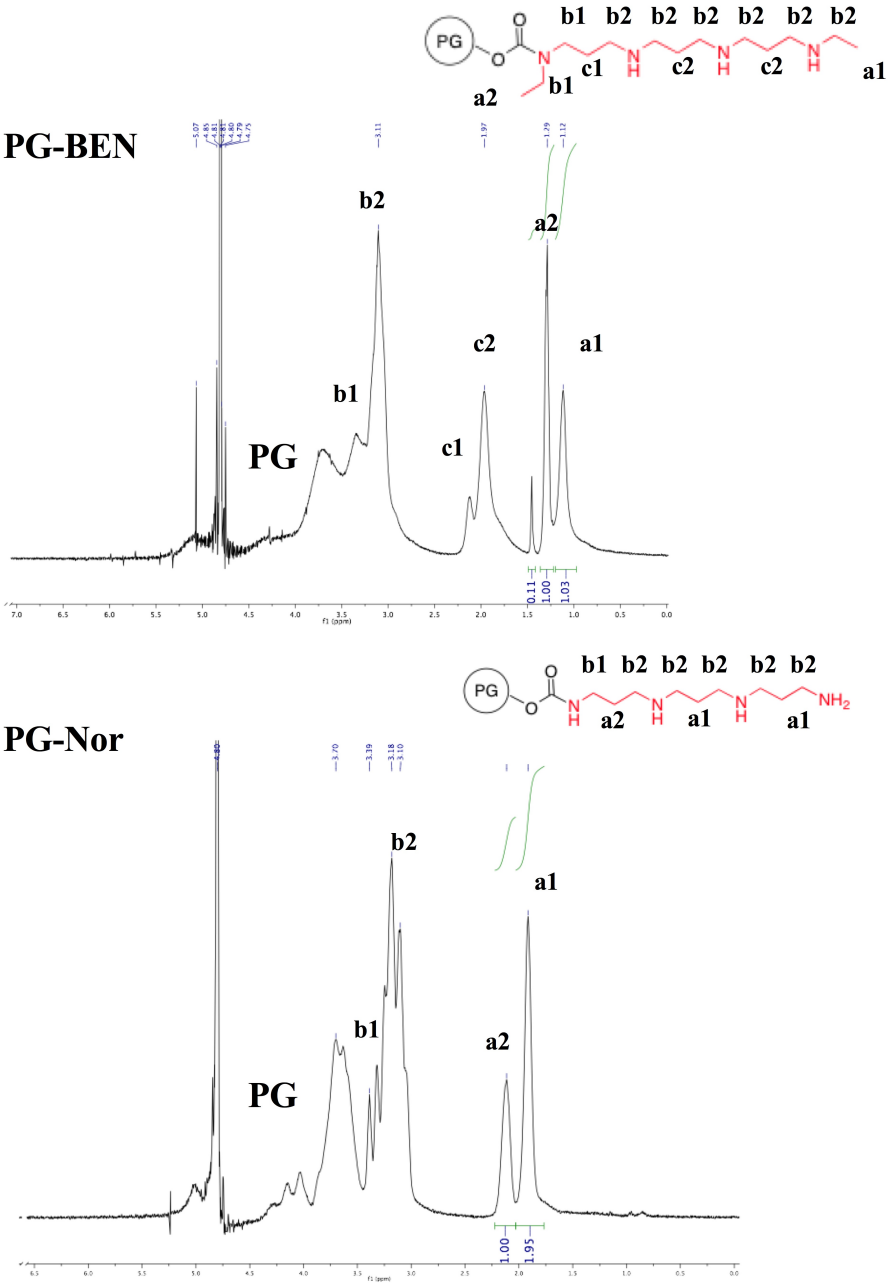


**Figure 19.** $^{1}$H-NMR spectra of PG-BEN (upper panel) and PG-Nor (lower panel). PG peak: CH and $CH_2$ in PG backbone.

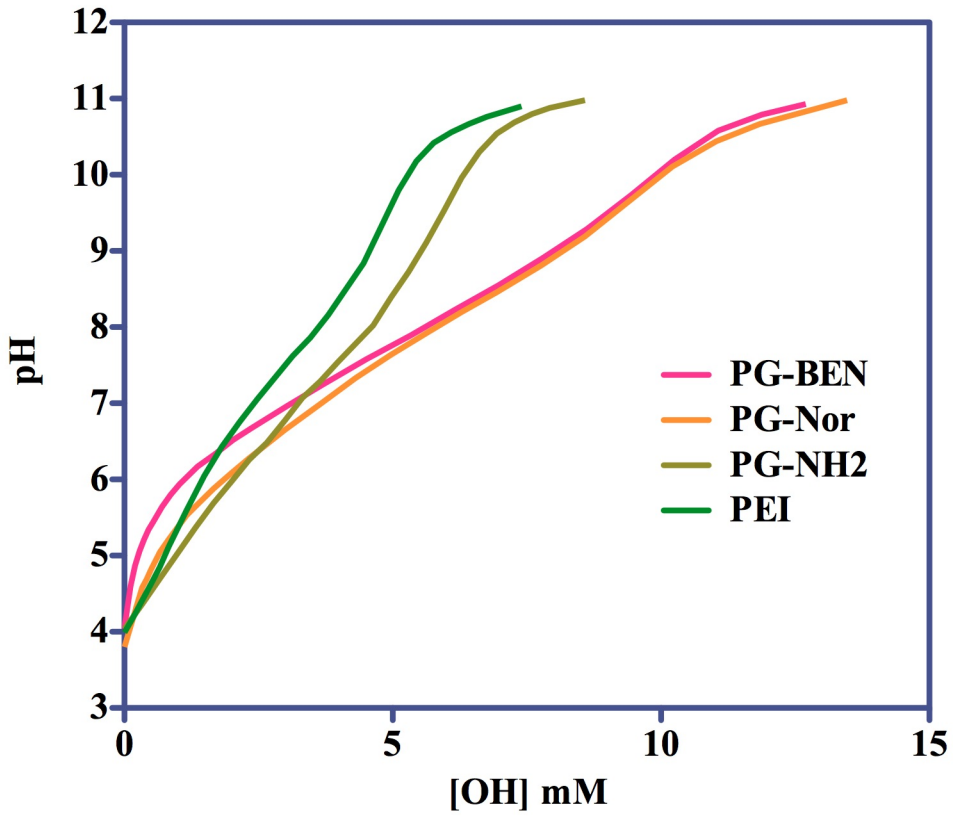


**Figure 20.** Acid-base titration curves of PG derivatives.

4.3.2 DNA/siRNA condensation and polyplex characterization

All the synthesized PG derivatives were able to condense DNA as documented by the results of the EtBr exclusion assay and agarose gel electrophoresis (Figure 21a and b). PG-BEN and PG-Nor were comparably efficient and condensed DNA at N/P ratios above 1. Control PEI required higher N/P ratios to fully condense DNA (N/P > 2), as did PG-$NH_2$ (N/P > 4). The strong DNA condensing ability of PG-BEN and PG-Nor are the result of high surface density of amines in the conjugates. As expected from the ability to condense DNA, all PG derivatives form positively charged polyplexes (Figure

21d). The polyplexes were smaller than 110 nm at all studied N/P ratios as measured by dynamic light scattering (Figure 21c).

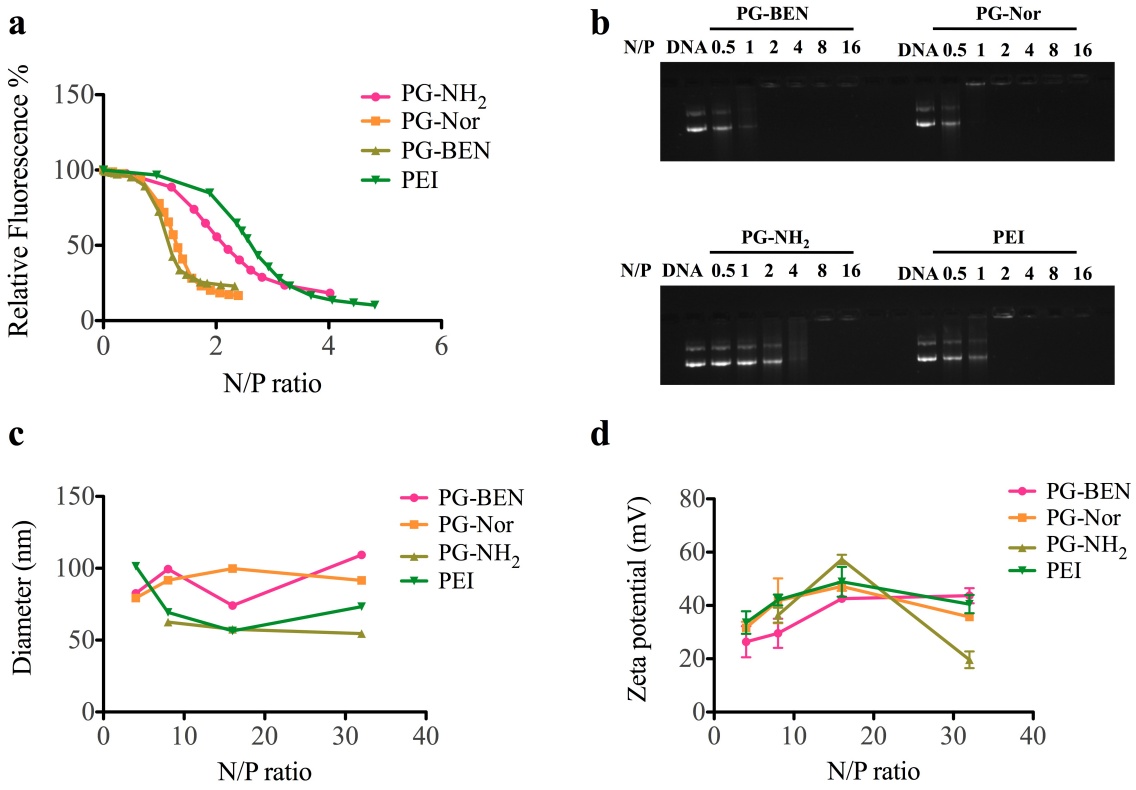


**Figure 21.** Physicochemical characterization of DNA polyplexes of PG derivatives. DNA condensation by (a) EtBr exclusion and (b) agarose gel eletrophoresis of PG derivatives and PEI polyplexes in 10 mM HEPES (pH 7.4); and dependence of (b) hydrodynamic particle size and (c) zeta potential of the polyplexes on different N/P ratios.

AFM was used to study the morphology of the DNA polyplexes. As shown in Figure 22, all polyplexes of PG derivatives were imaged at a constant N/P ratio of 16. PG-Nor/DNA polyplexes showed the most uniform particle sizes around 60-70 nm, with all the polyplexes spherical and homogeneously distributed. Similar result was also observed for PG-BEN/DNA polyplexes, where spherical particles were observed with

sizes around 50-80 nm. Interestingly, one PG-BEN/DNA polyplex showed DNA release on the surface of the particle (indicated by arrow head in Figure 22), demonstrating the need for higher N/P ratio of PG-BEN to achieve complete DNA condensation. PG-$NH_2$/DNA polyplexes showed different morphology than PG-BEN and PG-Nor polyplexes, with DNA release observed for almost all particles. This result indicated the ineffectiveness of PG-$NH_2$ to condense DNA even at N/P ratio of 16. DNA release was also observed from some PEI polyplexes, while the majority of PEI polyplexes were spherical particles with sizes around 40-70 nm. The fact that smaller sizes of polyplexes were observed from AFM than from dynamic light scattering (DLS) is a normal phenomenon that can be explained by the difference of the techniques: in DLS measurement, small polyplexes with weak scattering could be masked by the strong scattering from bigger polyplex aggregates, therefore DLS yielded higher value of particle size than AFM [312].

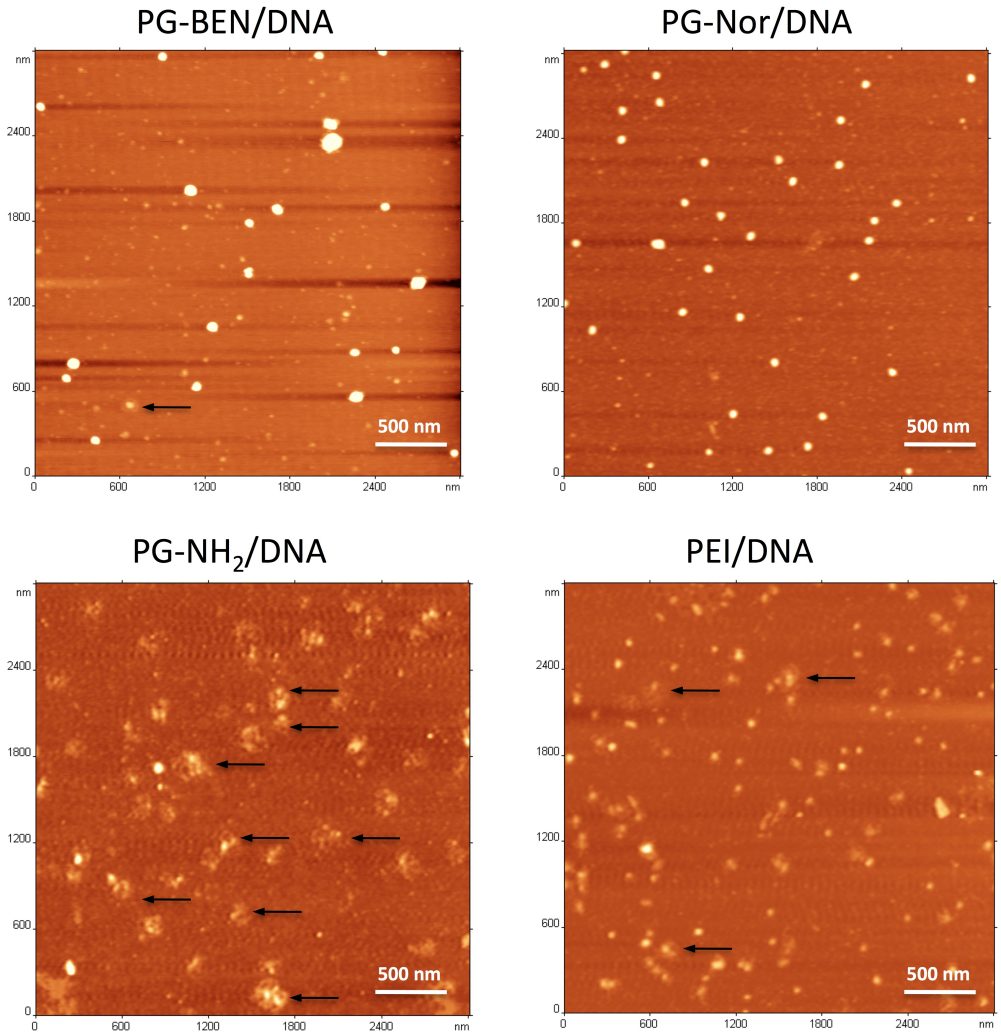


**Figure 22.** AFM images of different DNA polyplexes. All polyplexes were prepared at a N/P ratio of 16. Arrow heads indicate plasmid DNA released from the polyplexes.

Oppositely, although all the PG derivatives were able to sufficiently bind siRNA at lower N/P ratios (N/P ≥ 1 for PG-BEN and PG-Nor; N/P > 2 for PEI and PG-$NH_2$) as shown in EtBr exclusion assay and agarose gel retardation assay (Figure 23a and b), the PG/siRNA polyplexes showed much larger distribution in size and very small positive charge, with zeta potential lower than 10 mV for all polyplexes (Figure 23c and

d). The siRNA polyplexes were further analyzed by heparin replacement assay and RNase digestion assay (Figure 24). As shown in Figure 24 (upper panel), PG-Nor/siRNA polyplexes were the most stable, with dissociation occurred at heparin concentration of 160 μg/mL, which is 8-fold the amount of siRNA presented in the polyplexes. PG-BEN and PG-$NH_2$ polyplexes showed similar stability, with partial release of the siRNA occurred at heparin concentration of 80 μg/mL. These results indicated strong interactions between siRNA and all PG derivatives. However, result from RNase digestion assay showed an opposite trend (Figure 24, lower panel) that PG-$NH_2$ provided better protection for siRNA against RNase A, with complete siRNA degradation occurred at RNase concentration higher than 200 μg/mL. On the other hand, PG-BEN and PG-Nor showed lower protection ability against RNase A, with the complete siRNA degradation observed at RNase concentration higher than 40 μg/mL. This result suggests that, opposite to the ineffectiveness of condensing DNA, PG-$NH_2$/siRNA polyplexes may result in improved knockdown efficiency of the cargo siRNA compared with PG-BEN and PG-Nor polyplexes, due to the improved protection against RNase. These results indicates that, due to the structural difference of siRNA such as lower charge density and higher stiffness compared with DNA [313], PG-BEN and PG-Nor may not be able to fully condense siRNA molecules in comparison with forming DNA polyplexes.

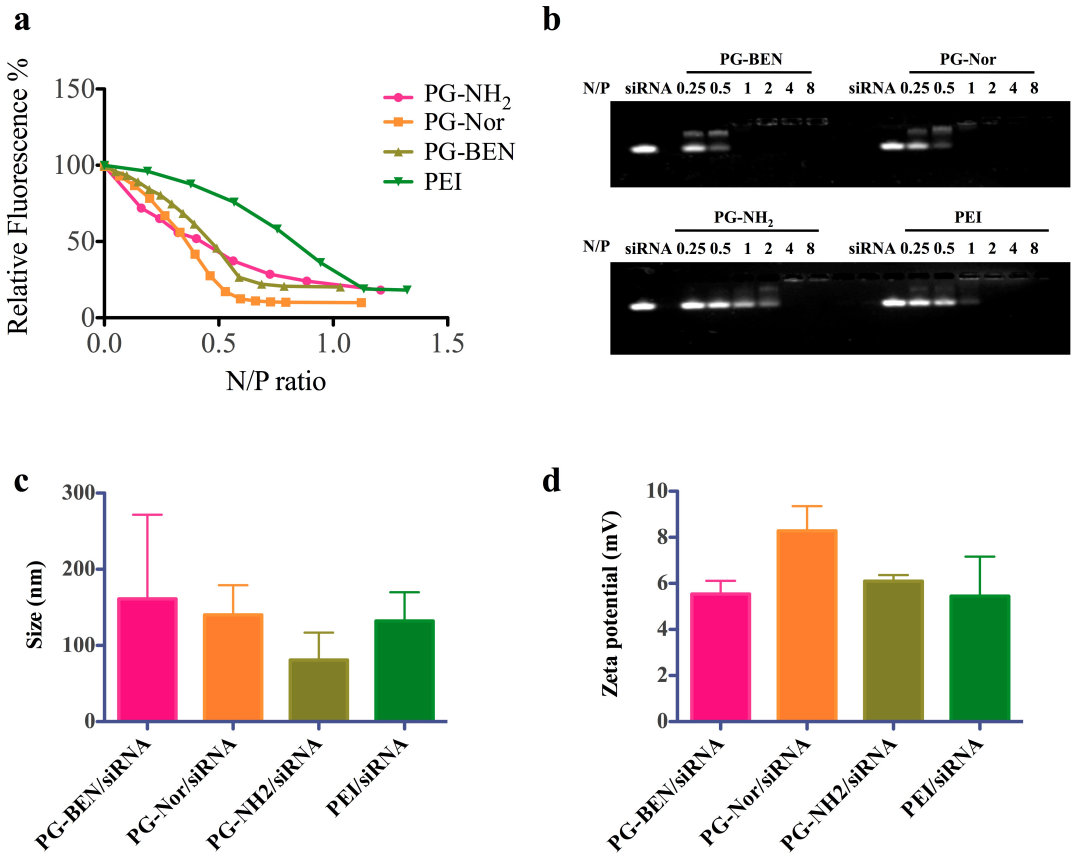


**Figure 23.** Physicochemical characterization of siRNA polyplexes of PG derivatives. (a) EtBr exclusion assay in 10 mM HEPES (pH 7.4); (b) agarose gel retardation assay of siRNA polyplexes at different N/P ratios; (c) hydrodynamic particle size and (d) zeta potential of the polyplexes at fixed N/P ratio (PG-BEN/siRNA 7, PG-Nor/siRNA 10, PG-$NH_2$/siRNA 24).

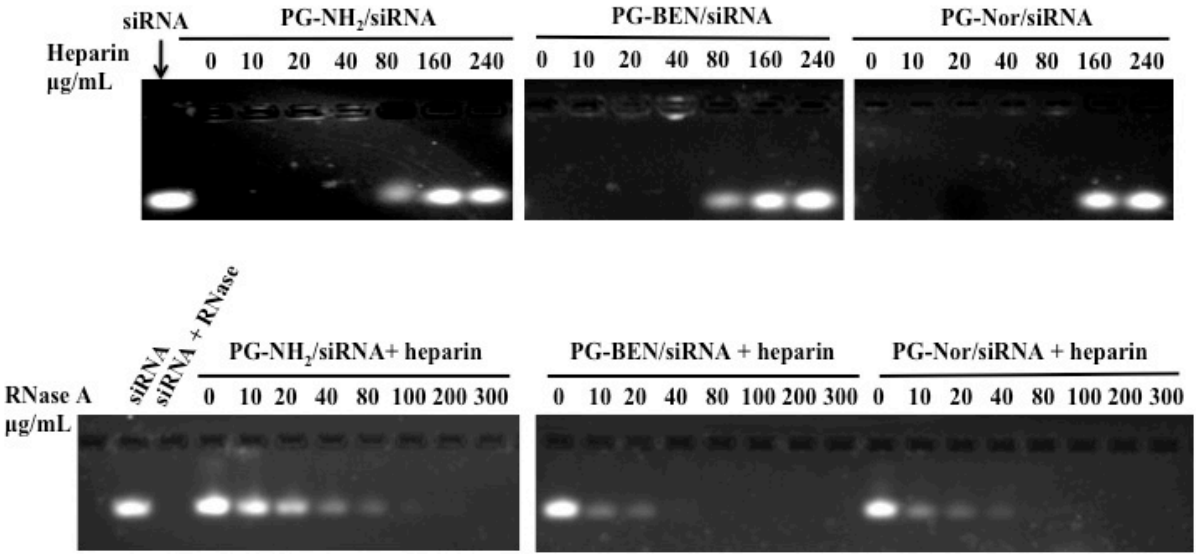


**Figure 24.** Agarose gel electrophoresis of siRNA polyplexes against heparin displacement (upper panel) and recovery of intact siRNA from the polyplexes challenged with RNase A (lower panel). Free siRNA and siRNA treated with RNase A (10 μg/mL) were loaded as references.

### 4.3.3 Transfection

Transfection activity of the PG-BEN and PG-Nor polyplexes was first measured in the presence of 10% FBS in B16F10 cells using luciferase reporter plasmid (Figure 25a). The PG-BEN and PG-Nor polyplexes showed consistently higher transfection activity than PG-$NH_2$ polyplexes. The transfection efficiency of PG-BEN and PG-Nor polyplexes was fully comparable or better than that of the control PEI polyplexes. These results demonstrate that the drug-based PG-BEN conjugate can protect DNA in the presence of serum and facilitate DNA delivery to cells, thus fulfilling its intended function as a gene delivery vector.

Even though PG-BEN and PG-Nor were highly efficient in DNA transfection, they exhibited poor ability to deliver siRNA (Figure 25b and c). Both PG-BEN and PG-Nor

polyplexes with siRNA mediated only negligible levels of silencing (~11%) of the luciferase gene in MDA-MB-231-Luc2 cells. In contrast, PG-$NH_2$ which demonstrated only low DNA transfection was highly active at delivery of siRNA. The levels of luciferase silencing by PG-$NH_2$ approached levels of a specialized commercial siRNA transfection reagent Lipofectamine$^{TM}$ RNAiMAX. This result confirms finding of many previous studies, which show that the properties that make for an efficient DNA delivery agent, are not necessarily the same as those for efficient siRNA delivery agent. It is likely that it is the lower binding affinity of PG-$NH_2$ to nucleic acids as suggested by the requirement for higher N/P ratios to condense DNA (Figure 21a) that is beneficial for siRNA delivery. In contrast, the affinity may not be sufficient to protect DNA and mediate intracellular DNA transport into nucleus [314, 315].

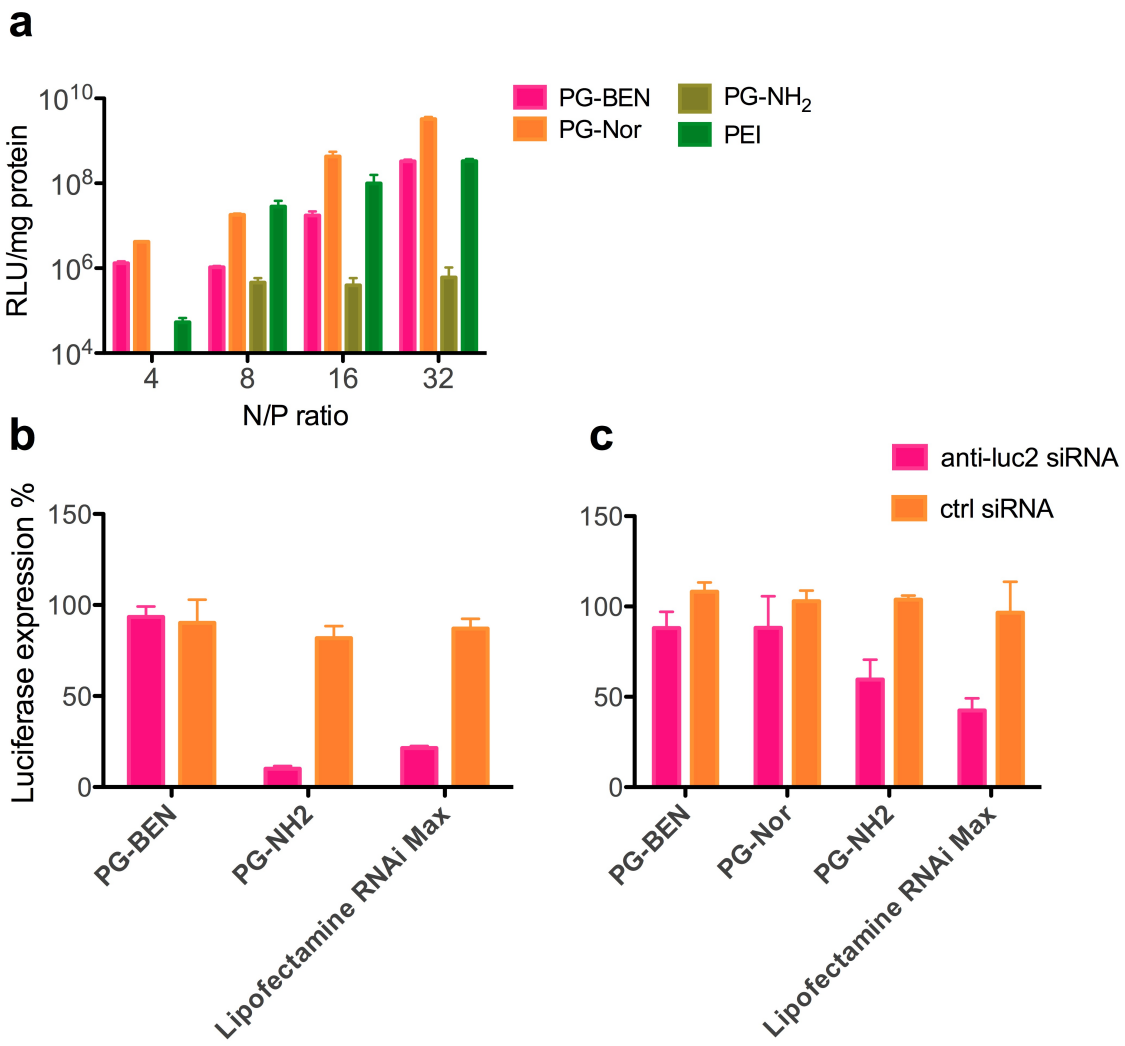


**Figure 25.** Transfection activity of polyplexes. (a) Luciferase gene transfection in B16F10 cells measured 24 h after 4 h incubation of cells with the DNA polyplexes in 10% FBS. Results are shown as mean relative light unit (RLU)/mg protein ± SD (n=3). siRNA silencing of luciferase expression in (b) B16F10-Luc2 cells and (c) MDA-MB-231-Luc2 cells stably expressing the luciferase gene. Results are expressed as percentage of (RLU)/mg protein ± SD (n=4) compared with untreated cells.

### 4.3.4 Cytotoxicity

The cytotoxicity of PG-BEN, PG-Nor and PG-$NH_2$ was tested in MDA-MB-231, B16F10 and HepG2 cells (Figure 26). HepG2 cells have been established as a reliable predictor of human hepatotoxicity and are thus widely used for *in vitro* cytotoxicity testing [316-318]. Because of the anticancer activity of BENSpm, we have tested whether its presence in PG-BEN imparts selective toxicity towards cancer cells by measuring toxicity also in MDA-MB-231 and B16F10 cancer cells. Indeed, PG-BEN was 11-times more toxic towards MDA-MB-231 cancer cells and 3.4-times more toxic towards B16F10 cancer cells than towards HepG2 cells, as determined from the ratios of the respective $IC_{50}$ values. In contrast, control PEI showed almost no selective toxicity towards the two cancer cell lines with its $IC_{50}$ ratios between 1.2 and 1.3. PG-Nor and PG-$NH_2$ demonstrated intermediate selectivity with $IC_{50}$ ratios of 5.2 and 6.1 in MDA-MB-231 and 2.7 and 1.5 in B16F10, respectively.

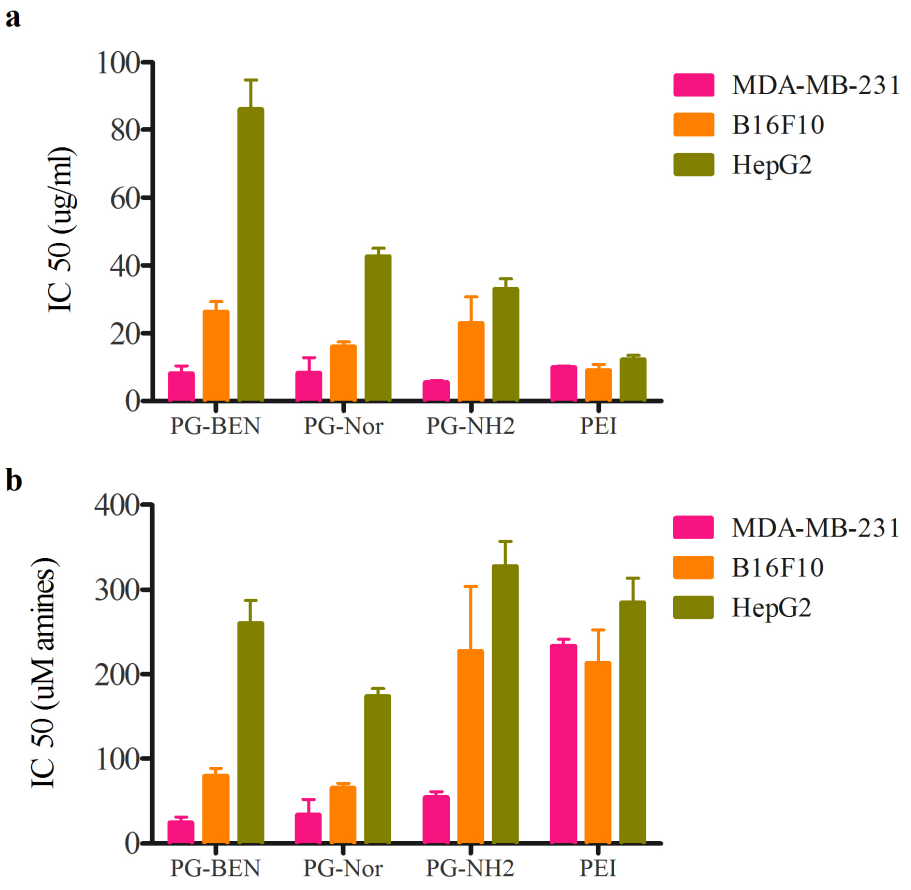


**c**

| Polymer | IC50 (μg/mL) | | | IC50 (μM amines) | | |
|---|---|---|---|---|---|---|
| | MDA-MB-231 | B16F10 | HepG2 | MDA-MB-231 | B16F10 | HepG2 |
| PG-BEN | 8.1 ± 1.6 | 26.4 ± 2.1 | 88.8 ± 4.3 | 24.5 ± 4.9 | 79.7 ± 6.4 | 260.0 ± 18.9 |
| PG-Nor | 8.2 ± 3.3 | 16.1 ± 1.0 | 42.7 ± 1.6 | 33.4 ± 13.3 | 65.4 ± 4.0 | 173.7 ± 6.7 |
| PG-$NH_2$ | 5.5 ± 0.5 | 22.9 ± 5.5 | 33.6 ± 0.9 | 54.5 ± 4.7 | 227.0 ± 54.4 | 327.4 ± 20.9 |
| PEI | 10.0 ± 0.2 | 9.1 ± 1.2 | 12.2 ± 0.9 | 233.5 ± 5.2 | 212.7 ± 28.0 | 284.7 ± 20.5 |

**Figure 26.** Toxicity of PG-BEN and PG-Nor. $IC_{50}$ values in MDA-MB-231, B16F10 and HepG2 cells determined by MTS assay expressed in (a) μg/mL of the polycation and (b) μM amino groups. (c) Summary of the results from (a) and (b).

Toxicity of polycations is strongly dependent on the number of protonated amines. It is thus informative to compare toxicity $IC_{50}$ values also in terms of molar concentrations of amines. While PG-BEN is 7.3-times less toxic than PEI and similarly,

PG-Nor and PG-$NH_2$ show about 3-times lower toxicity than PEI when measured in μg/mL, when expressed in terms of molarity of the amines, the picture changes substantially (Figure 26b). In such case, PEI becomes the least toxic among the tested polycations with its $IC_{50}$ values 5-10-fold higher than PG-BEN and PG-Nor in MDA-MB-231 and 2-4-fold higher in B16F10. In HepG2 cells, the difference between $IC_{50}$ (μM) values of PEI and PG derivatives were negligible with the ratios between 0.6 and 1.1. These results suggest that PG-BEN may have useful anticancer activity that cannot be fully explained by its polycationic character. The results also emphasize the importance of a proper selection of units when comparing toxicity of polycations with different chemical structures.

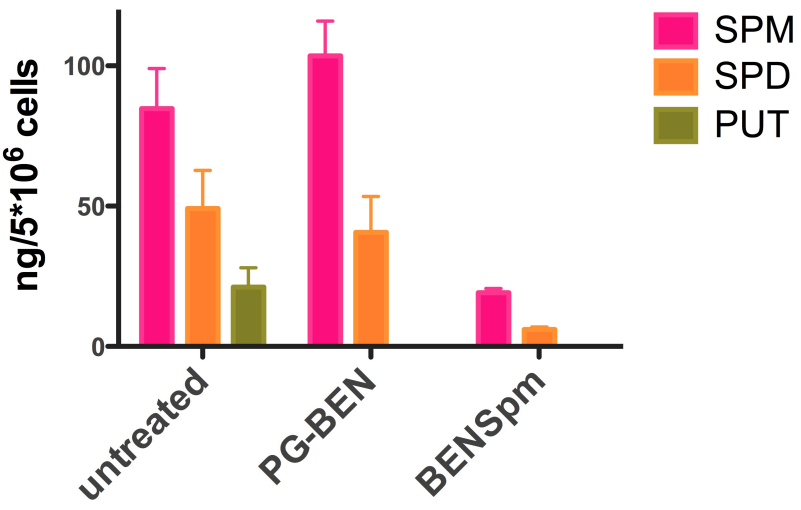


**Figure 27.** Effect of PG-BEN treatment on polyamine levels in MDA-MB-231 cells. The cells were treated with 6 µg/mL PG-BEN or equivalent concentration of free BENSpm (2.5 µg/mL) for 72 h, the cells were lysed in 5% perchloric acid and polyamine levels in the lysate analyzed by LC-MS/MS. Results are shown as mean polyamine levels in ng/5×$10^6$ cells ± SD (n=3).

4.3.5 Effect of PG-BEN treatment on cellular polyamine metabolism.

After confirming solid transfection activity of PG-BEN polyplexes with plasmid DNA, we investigated whether the mechanism of the observed anticancer effect of PG-BEN is through its effect on polyamine metabolism similar to the parent BENSpm. BENSpm down-regulates natural polyamine pathway in many types of cancer cells and that leads to cell growth inhibition and apoptosis. In order to analyze the effect of BENSpm and PG-BEN on the cellular polyamine metabolism, an LC-MS/MS method was developed to quantitatively analyze differences in the levels of different polyamines in the polyamine metabolic pathway. LC-MS/MS does not require any pre-column derivatization of the polyamines and provides superior sensitivity and reproducibility in the analysis of structurally similar natural polyamines [176, 319, 320]. The linearity ($r^2$ >

0.96) of the method was confirmed in the concentration range from 16 ng/mL to 2 µg/mL for all the analyzed natural polyamines, BENSpm, and norspermine.

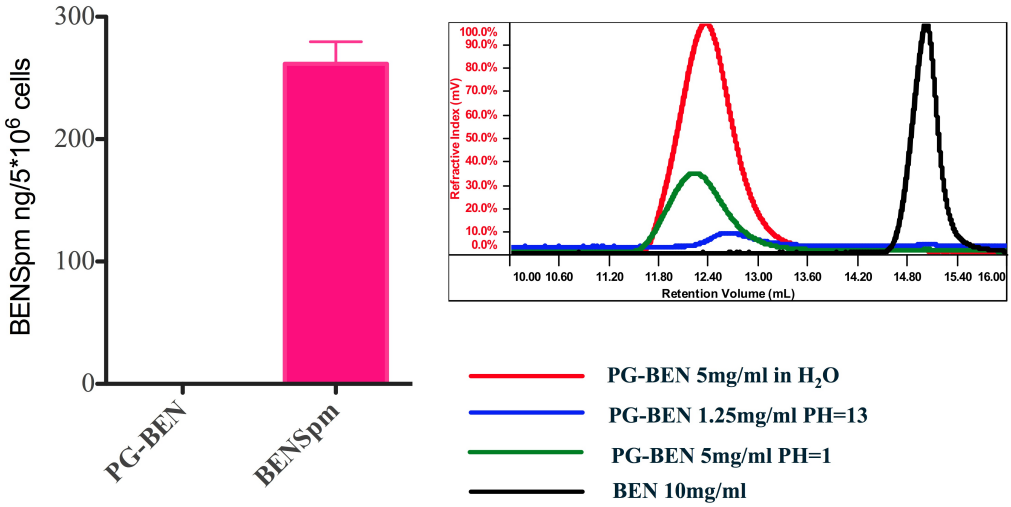


**Figure 28.** BENSpm content in MDA-MB-231 cell lysate (right panel) and size exclusion chromatography of PG-BEN and free BEN (left panel).

The effect of PG-BEN and BENSpm on polyamine metabolism was determined in MDA-MB-231 cells. The cells were treated with BENSpm or PG-BEN for 72 h and the levels of polyamines in cell lysate were analyzed by LC-MS/MS (Figure 27). The results show that BENSpm (2.5 µg/mL) down-regulated all natural polyamines as expected. In contrast, PG-BEN treatment had no effect on the levels of SPM and SPD and resulted only in decreased levels of PUT. This finding suggests that BENSpm was probably not efficiently released from PG-BEN. This hypothesis was confirmed when no detectable amount of free BENSpm were observed in cells treated with PG-BEN, compared with 262 ng/5×$10^6$ cell of BENSpm in BENSpm treated cells (Figure 28). Moreover, no BENSpm release was observed by SEC after incubation in both acidic and basic

solutions, indicating negligible hydrolysis capability of the polymer (Figure 28). Our results contradict previous report in which oligoamine was enzymatically released from PG conjugates [302]. Most likely explanation for the discrepancy is the use of different polyamine and insufficient levels of enzymes in MDA-MB-231 cells to cleave the carbamate bond in PG-BEN.

## 4.4 Conclusions

We have conjugated anticancer agent BENSpm to dendritic PG and demonstrated the utility of the conjugate for gene delivery. Compared with the lipid based BENSpm prodrug Lipo-SS-BEN that we discussed in Chapter 3, PG-BEN demonstrated ~10-75 fold increase in transfection efficiency in B16F10 cells. Because the sizes and zeta potential of PG-BEN polyplexes are comparable to Lipo-SS-BEN lipoplexes (sizes of polyplexes ~74-109 nm compared with ~ 99 nm of lipoplexes; zeta potential of polyplexes ~26-44 mV compared with ~31 mV of lipoplexes), the increased transfection capability of PG-BEN is most likely the result of improved extracellular stability of the carbamate linker in PG-BEN, compared with the dithiobenzyl carbamate linker in Lipo-SS-BEN. However, compromised drug function of polyamine depletion in PG-BEN treated cells documented by LC-MS/MS analysis indicated inefficient release of BENSpm from the PG-BEN vector. Therefore, alternative linker chemistry will have to be developed to take full advantage of BENSpm anticancer activity in BENSpm-based gene delivery vectors.

Moreover, PG-BEN showed favorable cytotoxicity profile by exhibiting selective toxicity towards breast cancer cells relative to hepatocytes. The selective toxicity,

however, was not fully related to the known mechanism of action of BENSpm through its effects on polyamine metabolism. The mechanism of the selective toxicity of PG-BEN towards cancer cells is also worth investigating.

# CHAPTER 5

# POLYCATIONIC BENSPM PRODRUG USING SELF-IMMOLATIVE LINKER AS DUAL DRUG/GENE DELIVERY SYSTEM

## 5.1 Introduction

Gene therapy shows promise for cancer treatment, however, this potentially powerful therapeutic modality is greatly hampered by the lack of desirable drug delivery systems that can accommodate various agent payloads and overcome multiple barriers such as to prevent degradation, to limit susceptibility to serum, and to improve bioavailability [321]. Polyplexes continue to gain strength as promising gene delivery vectors but the relatively low transfection activity and high toxicity associated with polycations hamper their success in clinical applications [322, 323]. Traditional ways to address the problems include combining the therapeutic gene with small-molecule drugs to enhance the therapeutic activity of the transgene [324-326]. For example, Wang and colleagues developed a nanoparticle system for co-delivery of paclitaxel with an interleukin-12-encoded plasmid. The authors demonstrated enhanced gene transfection as well as superior tumor suppression both in vitro and in vivo in tumor models [67]. A typical way to address the current problems with toxicity of polyplexes is to design biodegradable polycations that degrade into less toxic byproducts [327, 328]. Incorporation of intracellular stimuli-triggered degradation is among the most favored strategies in designing polycationic gene delivery system [329]. Examples include (i) pH-sensitive polymers containing hydrolytically sensitive bonds such as esters, (ii)

redox-responsive polymers containing disulfide bonds that are cleaved in the reductive environment of the cytoplasm, and (iii) enzymatically cleavable polymers [330-334].

The field of combination drug/nucleic acid carriers is quickly developing, with emerging novel designs of delivery vectors. Besides traditional polymeric delivery systems, new concepts such as self-assembled nucleic acid nanostructures [335], single nucleic acid encapsulation [336], multilayered polymer-nucleic acids nanocapsule [337] as well as other multifunctional nanocarriers [338] are drawing increasing attention. In order to achieve both drug/gene combination delivery and designing biodegradable delivery vector, we proposed a novel design of dual delivery vectors that not only deliver therapeutic nucleic acids but also utilizes pharmacologic effect of a cationic drug to augment the activity of the nucleic acid. To achieve this, we synthesized polycations based on a polyamine analogue BENSpm, which was originally developed to treat cancer. BENSpm contains four secondary amines that can provide positive charges under physiological conditions to bind with nucleic acids via electrostatic interactions. Thus, conjugation of BENSpm with a lipid or a polymer by appropriate linker can provide a prodrug gene delivery carrier, which can be engineered to release free BENSpm under physiological conditions. In the previous chapters (Chapter 3 and Chapter 4), Lipo-SS-BEN demonstrated satisfactory prodrug function, however, the gene delivery function was compromised by the instability of the vector. We suspected that the breakage of dithiobenzyl carbamate linker occurred before the cellular uptake. Therefore, we explored a more stable linker strategy. PG-BEN with carbamate linker between the PG core and BENSpm showed superior transfection efficiency, however, the release of BENSpm was negligible in the intracellular space. In order to improve the

dual function of the BENSpm base drug/gene delivery vector, a better linkage strategy is further explored in this chapter. We decided to use bis(2-hydroxyethyl) disulfide as a self-immolative linker to synthesize polymer prodrugs of BENSpm. The rationale behind this design is that incorporating disulfide bond into the prodrug vector allows selective degradation in the reducing intracellular space and that after the disulfide bond cleavage, the intermediate will further undergo slow intramolecular cyclization to give free BENSpm [339].

## 5.2 Materials and Methods

### 5.2.1 Materials

Plasmid DNA containing luciferase reporter gene (gWiz-Luc) was from Aldevron (Fargo, ND). Dulbecco's modified eagle medium (DMEM), Dulbecco's phosphate buffered saline (PBS), Hanks' balanced salt solution (HBSS), RPMI 1640 medium, fetal bovine serum (FBS), L-glutamine, Penicillin-Streptomycin and Snakeskin® dialysis tubing (molecular weight cutoff = 3.5 kDa) were from Thermo Scientific (Waltham, MA). G418 sulfate was from Mediatech, Inc. (Manassas, VA). Eagle's minimum essential medium (EMEM) was from Corning (Manassas, VA). HepG2 cell line was purchased from American Type Culture Collection (ATCC; Manassas, VA). MDA-MB-231 cell line was a kind gift from Dr. Jing Li, Karmanos Cancer Institute (Detroit, MI). B16F10 cell line was a kind gift from Dr. Rakesh Singh, University of Nebraska Medical Center (Omaha, NE). HEK 293T cell line was a kind gift from Dr. Gensheng Wu, Karmanos Cancer Institute (Detroit, MI). Human epithelial osteosarcoma U2OS cell line was purchased from Thermo Scientific (Waltham, MA). DharmaFECT-4 siRNA transfection

reagent, siGenome SMARTpool siRNAs: PLK-1 (polo-like kinase 1), sHH (sonic hedgehog), Bcl-2 and negative control siRNA (ON-TARGET plus Non-targeting siRNA #1) were purchased from Dharmacon (Lafayette, CO). SignalSilence® siRNAs: Akt-2, survivin, PARP and Stat-3 were from Cell Signaling Technology (Beverly, MA). Hif-1α siRNA was purchased from Santa Cruz Biotechnology (Santa Cruz, CA). 1,1'-carbonyldiimidazole (CDI), bis(2-hydroxyethyl) disulfide (DSOH), spermidine trihydrochloride, putrescine dihydrochloride and polyethylenimine (PEI, 25 kDA, branched) were purchased from Sigma-Aldrich (St. Louis, MO). Dichloromethane (99.9%, extra dry, AcroSeal™), tetrahydrofuran (THF, 99.85%, extra dry, AcroSeal™), 5-sulfosalicylic acid dihydrate (SSA), 1,7-diaminoheptane (DAH), dansyl chloride (5-dimethylamino-1-naphthalenesulfonyl chloride, 98%) and 1,6-hexanediol were from Acros Organics (Fair Lawn, NJ). L-Proline was from Alfa Aesar (Ward Hill, MA). Spermine (SPM) was from MP Biomedicals™ (Santa Ana, CA). BENSpm was synthesized as previously described [155]. Recombinant human TRAIL/Apo2L protein was purchased from PeproTech (Rocky Hill, NJ). All other reagents and chemicals were obtained from Fisher Scientific or VWR International unless otherwise stated.

### 5.2.2 Synthesis and characterization of polymeric BENSpm prodrugs

*Polymer analysis.* NMR spectra were recorded on 400MHz Bruker NMR spectrometer and chemical shifts (δ) were expressed in ppm. The composition of the polymers was determined by elemental analysis from N, S, H and Cl content (Atlantic Microlab, Inc., Norcross, GA). Weight-average molecular weight ($M_w$) and polydispersity

index (PDI) of polymers were determined by Size Exclusion Chromatography (SEC) using Agilent Technologies 1260 Infinity GPC-SEC system Agilent 1260 Infinity equipped with isocratic pump, degasser, variable wavelength detector, thermostated column compartment and autosampler from Agilent Technologies, Inc. (Santa Clara, CA). Wyatt miniDWAN™ TREOS multi-angle light scattering detector and Optilab® T-rEX™ differential refractometer (Wyatt Technology Corporation, Santa Barbara, CA) were used to determine the molecular weights. The columns used were single-pore AquaGel™ columns PAA-202 and PAA-203 from PolyAnalytik (London, ON, Canada). Sodium acetate buffer (0.3 M, pH 5.0) was used as the mobile phase at a flow rate of 0.3 mL/min. Astra 6.1 software was used for chromatographic data processing.

*Synthesis of disulfide-containing BENSpm carbamate prodrug (DSS-BEN).* Reactions were carried out under inert atmosphere with the exclusion of water. Briefly, DSOH (403.2 mg, 2.6 mmol) was dissolved in the mixture of $CH_2Cl_2$ (3.3 mL) and THF (0.7 mL). Then, a solution of CDI (887.5 mg, 5.5 mmol) in 3.5 mL $CH_2Cl_2$ was added dropwise to the ice cold solution of DSOH under nitrogen, and the reaction was kept on thawing ice for 1 h. A solution of BENSpm (2.6 mmol, 640 mg) in $CH_2Cl_2$ was then added and the reaction was kept reflux for 18 h at 45 °C. The reaction mixture was then allowed to cool down to room temperature and the final product was precipitated out in ether (25 mL) and washed twice with 20 mL ether. The residual solvents were removed under vacuum. Water (25 mL) was then added and 6 N HCl was added dropwisely until the material dissolved completely. The product was further dialyzed in 3.5 L water using dialysis tubing with molecular weight cutoff = 3.5 kDa. The solvent was changed three times against water with pH adjusted to 4.0 using HCl and finally dialyzed against

distilled water. The product was then freeze-dried. A total of 371.8 mg of DSS-BEN hydrochloride was obtained (yield= 34.2%).

*Synthesis of non-reducible BENSpm carbamate prodrug (DCC-BEN).* Reactions were carried out under inert atmosphere with the exclusion of water. To a solution of 1,6-hexanediol (437.3 mg, 3.7 mmol) in 15 ml $CH_2Cl_2$ and 1 mL THF, a solution of CDI (1,260 mg, 7.77 mmol) in 5 mL $CH_2Cl_2$ was added dropwise under stirring. The reaction was kept on thawing ice bath for 1 h and 10 mL solution of BENSpm (904 mg, 3.7 mmol) in $CH_2Cl_2$ was added. The reaction mixture was then refluxed for 96 h. The reaction product was then precipitated out in ether and dissolved in 25 mL water with addition of HCl. Polymer was isolated by freeze-drying after extensive dialysis against distilled water acidified with HCl to pH 4.0 and a final dialysis against distilled water. The product was then freeze-dried to afford the final product as HCl salt of 143.3 mg DCC-BEN (yield= 10%).

### 5.2.3 Polymer degradation studies

Degradation studies of DSS-BEN and DCC-BEN were carried out following published procedures [340]. Briefly, DSS-BEN or DCC-BEN (10 mg) was dissolved in 900 µL of 0.1 M phosphate buffered $D_2O$:acetone-$d_6$ (3:2) and the solution was purged with argon for 10 minutes. DTT (15 mg, 0.097 mmol) was added to the solution of DSS-BEN or DCC-BEN immediately before NMR acquisition and the solution was incubated at 25 °C. The extent of depolymerization was monitored using 1H NMR spectrum. Percentage of polymer degradation was quantified by the reduction of integrated methylene peaks next to carbamate at the N end in the polymer (3.35-3.55 ppm for

DSS-BEN; 3.23-3.50 ppm for DCC-BEN) relative to the solvent peak of $D_2O$ (4.8 ppm) in the sample. The degradation of polymers was plotted using curve fitting of nonlinear regression model with first-order kinetic using GraphPad Prism software.

### 5.2.4 Cell culture

Murine melanoma cell line B16F10 and human embryonic kidney cell line HEK 293T cells were cultured in DMEM supplemented with 10% FBS. MDA-MB-231 human breast cancer cells were cultured in RPMI supplemented with 10% FBS. HepG2 cells were cultured in EMEM supplemented with 10% FBS. Human epithelial osteosarcoma U2OS cells were cultured in DMEM supplemented with 2 mM L-Glutamine, 10% FBS, 1% Pen-Strep and 0.5 mg/ml G418. All cells were kept at 37 °C in incubator with 5% $CO_2$.

### 5.2.5 Polyamine analysis

Cells were treated with BENSpm (2.5 μg/mL), DSS-BEN (5.7 μg/mL) or DCC-BEN (5.7 μg/mL) for 24, 48, 72 h. Intracellular polyamines (SPM, SPD, PUT) and polyamine analog BENSpm were then extracted from cell pellets with 5% SSA, modified with dansyl, and analyzed by reverse phase HPLC as described previously [341]. Briefly, cell pellet was harvested and cells were counted after treatment. For every $10^7$ cells, 200 μL of 5% SSA was added. Cell suspension was then sonicated for 30 s, allowed to stand on ice for 60 min and mixed once at 30 min. Cell debris was then centrifuged for 5 min at 12,000 g. Fifty μL of the supernatant was transferred to a new 1.7 mL centrifuge tube and mixed with 50 μL of internal standard (40 μM DAH stock

solution in 0.1 N HCl). Two hundred µL of saturated sodium carbonate and 200 µL of dansyl chloride (10 mg/mL in acetone) were then added. The reaction mixture was then vortexed for 10 s and incubated at 70 °C for 10 min and kept in dark. The samples were then allowed to cool to room temperature and 100 µL of freshly prepared proline solution (250 mg/mL) was added. The sample was then kept in dark for additional 10 min and loaded onto a Bond-Elut $C_{18}$ column (1 mL, with adapters, Agilent Technology). After loading, column was washed with two column volumes of 35% acetonitrile. Dansylated polyamine samples were then eluted with 100% acetonitrile. Fifty µL of samples were injected onto Eclipse Plus $C_{18}$, 4.6 x 150 mm column (5 µm particle size, Agilent Technology, Santa Clara, CA) and eluted by a two-solvent gradient using 1260 Infinity Quaternary LC System (Agilent Technology, Santa Clara, CA). Solvent A was 10 mM phosphate buffer, pH 4.4. Solvent B was 100% acetonitrile. At 2 mL/min, the gradient began at 45% solvent A and progressed linearly to 80% solvent B over 14 min and increased to 90% solvent B at 15 min and the gradient was maintained until 20 min, then the gradient of solvent A decreased linearly to 45% till 26 min. Compounds were detected using 1260 Infinity Fluorescence Detector (Agilent Technology, Santa Clara, CA) with an excitation wavelength of 340 nm and an emission wavelength of 515 nm. The data were collected and analyzed using OpenLAB CDS Chemstation Edition software (Agilent Technology). BENSpm and polyamine analogue levels were then calculated based upon internal standard levels and external standard curves. The results for natural polyamines were expressed as amount of polyamine (ng) per ten million cells (ng/$10^7$ cells). The relative BENSpm release (%) was calculated as the

amount of BENSpm detected ([M]) in DSS-BEN treated cells divided by [M] in free BENSpm treated cells: $[M]_{DSS\text{-}BEN}/[M]_{BENSpm} \times 100\%$.

5.2.6 EtBr exclusion assay

The ability of DSS-BEN and DCC-BEN to condense gWiz-Luc plasmid DNA was determined by EtBr exclusion assay by measuring the changes in EtBr/DNA fluorescence. One mL DNA solution at a concentration of 20 μg/mL in 10 mM HEPES buffer (pH 7.4) was mixed with EtBr (1 μg/mL) and fluorescence was measured and set to 100% using an excitation wavelength of 540 nm and an emission wavelength of 590 nm using Quantech™ Fluorometer from Thermo Scientific (Waltham, MA). Fluorescence readings were then taken following a stepwise addition of a polycation solution, and the condensation curve for each polycation was constructed.

5.2.7 Gel retardation assay and release of DNA from polyplexes under reductive environment

Twenty μL polyplexes of DSS-BEN and DCC-BEN at different w/w ratios with 20 μg/mL gWiz-Luc DNA were loaded onto a 0.8% agarose gel containing 0.5 μg/mL EtBr and run for 60 min at 120 V in 0.5× Tris/Borate/EDTA (TBE) running buffer. For testing the disassembly of polyplexes in reductive environment, DSS-BEN and DCC-BEN polyplexes were prepared at w/w ratio of 8, and were incubated with different concentration of heparin -/+ GSH (20 mM) for 30 min before loaded onto the gel. The gels were visualized under UV illumination on a KODAK Gel Logic 100 Imaging System.

### 5.2.8 Size and zeta potential of polyplexes

Hydrodynamic diameter and zeta potential of DSS-BEN/DNA and DCC-BEN/DNA polyplexes were determined by dynamic light scattering (DLS) using a ZEN3600 Zetasizer Nano-ZS Particle Size Analyzer (Malvern Instruments Ltd., Worcestershire, UK). Polyplexes were prepared at a desired weight-to-weight (w/w) ratio of 2, 4, 6, 8 by adding a pre-determined amount of polymer to the solution of plasmid DNA in 10 mM HEPES (pH 7.4) to achieve a final DNA concentration of 20 μg/mL (200 μL). The polyplexes were incubated for 30 min at room temperature and then diluted to 1 mL for size and zeta potential measurement.

### 5.2.9 Cytotoxicity

Toxicity was evaluated by MTS assay. The cells were seeded in 96-well microplates at a density of 10,000 cells/well. After 24 h, culture medium was replaced by 200 μL of serial dilutions of DSS-BEN or DCC-BEN in serum-supplemented medium and the cells were incubated for 24 h. Then the solutions were aspirated and replaced by a mixture of 100 μL serum-free media and 20 μL of MTS reagent (CellTiter 96® AQueous Non-Radioactive Cell Proliferation Assay, Promega). After 1.5 h incubation, the absorbance was measured using SpectraMax® M5e Multi-Mode Microplate Reader (Molecular Devices, CA) at a wavelength of 490 nm. The relative cell viability (%) was calculated as $[A]_{sample}/[A]_{untreated} \times 100\%$. The $IC_{50}$ were calculated as the polymer concentration that inhibits growth of 50% of cells relative to untreated cells. The $IC_{50}$ values were calculated using GraphPad Prism.

5.2.10 Determination of maximum tolerated dose (MTD) in mouse

Animal experiment was performed under a protocol approved by the University of Nebraska Medical Center Institutional Animal Care and Use Committee. Fifteen-week-old female BALB/c nude mice were administered by tail vein injection of DSS-BEN or DCC-BEN polyplexes (w/w 4) in 200 µL solution of 0.27 M mannitol in 5 mM HEPES at concentrations of 0.8, 1.6, 2.4 and 3.2 mg/kg body weight for the corresponding polymer. Mice were monitored for 3 h after injection for acute toxicity. MTD was considered the highest dose in which no mortality was observed.

5.2.11 Transfection of DNA polyplexes

All transfection experiments were conducted in 48-well plates following a previously published protocol [342]. Cells were seeded at a density of 50,000 cells/well for MDA-MB-231 cells and HEK 293T cells, 40,000 cells/well for B16F10 cells and 20,000 cells/well for U2OS cells 24 h prior to transfection. On the day of transfection, cells were incubated with the polyplexes (DNA conc. 2.35 µg/mL) in 170 µL of media with or without 10% FBS. After 4 h incubation, polyplexes were completely removed and the cells were cultured in complete culture medium for 24 h prior to measuring luciferase expression. The medium was discarded and the cells were lysed in 100 µL of 0.5x cell culture lysis reagent buffer (Promega, Madison, WI) for 30 min. To measure the luciferase content, 100 µL of 0.5 mM luciferin solution was automatically injected into each well of 20 µL of cell lysate and the luminescence was integrated over 10 s using GloMax 96 Microplate Luminometer (Promega, Madison, WI). Total cellular protein in the cell lysate was determined by the bicinchoninic acid protein assay using

calibration curve constructed with standard bovine serum albumin solutions (Pierce, Rockford, IL). Transfection activity was expressed as relative light units (RLU)/mg cellular protein ± SD (n=4).

5.2.12 Combination of DSS-BEN and DCC-BEN with TRAIL protein

MDA-MB-231 cells were seeded in 96-well plates at a density of 3,000 cells/well. After 24 h, culture medium was replaced by 200 µL of serial dilutions of BENSpm, DSS-BEN, DCC-BEN, TRAIL protein or the combination of each reagent with TRAIL in serum-supplemented medium. Cells were further incubated for 120 h and medium was changed once with fresh medium containing the same concentration of agents at 48 h. Cell viability was then measured by MTS assay as described above. Quantification of synergistic effect was evaluated by CI value calculated using CompuSyn software (ComboSyn, Inc., Paramus, NJ).

5.2.13 Combination of DSS-BEN and DCC-BEN with different siRNAs

Reverse transfection method was used for siRNA knockdown. For each well of 96-well plate, particles containing siRNA were prepared by mixing 10 µL siRNA solution in HBSS (conc. 200 nM, 2 pmol per well) and 10 µL DharmaFECT4 solution (0.1 µL DharmaFECT4 solution in 10 µL HBSS), the mixture was allowed to stand for 20 min at room temperature, and the total amount of 20 µL of siRNA complexes was added to each well. Eighty µL of U2OS cell suspension containing either fresh medium, BENSpm, DSS-BEN or DCC-BEN was then added to each well (50,000 cells/mL, 4,000 cells/well). Final concentration of BENSpm, DSS-BEN, or DCC-BEN was 2.5 µg/mL, 5.7

μg/mL, 5.7 μg/mL, respectively (the doses of DSS-BEN and DCC-BEN are equivalent to 2.5 μg/mL BENSpm as determined by elemental analysis). The cells were further incubated for 72 h and cell viability was then measured using CellTiter-Blue® Cell Viability Assay (Promega, Madison, WI). Twenty μL of CellTiter-Blue reagent was added into each well and incubated for 1.5 h in the incubator before recording the fluorescent intensity ($560_{Ex}/590_{Em}$). The relative cell viability (%) was calculated as the relative fluorescence $[F]_{sample}/[F]_{untreated} \times 100\%$. Data were analyzed by Student's *t*-test, and statistical significant difference was determined as $p < 0.02$.

## 5.3 Results and Discussion

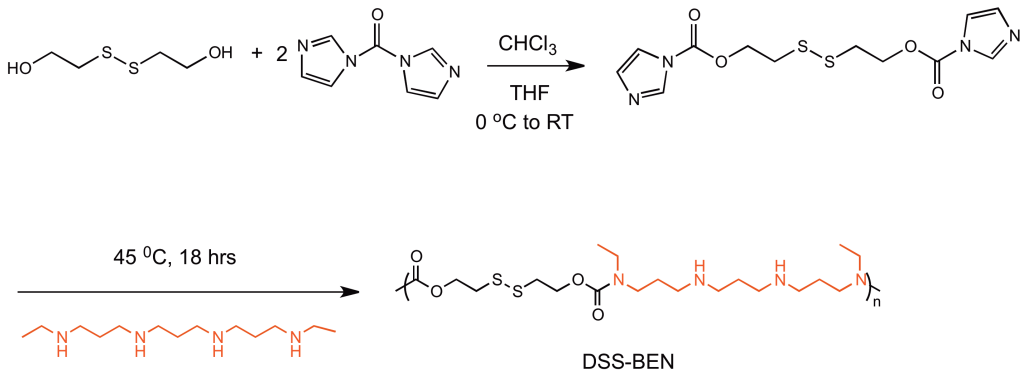


**Scheme 8.** Synthesis of DSS-BEN

In order to design a self-immolative prodrug/gene delivery vector with high content of BENSpm and intracellularly selective drug release mechanism, we designed a simple two-step reaction. Activation of DSOH with CDI was followed by polymerization with BENSpm via carbamate bond to form DSS-BEN polymer (Scheme 8). As the non-degradable counterpart, control polymer DCC-BEN without the disulfide bond was also

synthesized for this study (Scheme 9). The synthesized DSS-BEN was expected to undergo intracellular reduction by reacting with intracellular reducing reagents such as GSH. The resulting thiolated intermediate is subject to intramolecular cyclization, which generates BENSpm and a small cyclic molecule 1,3-oxathiolan-2-one (Scheme 10).

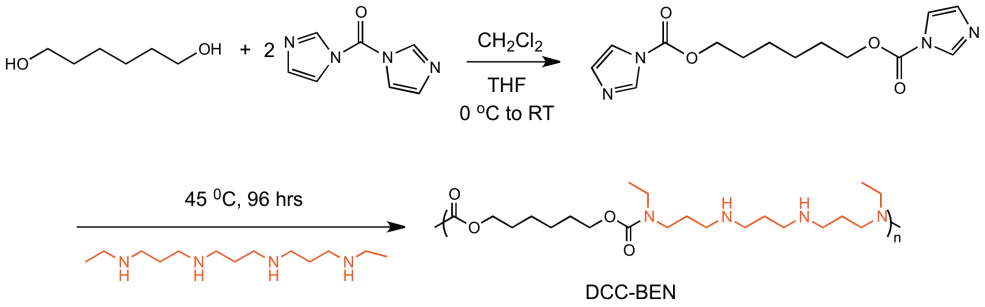


**Scheme 9.** Synthesis of DCC-BEN

5.3.1 Synthesis and characterization of DSS-BEN and DCC-BEN

DSS-BEN and non-degradable control DCC-BEN were synthesized using 1: 1 ratio of BENSpm with activated DSOH or 1,6-hexanediol in dichloromethane (Scheme 8 and Scheme 9). The success of the synthesis was confirmed by $^{1}$H-NMR (Figure 29) and elemental analysis (Table 6). The patterns of peak broadening in the NMR spectra for both DSS-BEN and DCC-BEN proved the formation of polymers [343]. From the NMR spectra of DSS-BEN, ratio between the integration of peak a to peak c and e equals 1: 2, which indicates the molar ratio between DSOH and BENSpm in the polymer is around 1: 1. This result was also confirmed by the elemental analysis (2 mol S in 1 mol DSOH, 4 mol N in 1 mol BENSpm), where the molar ratio between BENSpm and DSOH equals 1: 1.14. These results suggested that the structure of the polymer is mostly linear, however, due to the similar reactivity of the four secondary amines in

BENSpm, it is not possible to determine which two amines were conjugated with the DSOH based on our current detection methods. Similar result was also obtained with DCC-BEN. In the NMR spectra of DCC-BEN, ratio of peak a to the addition of peak e and peak f equals 1: 2.01. It can be calculated from the elemental analysis that the ratio between BENSpm and hexanediol is 1: 1.22 (6 mol C in 1 mol hexanediol, 4 mol N and 13 mol C in 1 mol BENSpm), indicating the structure of the polymer is mostly linear, with most of the polymer molecules terminated with hexanediol. Moreover, both polymers contain equal amount of 44% BENSpm in the total weight (Table 6).

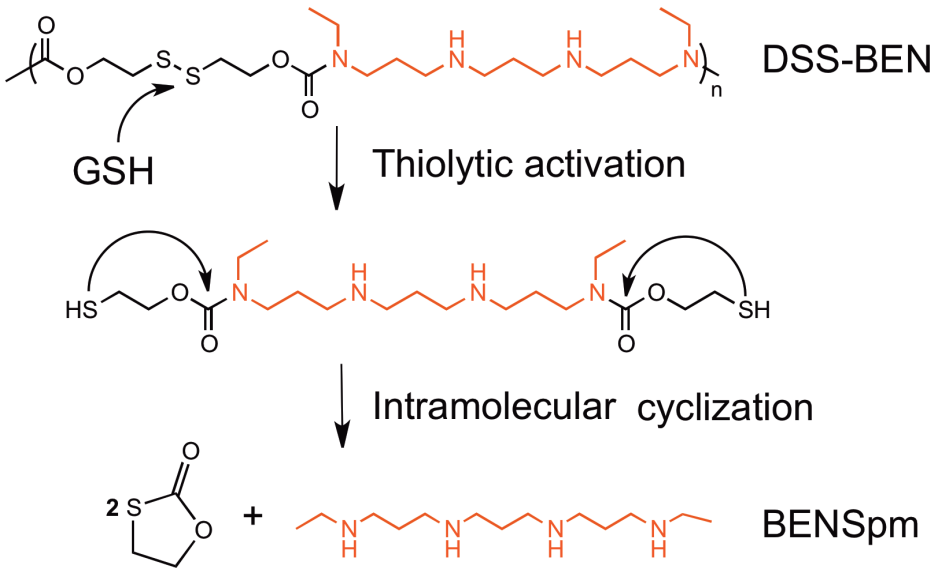


**Scheme 10.** Intracellular release mechanism of BENSpm from DSS-BEN.

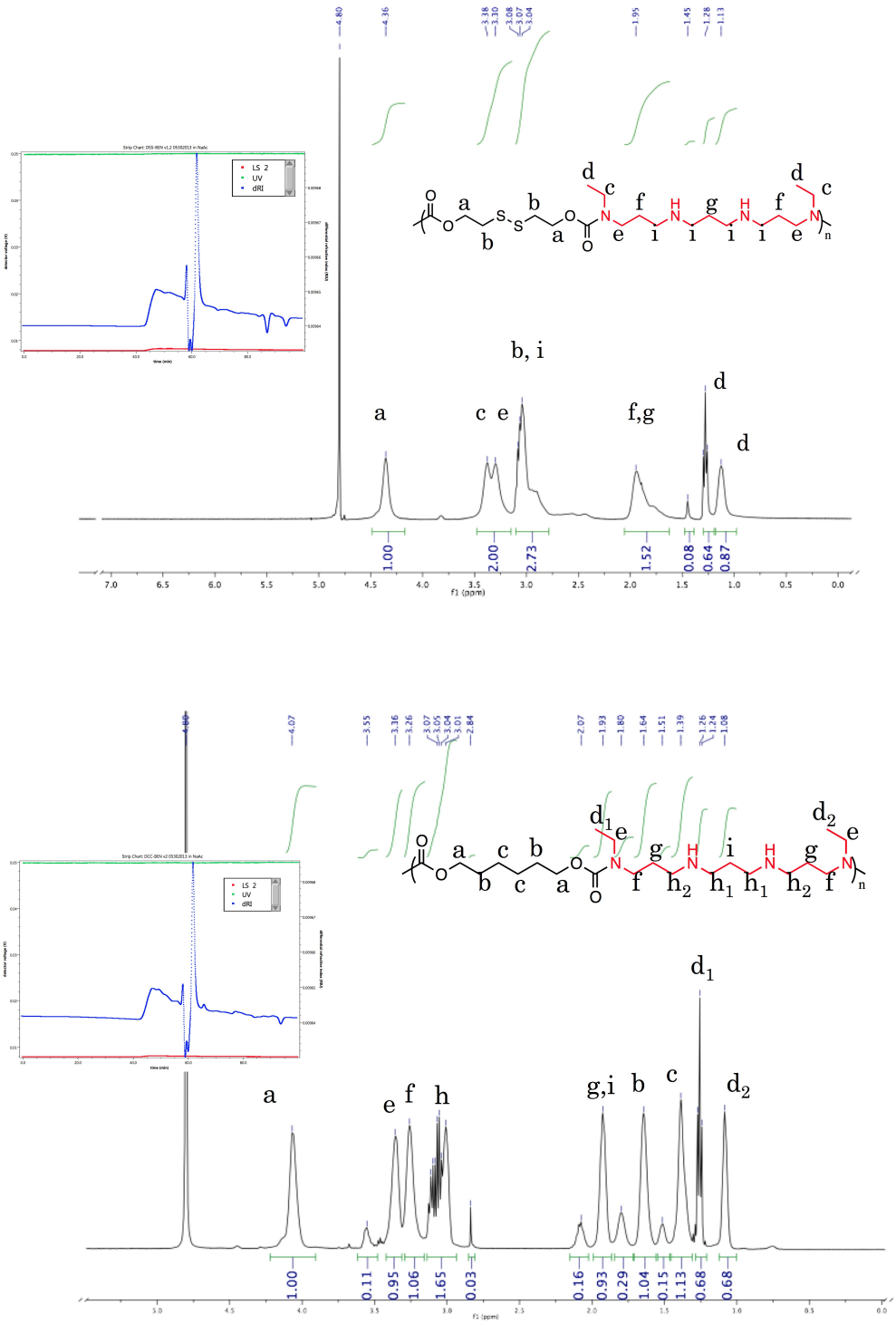


**Figure 29.** $^{1}$H-NMR and SEC spectra (small figures) of DSS-BEN (upper panel) and DCC-BEN (lower panel).

SEC (Figure 29) showed that DSS-BEN has the molecular weight around 3.8 kDa, while the DCC-BEN has lower molecular weight around 2.8 kDa. The low molecular weight of the DCC-BEN partially explained the low yield (10%), as the polymer was purified by dialysis with the molecular weight cutoff of 3.5 kDa. The *dn/dc* value was determined experimentally as 0.1693 g/mL using a serial dilution of DSS-BEN. It can be calculated from the molecular weight of both polymers that the number of repeating unit (*n*) in the polymers (as shown in the structure of DSS-BEN in Scheme 8 and DCC-BEN in Scheme 9) equals 8 and 7 for DSS-BEN and DCC-BEN, respectively. The polymerizations for both DSS-BEN and DCC-BEN have been carried out at different temperatures (60 °C in chloroform and 45 °C in dichloromethane) and using different reaction times (24, 48, 72, 96 h). However, no significant increase in the molecular weight was observed under either elevated temperature or prolonged reaction time.

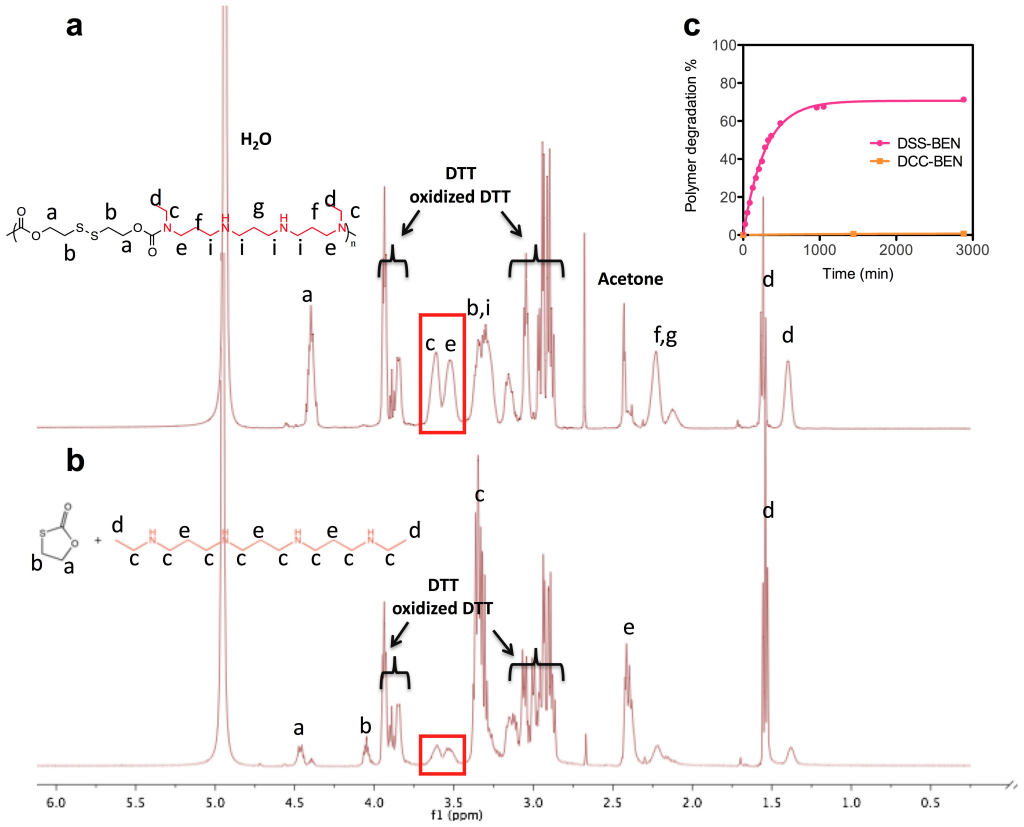


**Figure 30.** $^{1}$H NMR spectra of DSS-BEN (a) immediately after DTT addition in 0.1 M pH 7.4 phosphate buffered $D_2O$:acetone (3:2) at 25 °C; (b) after 16 h under the same conditions; (c) degradation kinetics of DSS-BEN and DCC-BEN as calculated from the $^{1}$H NMR.

The synthesized DSS-BEN was expected to undergo intracellular reduction by reacting with intracellular reducing reagents such as GSH (Scheme 10). In order to verify the proposed degradation mechanism of DSS-BEN, we investigated the degradation kinetic of DSS-BEN in comparison with non-reducible DCC-BEN by 1H NMR spectroscopy. With the presence of reducing agent DTT, multiple changes of the chemical shift were observed from the NMR spectrum for DSS-BEN after 16 h

incubation (Figure 30a and 30b). Reduction of peak c and peak e in Figure 30a compared with the corresponding peaks in Figure 30b indicated the cleavage of carbamate bond in the polymer backbone. Peak a and peak b in Figure 30b represented the methylene peaks of the 1,3-oxathiolan-2-one cyclic product in the reaction mixture. These results proved the proposed mechanism of intramolecular cyclization of the self-immolate linkage. Oppositely, no difference in the spectrum was observed for DCC-BEN under the same condition (data not shown), therefore verified the need of designing self-immolative linker to facilitate the carbamate cleavage in the polymer backbone. The degree of polymer degradation was calculated as the percentage of reduction in the integration of peak a and e (Figure 30a) relative to the peak integration at time 0 (immediately after DTT addition). As shown in Figure 30c, curve fitting of the degradation result demonstrated that DSS-BEN depolymerization followed first-order kinetic, with a rate constant of $3.5 \times 10^{-3}\,min^{-1}$ and a corresponding half-life of 198 min. This result is in well agreement with former reports that the degradation of several self-immolative polymers containing similar cyclizing spacers followed the kinetics between zero and first order [340, 344]. Co-incubation of DCC-BEN with DTT resulted in no change in the NMR spectrum, and the calculated degree of depolymerization was lower than 0.7% within 48 h. In all, these results demonstrated the success of designing DSS-BEN as an effective self-immolative BENSpm prodrug.

**Table 6.** Elemental analysis and calculated BENSpm content in DSS-BEN and DCC-BEN

| Weight % | C | H | N | S | Cl | BENSpm |
|---|---|---|---|---|---|---|
| DSS-BEN | 44.1 | 7.9 | 10.2 | 13.3 | 8.5 | 44.0 |
| DCC-BEN | 49.7 | 9.3 | 10.1 | NA | 11.3 | 43.9 |

5.3.2 Prodrug function of DSS-BEN and DCC-BEN in various cell lines

The prodrug function of DSS-BEN and DCC-BEN was evaluated using HPLC to quantitatively determine the intracellular levels of BENSpm and their effect of depleting natural polyamines. We first verified that BENSpm could be released from the DSS-BEN. As shown in Figure 31, BENSpm was detected in all cell lines tested after the treatment with DSS-BEN, the highest amount of BENSpm release (67.5%) was observed in U2OS cells followed 72 h treatment with DSS-BEN. In comparison, in all untreated groups and DCC-BEN treated groups, no detectable amount of BENSpm was observed, and thus was not depicted in the figure. This result confirmed the success of degradable design of DSS-BEN, and the cell line-dependence of BENSpm release may be caused by the difference in intracellular redox potential of the different cell lines.

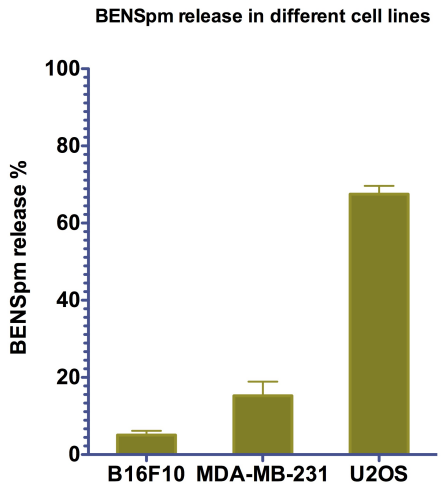


**Figure 31.** BENSpm release after 72 h treatment of DSS-BEN in different cell lines determined by HPLC analysis.

In order to test the drug effect of DSS-BEN and DCC-BEN in comparison with BENSpm, we further evaluated the intracellular polyamine levels. As shown in Figure 32a, BENSpm treatment efficiently depleted all the natural polyamines in B16F10 cells when treated for at least 24 h. Treatment with DSS-BEN resulted in less polyamine depletion because less than 15% of BENSpm was released from DSS-BEN in B16F10 cells. It is reasonable to conclude that limited BENSpm release and insufficient time were the major causes for the compromised drug effect. In contrast, significant down-regulation of polyamines was observed in U2OS cells after 72 h treatment with DSS-BEN (Figure 32b), suggesting that BENSpm release from DSS-BEN is strongly cell line-dependent. DCC-BEN failed to down-regulate the polyamines in both B16F10 cells and U2OS cells. Although in MDA-MB-231 cells, DCC-BEN showed moderate down-regulation of polyamines, it was considered less relevant with the BENSpm drug effect, as no BENSpm release was detected 72 h after DCC-BEN treatment. In all, these

results demonstrated that DSS-BEN could release BENSpm in the intracellular environment and exhibit the drug effect for polyamine depletion.

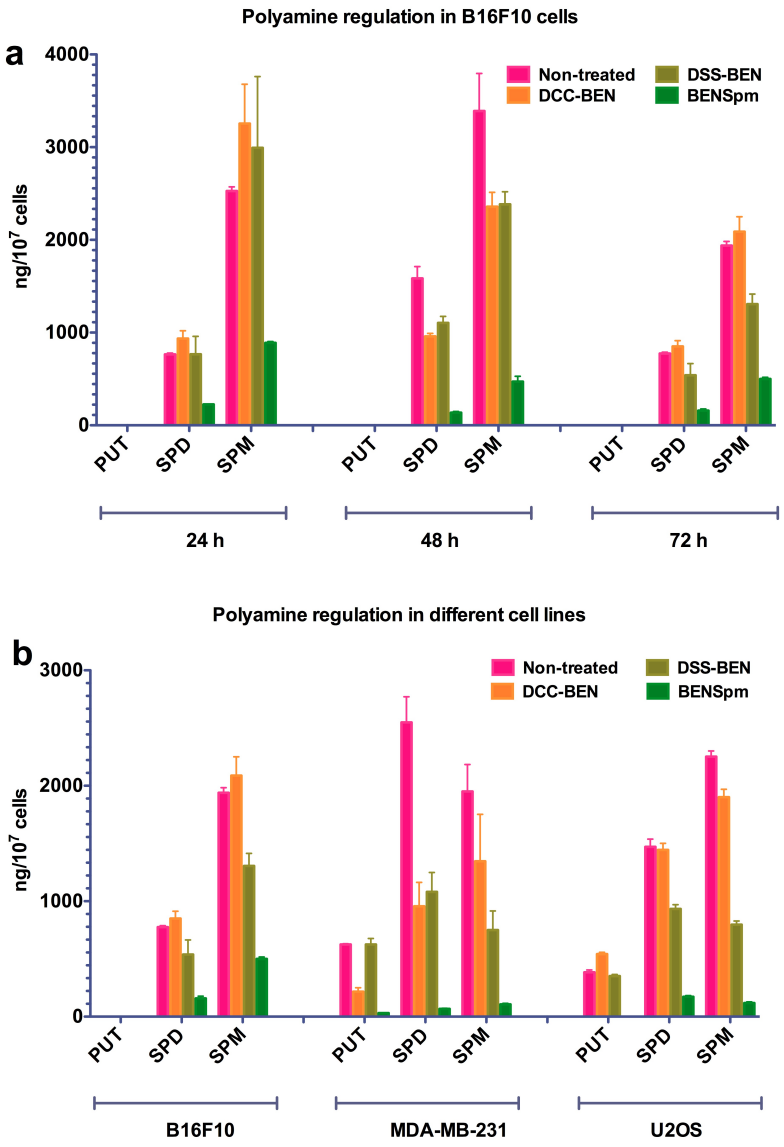


**Figure 32.** Polyamine concentration in different cell lines determined by HPLC analysis. (a) Time dependence of polyamine production in B16F10 cells after treatment with BENSpm, DSS-BEN or DCC-BEN; (b) Cell line dependence of polyamine production in B16F10, MDA-MB-231 and U2OS cells after 72 h treatment.

### 5.3.3 DNA condensation and polyplex characterization

In order to test the function of DSS-BEN and DCC-BEN as gene delivery vectors, we first investigated the ability of DSS-BEN and DCC-BEN to condense DNA using EtBr exclusion assay (Figure 33a). Results showed that the parent BENSpm could not condense DNA, indicated by the decrease of fluorescence intensity by less than 30%. In contrast, DSS-BEN could efficiently condense DNA at w/w ratio > 4, however, DCC-BEN only showed partial DNA condensation ability with only 50% decrease in fluorescence intensity at w/w 10. Gel retardation assay showed that both DSS-BEN and DCC-BEN could confine DNA to the start of the gel at w/w ratio higher than 0.5 and 1, respectively (Figure 33b). However, fluorescence was observed in the wells even at the highest w/w ratio (w/w 16) used. Because the fluorescence emission is a result of intercalation of DNA by EtBr, it can be concluded that both DSS-BEN and DCC-BEN formed lose polyplexes structure with DNA. Therefore the partially condensed DNA molecules could remain active to interact with EtBr.

The DSS-BEN/DNA and DCC-BEN/DNA polyplexes were further analyzed for the size and zeta potential (Figure 33c and 33d). DSS-BEN efficiently condensed DNA into positively charged nanoparticles, with small particle sizes ~70-100 nm for all the tested w/w ratios. However, DCC-BEN could not condense DNA at w/w 2 and the particle sizes were above 100 nm at higher w/w ratios, with zeta potential generally smaller than DSS-BEN polyplexes. Despite the structural similarity between DSS-BEN and DCC-BEN, possible explanation for the discrepancy in DNA condensation ability is that the flexible disulfide-disulfide exchange between DSS-BEN polymer chains may facilitate encapsulation of DNA molecule as well as stabilization of the polyplexes [345].

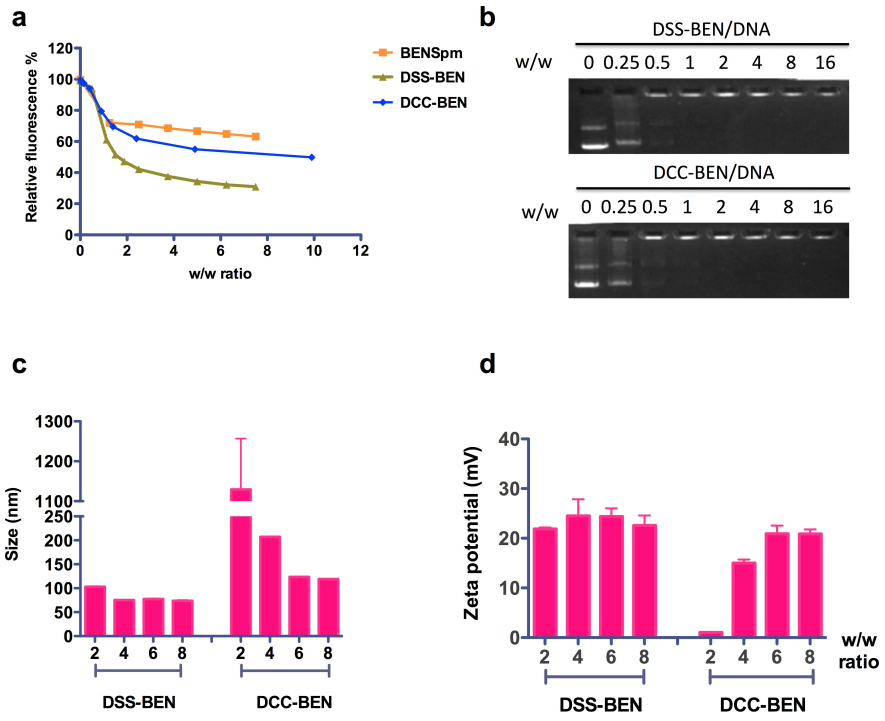


**Figure 33.** Physiochemical characterization of DNA polyplexes of DSS-BEN and DCC-BEN polyplexes. (a) EtBr exclusion assay in 10 mM HEPES (pH 7.4); (b) gel retardation assay; (c) hydrodynamic particle size and (d) zeta potential of the polyplexes at different w/w ratios.

The effect of disulfide reduction mediated by GSH on the polyplexes against polyelectrolyte exchange with heparin was evaluated by agarose gel electrophoresis (Figure 34). We hypothesized that disulfide reduction of DSS-BEN would not only facilitate the BENSpm release from the polymer, but also result in the intracellular release of DNA from the polyplexes. In the absence of a reducing agent, both the DSS-BEN and DCC-BEN polyplexes showed the first sign of DNA release at a heparin concentration of 120 µg/mL. However, in the presence of 20 mM GSH that mimic the redox status in the cell nuclei [346], DNA release was observed even without the involvement of heparin. On the other hand, DCC-BEN polyplexes showed only slight

difference in DNA release with the presence of GSH. These results confirmed our hypothesis that disulfide-containing polymer DSS-BEN possesses the advantage of redox-responsive DNA release in the intracellular environment. Therefore, DSS-BEN is expected to have better transfection capability over DCC-BEN.

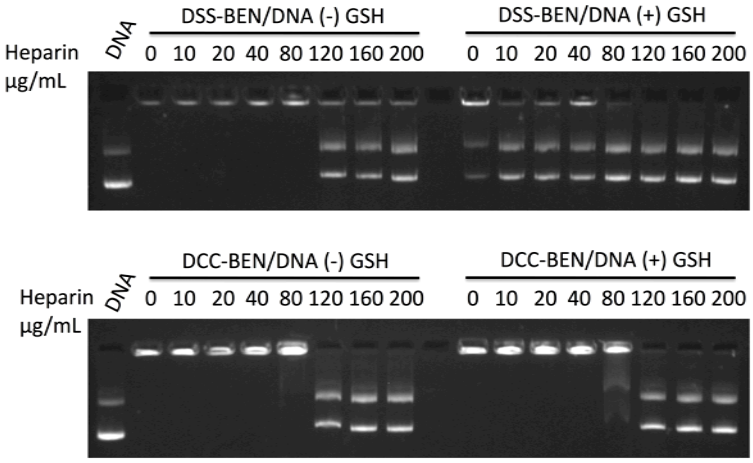


**Figure 34.** DNA release from DSS-BEN (upper panel) and DCC-BEN (lower panel) polyplexes after incubation with heparin -/+ GSH (20 mM). All polyplexes were prepared at w/w ratio 8.

### 5.3.4 Cytotoxicity

Toxicity associated with the use of polycations remains a major hindrance for polycation-based gene delivery systems. One of the most effective strategies to reduce the vector toxicity is to incorporate degradable moiety into the polymer backbone [347-350]. Because of the bioreducible nature of DSS-BEN, we expected it to have lower toxicity compared with the non-degradable control DCC-BEN. As shown in Figure 35, $IC_{50}$ values of DSS-BEN were generally 1.5-2 fold higher than DCC-BEN, and 3-4 fold higher than PEI. Interestingly, DSS-BEN showed selective toxicity in MDA-MB-231, with the $IC_{50}$ comparable to that of DCC-BEN and PEI, whereas no cell line dependence was

observed for DCC-BEN ($IC_{50}$ 12-20 µg/mL) and PEI ($IC_{50}$ 6-12 µg/mL). We then also determined the MTD of DSS-BEN and DCC-BEN in BALB/c nude mice after i.v. injection. The determined MTD was 1.6 mg/kg body weight for DSS-BEN and 0.8 mg/kg body weight for DCC-BEN. MTD values of both BENSpm polymers was lower than the reported MTD of PEI [351]. The fact that PEI was more toxic in vitro, while less toxic in vivo suggests that other factors play a role in *in vivo* toxicity that are not captured in the simple *in vitro* assays.

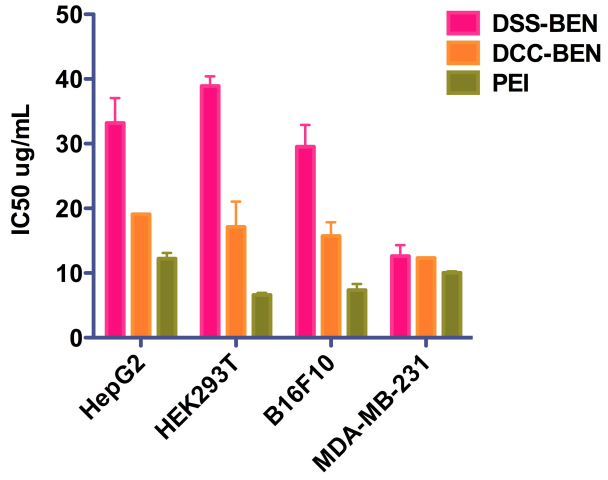


**Figure 35**. $IC_{50}$ values of DSS-BEN, DCC-BEN and PEI in various cell lines. Cell viability was measured by MTS assay after 24 h treatment.

### 5.3.5 Transfection

Luciferase transfection assay was used to assess the capability of DSS-BEN and DCC-BEN as gene delivery vectors in various cell lines. Cells were transfected with DSS-BEN or DCC-BEN polyplexes prepared at different w/w ratios in the presence or absence of serum (Figure 36). DSS-BEN polyplexes showed comparable transfection with PEI in all tested cell lines. Interestingly, DSS-BEN polyplexes showed low

sensitivity to w/w ratio and the presence of serum, especially in B16F10 and HEK 293T cells. In contrast, transfection of DCC-BEN polyplexes showed strong dependence on w/w ratio. The transfection efficiency of DCC-BEN was consistently lower than that of DSS-BEN polyplexes in all cell lines tested. Compared with DCC-BEN, higher transfection efficiency of DSS-BEN can be explained by the redox-responsive nature of the polymer, which can reduce the vector cytotoxicity and facilitate intracellular DNA release. This result verified the success of designing DSS-BEN as an efficient gene delivery vector.

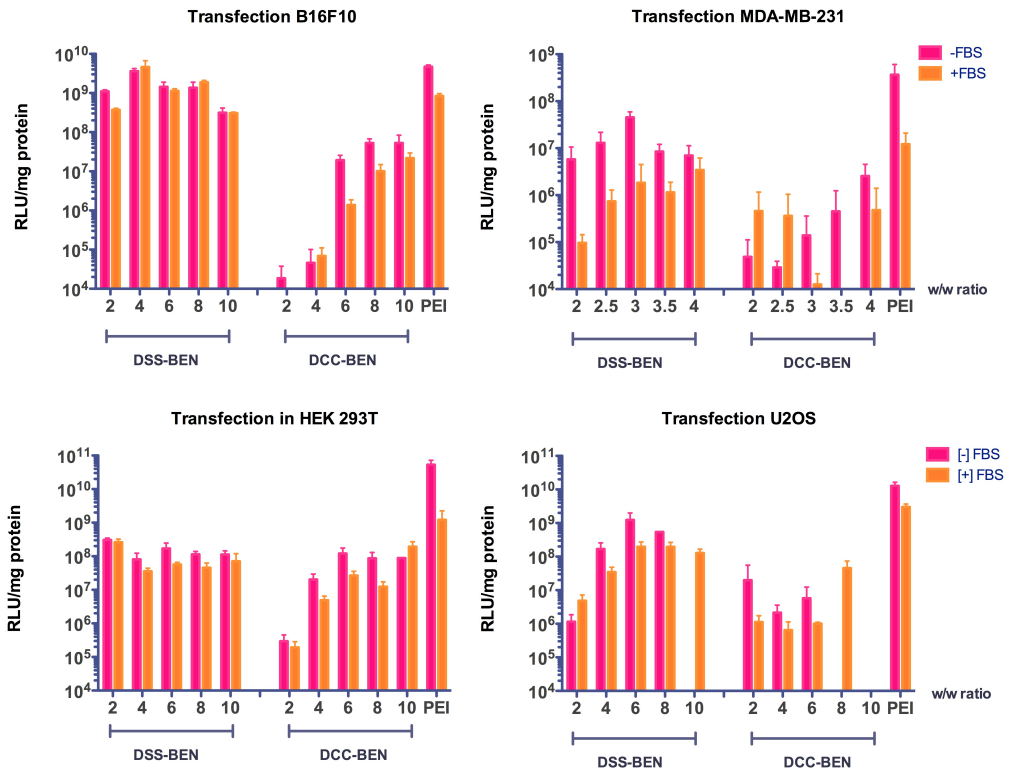


**Figure 36.** Transfection activity of DSS-BEN and DCC-BEN polyplexes in different cell lines. Results are shown as mean relative light unit (RLU)/mg protein ± SD (n=4).

5.3.6 Combination of DSS-BEN with nucleic acids and proteins

BENSpm was reported to act synergistically with different therapeutic agents such as 5-FU, PTX, histone deacetylase inhibitor MS-275 and recombinant proteins TNF or TRAIL [199, 265, 352, 353]. In order to utilize the synergistic effect of BENSpm in DSS-BEN, it is important to evaluate the effectiveness of DSS-BEN in combination with different therapeutic agents, including siRNA or proteins.

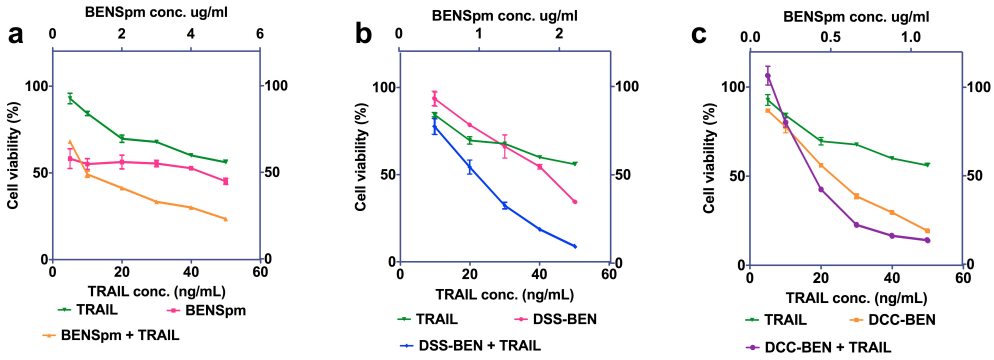


| TRAIL (ng/mL) | CI value | | |
|---|---|---|---|
| | BENSpm + TRAIL (100: 1) | DSS-BEN + TRAIL (100:1) | DCC-BEN + TRAIL (50:1) |
| 10 | 0.31 | 1.10 | 1.82 |
| 20 | 0.27 | 0.90 | 0.95 |
| 30 | 0.26 | 0.68 | 0.73 |
| 40 | 0.29 | 0.57 | 0.74 |
| 50 | 0.25 | 0.41 | 0.84 |

**Figure 37.** Combination treatment of (a) BENSpm; (b) DSS-BEN and (c) DCC-BEN with TRAIL in MDA-MB-231 cells. Dose axis of DSS-BEN and DCC-BEN was normalized to corresponding BENSpm content, results were shown as relative cell viability compared with non-treated cells ± SD (n=3).

The synergistic effect of DSS-BEN and TRAIL combination was determined in MDA-MB-231 cells and compared with BENSpm and DCC-BEN. The cells were treated

with DSS-BEN, DCC-BEN, BENSpm or TRAIL protein alone, or in the combination with TRAIL at fixed weight ratios (BENSpm: TRAIL 100:1; DSS-BEN: TRAIL 100:1 and DCC-BEN: TRAIL 50:1) for 120 h (Figure 37). CI value analysis showed that for all the doses tested, BENSpm showed strongest synergistic effect with TRAIL (CI < 0.32). DSS-BEN also showed synergism at high doses (CI = 0.41-0.68), while additive effect was observed at low doses (CI = 0.9-1.10). Compromised synergism may be owing to the less amount of BENSpm presented in DSS-BEN (44% weight loading) in combination with TRAIL, compared with the BENSpm free drug and TRAIL combination. Nevertheless, the results provided evidence of the prodrug functionality of DSS-BEN, which could maintain the enhancing potential of BENSpm. In contrast, DCC-BEN only showed slight synergism with TRAIL at high doses, as indicated by the CI values higher than 0.73, and additive effect or antagonism at low doses tested (CI = 0.95-1.82).

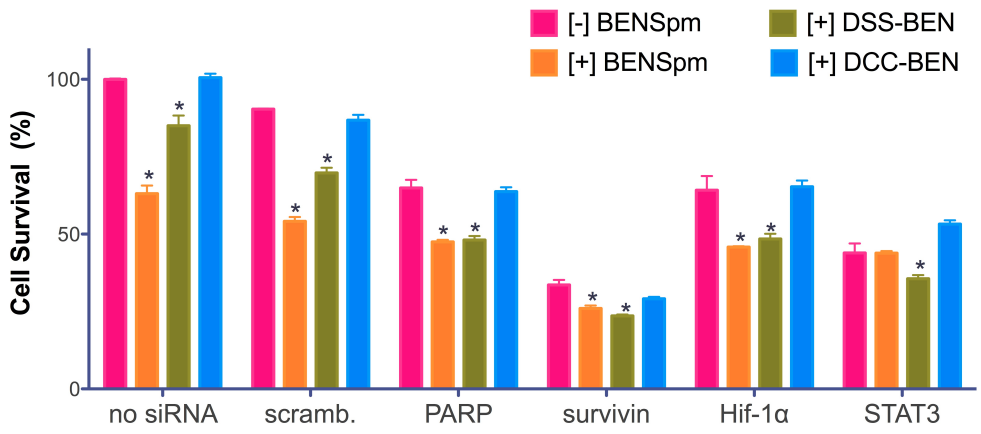


**Figure 38.** Combination of BENSpm, DSS-BEN and DCC-BEN with different siRNAs in U2OS cells for 72 h. Result are shown as mean cell viability ± SD (n=3). $^{*}p < 0.02$ indicates significant difference of cell viability in comparison with the (-) BENSpm groups.

Effect of DSS-BEN in combination with a panel of siRNAs was also investigated (Figure 38). U2OS cell line was used for the combination study because of the sensitivity to various siRNAs. A panel of siRNAs was chosen based on documented effectiveness of the target in cancer treatment, either alone or in combination with different therapeutic agents [354-364]. Doses of BENSpm, DSS-BEN or DCC-BEN used contained the equivalent amount of BENSpm (2.5 μg/mL). The results showed that BENSpm achieved the strongest cell growth inhibition (37%). DSS-BEN treatment showed compromised growth inhibition to U2OS cells (15%). It is possible that longer time is needed for efficient BENSpm release from DSS-BEN in order to take the drug action. As predicted, DCC-BEN alone at the equivalent BENSpm dose did not show any cell growth inhibition. This result supports our hypothesis that efficient BENSpm release is important for the drug function. When the cells were treated with 20 nM of different siRNAs, the data demonstrated that PLK-1 knockdown was lethal to U2OS cells (less than 10% viable cells detected). Significant cell killing could also be observed in cells treated with siRNA against Bcl-2, sHH, Akt2, and survivin. Combination of these siRNAs with BENSpm, DSS-BEN and DCC-BEN did not lead to any significant enhancement of siRNA activity. In contrast, the activity of siRNAs against PARP and Hif-1$\alpha$ was enhanced by the combination with BENSpm and DSS-BEN by almost 20%. Combination of the same siRNA treatments with DCC-BEN showed no additional induction of cell killing. To summarize, results from the combination experiments proved that DSS-BEN could well-maintain the synergistic potential of BENSpm.

## 5.4 Conclusions

We have successfully developed polymeric prodrug of anticancer drug BENSpm and confirmed its dual functionality as a prodrug and a gene delivery vector. Presence of free BENSpm in cells treated with DSS-BEN confirmed the success of our self-immolative linker strategy. We have also demonstrated that DSS-BEN can act synergistically with several therapeutic agents, making it a promising delivery platform for combination therapy in cancer by co-delivering a variety of therapeutic agents. Moreover, this kind of self-immolative linker can also be incorporated into prodrug design for a growing number of other similar drugs that possess cationic amines, such as difluoromethylornithine or AMD3100, and thus may be applied to other diseases: such as Barrett's esophagus and myelokathexis [365-367], for which polyamine drugs are promising therapeutics. In all, DSS-BEN is a promising dual delivery vector, and development of this kind of dual delivery platform warrants further investigation.

## REFERENCES

[1] Y. Zhu, J. Li, D. Oupicky, Intracellular Delivery Considerations for RNAi Therapeutics, in: K.A. Howard (Ed.) RNA Interference from Biology to Therapeutics, Springer US, 2013, pp. 79-95.

[2] J. Li, Y. Wang, Y. Zhu, D. Oupicky, Recent advances in delivery of drug-nucleic acid combinations for cancer treatment, J Control Release, (2013).

[3] S.A. Rosenberg, P. Aebersold, K. Cornetta, A. Kasid, R.A. Morgan, R. Moen, E.M. Karson, M.T. Lotze, J.C. Yang, S.L. Topalian, et al., Gene transfer into humans--immunotherapy of patients with advanced melanoma, using tumor-infiltrating lymphocytes modified by retroviral gene transduction, N. Engl. J. Med., 323 (1990) 570-578.

[4] T. Wirth, N. Parker, S. Yla-Herttuala, History of gene therapy, Gene, 525 (2013) 162-169.

[5] D. Takefman, W. Bryan, The state of gene therapies: the FDA perspective, Mol. Ther., 20 (2012) 877-878.

[6] S.L. Ginn, I.E. Alexander, M.L. Edelstein, M.R. Abedi, J. Wixon, Gene therapy clinical trials worldwide to 2012 - an update, J Gene Med, 15 (2013) 65-77.

[7] H. Matsubara, Y. Mizutani, F. Hongo, H. Nakanishi, Y. Kimura, S. Ushijima, A. Kawauchi, T. Tamura, T. Sakata, T. Miki, Gene therapy with TRAIL against renal cell carcinoma, Mol. Cancer Ther., 5 (2006) 2165-2171.

[8] T. Wenger, J. Mattern, T.L. Haas, M.R. Sprick, H. Walczak, K.M. Debatin, M.W. Buchler, I. Herr, Apoptosis mediated by lentiviral TRAIL transfer involves transduction-dependent and -independent effects, Cancer Gene Ther., 14 (2007) 316-326.

[9] H. Tsurushima, X. Yuan, L.E. Dillehay, K.W. Leong, Radioresponsive tumor necrosis factor-related apoptosis-inducing ligand (TRAIL) gene therapy for malignant brain tumors, Cancer Gene Ther., 14 (2007) 706-716.

[10] M.L. Lucas, L. Heller, D. Coppola, R. Heller, IL-12 plasmid delivery by in vivo electroporation for the successful treatment of established subcutaneous B16.F10 melanoma, Mol. Ther., 5 (2002) 668-675.

[11] K. Anwer, M.N. Barnes, J. Fewell, D.H. Lewis, R.D. Alvarez, Phase-I clinical trial of IL-12 plasmid/lipopolymer complexes for the treatment of recurrent ovarian cancer, Gene Ther., 17 (2010) 360-369.

[12] F. Lohr, D.Y. Lo, D.A. Zaharoff, K. Hu, X. Zhang, Y. Li, Y. Zhao, M.W. Dewhirst, F. Yuan, C.Y. Li, Effective tumor therapy with plasmid-encoded cytokines combined with in vivo electroporation, Cancer Res, 61 (2001) 3281-3284.

[13] D.M. Mahvi, M.B. Henry, M.R. Albertini, S. Weber, K. Meredith, H. Schalch, A. Rakhmilevich, J. Hank, P. Sondel, Intratumoral injection of IL-12 plasmid DNA--results of a phase I/IB clinical trial, Cancer Gene Ther., 14 (2007) 717-723.

[14] M. Nakase, M. Inui, K. Okumura, T. Kamei, S. Nakamura, T. Tagawa, p53 gene therapy of human osteosarcoma using a transferrin-modified cationic liposome, Mol. Cancer Ther., 4 (2005) 625-631.

[15] Y. Taniyama, K. Tachibana, K. Hiraoka, T. Namba, K. Yamasaki, N. Hashiya, M. Aoki, T. Ogihara, K. Yasufumi, R. Morishita, Local delivery of plasmid DNA into rat carotid artery using ultrasound, Circulation, 105 (2002) 1233-1239.

[16] Y. Zou, G. Zong, Y.H. Ling, M.M. Hao, G. Lozano, W.K. Hong, R. Perez-Soler, Effective treatment of early endobronchial cancer with regional administration of liposome-p53 complexes, J. Natl. Cancer Inst., 90 (1998) 1130-1137.

[17] D. Kobelt, M. Schleef, M. Schmeer, J. Aumann, P.M. Schlag, W. Walther, Performance of high quality minicircle DNA for in vitro and in vivo gene transfer, Mol. Biotechnol., 53 (2013) 80-89.

[18] P. Mayrhofer, M. Schleef, W. Jechlinger, Use of minicircle plasmids for gene therapy, Methods Mol Biol, 542 (2009) 87-104.

[19] M.J. Osborn, R.T. McElmurry, C.J. Lees, A.P. DeFeo, Z.Y. Chen, M.A. Kay, L. Naldini, G. Freeman, J. Tolar, B.R. Blazar, Minicircle DNA-based gene therapy coupled with immune modulation permits long-term expression of alpha-L-iduronidase in mice with mucopolysaccharidosis type I, Mol. Ther., 19 (2011) 450-460.

[20] L.E. Gracey Maniar, J.M. Maniar, Z.Y. Chen, J. Lu, A.Z. Fire, M.A. Kay, Minicircle DNA vectors achieve sustained expression reflected by active chromatin and transcriptional level, Mol. Ther., 21 (2013) 131-138.

[21] J. Wu, X. Xiao, P. Zhao, G. Xue, Y. Zhu, X. Zhu, L. Zheng, Y. Zeng, W. Huang, Minicircle-IFNgamma induces antiproliferative and antitumoral effects in human nasopharyngeal carcinoma, Clinical cancer research : an official journal of the American Association for Cancer Research, 12 (2006) 4702-4713.

[22] J.H. Park, M. Lee, S.W. Kim, Non-viral adiponectin gene therapy into obese type 2 diabetic mice ameliorates insulin resistance, J Control Release, 114 (2006) 118-125.

[23] J.H. Chan, S. Lim, W.S. Wong, Antisense oligonucleotides: from design to therapeutic application, Clin. Exp. Pharmacol. Physiol., 33 (2006) 533-540.

[24] N. Dias, C.A. Stein, Antisense oligonucleotides: basic concepts and mechanisms, Mol. Cancer Ther., 1 (2002) 347-355.

[25] A.L. Southwell, N.H. Skotte, C.F. Bennett, M.R. Hayden, Antisense oligonucleotide therapeutics for inherited neurodegenerative diseases, Trends Mol. Med., 18 (2012) 634-643.

[26] Y. Imai, S. Boyle, G.M. Varela, E. Caron, X. Yin, R. Dhir, M.J. Graham, R.S. Ahima, Effects of perilipin 2 antisense oligonucleotide treatment on hepatic lipid metabolism and gene expression, Physiol Genomics, 44 (2012) 1125-1131.

[27] H. Miyake, M. Fujisawa, Promise of antisense oligodeoxynucleotide-based therapy for bladder cancer, Expert Rev Anticancer Ther, 8 (2008) 1851-1854.

[28] R.A. Smith, T.M. Miller, K. Yamanaka, B.P. Monia, T.P. Condon, G. Hung, C.S. Lobsiger, C.M. Ward, M. McAlonis-Downes, H. Wei, E.V. Wancewicz, C.F. Bennett, D.W. Cleveland, Antisense oligonucleotide therapy for neurodegenerative disease, J. Clin. Invest., 116 (2006) 2290-2296.

[29] A. Fire, S.Q. Xu, M.K. Montgomery, S.A. Kostas, S.E. Driver, C.C. Mello, Potent and specific genetic interference by double-stranded RNA in Caenorhabditis elegans, Nature, 391 (1998) 806-811.

[30] J.C. Burnett, J.J. Rossi, K. Tiemann, Current progress of siRNA/shRNA therapeutics in clinical trials, Biotechnol. J., 6 (2011) 1130-1146.

[31] J.K. Watts, D.R. Corey, Clinical status of duplex RNA, Bioorg. Med. Chem. Lett., 20 (2010) 3203-3207.

[32] B.L. Davidson, P.B. McCray, Jr., Current prospects for RNA interference-based therapies, Nat. Rev. Genet., 12 (2011) 329-340.

[33] T. Tokatlian, T. Segura, siRNA applications in nanomedicine, Wiley Interdisciplinary Reviews-Nanomedicine and Nanobiotechnology, 2 (2010) 305-315.

[34] H. Xia, Q. Mao, H.L. Paulson, B.L. Davidson, siRNA-mediated gene silencing in vitro and in vivo, Nat. Biotechnol., 20 (2002) 1006-1010.

[35] N. Senzer, M. Barve, J. Kuhn, A. Melnyk, P. Beitsch, M. Lazar, S. Lifshitz, M. Magee, J. Oh, S.W. Mill, C. Bedell, C. Higgs, P. Kumar, Y. Yu, F. Norvell, C. Phalon, N. Taquet, D.D. Rao, Z. Wang, C.M. Jay, B.O. Pappen, G. Wallraven, F.C. Brunicardi, D.M. Shanahan, P.B. Maples, J. Nemunaitis, Phase I trial of "bi-shRNAi(furin)/GMCSF DNA/autologous tumor cell" vaccine (FANG) in advanced cancer, Mol. Ther., 20 (2012) 679-686.

[36] S. Seth, R. Johns, M.V. Templin, Delivery and biodistribution of siRNA for cancer therapy: challenges and future prospects, Ther Deliv, 3 (2012) 245-261.

[37] G. Tavernier, O. Andries, J. Demeester, N.N. Sanders, S.C. De Smedt, J. Rejman, mRNA as gene therapeutic: how to control protein expression, J Control Release, 150 (2011) 238-247.

[38] L. He, G.J. Hannon, MicroRNAs: small RNAs with a big role in gene regulation, Nat. Rev. Genet., 5 (2004) 522-531.

[39] Y. Lee, K. Jeon, J.T. Lee, S. Kim, V.N. Kim, MicroRNA maturation: stepwise processing and subcellular localization, EMBO J., 21 (2002) 4663-4670.

[40] J. Krutzfeldt, N. Rajewsky, R. Braich, K.G. Rajeev, T. Tuschl, M. Manoharan, M. Stoffel, Silencing of microRNAs in vivo with 'antagomirs', Nature, 438 (2005) 685-689.

[41] M. Yang, J. Mattes, Discovery, biology and therapeutic potential of RNA interference, microRNA and antagomirs, Pharmacol. Ther., 117 (2008) 94-104.

[42] E. Song, P. Zhu, S.K. Lee, D. Chowdhury, S. Kussman, D.M. Dykxhoorn, Y. Feng, D. Palliser, D.B. Weiner, P. Shankar, W.A. Marasco, J. Lieberman, Antibody mediated in vivo delivery of small interfering RNAs via cell-surface receptors, Nat. Biotechnol., 23 (2005) 709-717.

[43] Y.P. Liu, B. Berkhout, miRNA cassettes in viral vectors: Problems and solutions, Biochim. Biophys. Acta, (2011).

[44] N.M. Rao, Cationic lipid-mediated nucleic acid delivery: beyond being cationic, Chem. Phys. Lipids, 163 (2010) 245-252.

[45] A. Schroeder, C.G. Levins, C. Cortez, R. Langer, D.G. Anderson, Lipid-based nanotherapeutics for siRNA delivery, J Intern Med, 267 (2010) 9-21.

[46] T. Tagami, T. Suzuki, M. Matsunaga, K. Nakamura, N. Moriyoshi, T. Ishida, H. Kiwada, Anti-angiogenic therapy via cationic liposome-mediated systemic siRNA delivery, Int. J. Pharm., (2011).

[47] A.K. Kundu, P.K. Chandra, S. Hazari, Y.V. Pramar, S. Dash, T.K. Mandal, Development and optimization of nanosomal formulations for siRNA delivery to the liver, Eur J Pharm Biopharm, (2011).

[48] C.W. Chen, D.W. Lu, M.K. Yeh, C.Y. Shiau, C.H. Chiang, Novel RGD-lipid conjugate-modified liposomes for enhancing siRNA delivery in human retinal pigment epithelial cells, Int J Nanomedicine, 6 (2011) 2567-2580.

[49] Y. Inoh, T. Furuno, N. Hirashima, D. Kitamoto, M. Nakanishi, Rapid delivery of small interfering RNA by biosurfactant MEL-A-containing liposomes, Biochem. Biophys. Res. Commun., 414 (2011) 635-640.

[50] P.M. LoRusso, R. Canetta, J.A. Wagner, E.P. Balogh, S.J. Nass, S.A. Boerner, J. Hohneker, Accelerating cancer therapy development: the importance of combination strategies and collaboration. Summary of an institute of medicine workshop, Clinical cancer research : an official journal of the American Association for Cancer Research, 18 (2012) 6101-6109.

[51] J.H. Lee, A. Nan, Combination drug delivery approaches in metastatic breast cancer, J Drug Deliv, 2012 (2012) 915375.

[52] G. Szakacs, J.K. Paterson, J.A. Ludwig, C. Booth-Genthe, M.M. Gottesman, Targeting multidrug resistance in cancer, Nat Rev Drug Discov, 5 (2006) 219-234.

[53] S.M. McAuliffe, S.L. Morgan, G.A. Wyant, L.T. Tran, K.W. Muto, Y.S. Chen, K.T. Chin, J.C. Partridge, B.B. Poole, K.H. Cheng, J. Daggett, Jr., K. Cullen, E. Kantoff, K. Hasselbatt, J. Berkowitz, M.G. Muto, R.S. Berkowitz, J.C. Aster, U.A. Matulonis, D.M. Dinulescu, Targeting Notch, a key pathway for ovarian cancer stem cells, sensitizes tumors to platinum therapy, Proc. Natl. Acad. Sci. U. S. A., 109 (2012) E2939-2948.

[54] D. Hanahan, R.A. Weinberg, The hallmarks of cancer, Cell, 100 (2000) 57-70.

[55] H. Ganjavi, M. Gee, A. Narendran, N. Parkinson, M. Krishnamoorthy, M.H. Freedman, D. Malkin, Adenovirus-mediated p53 gene therapy in osteosarcoma cell lines: sensitization to cisplatin and doxorubicin, Cancer Gene Ther., 13 (2006) 415-419.

[56] M. Jiang, Z. Liu, Y. Xiang, H. Ma, S. Liu, Y. Liu, D. Zheng, Synergistic antitumor effect of AAV-mediated TRAIL expression combined with cisplatin on head and neck squamous cell carcinoma, BMC Cancer, 11 (2011) 54.

[57] B. Su, A. Cengizeroglu, K. Farkasova, J.R. Viola, M. Anton, J.W. Ellwart, R. Haase, E. Wagner, M. Ogris, Systemic TNFalpha gene therapy synergizes with liposomal doxorubicine in the treatment of metastatic cancer, Mol. Ther., 21 (2013) 300-308.

[58] K. Nakamura, A.S. Abu Lila, M. Matsunaga, Y. Doi, T. Ishida, H. Kiwada, A double-modulation strategy in cancer treatment with a chemotherapeutic agent and siRNA, Mol. Ther., 19 (2011) 2040-2047.

[59] Z. Khan, R.P. Tiwari, N. Khan, G. Prasad, P.S. Bisen, Induction of apoptosis and sensitization of head and neck squamous carcinoma cells to cisplatin by targeting survivin gene expression, Curr. Gene Ther., (2012).

[60] Q. Hu, W. Li, X. Hu, Q. Hu, J. Shen, X. Jin, J. Zhou, G. Tang, P.K. Chu, Synergistic treatment of ovarian cancer by co-delivery of survivin shRNA and paclitaxel via supramolecular micellar assembly, Biomaterials, 33 (2012) 6580-6591.

[61] M.M. Janat-Amsbury, J.W. Yockman, M. Lee, S. Kern, D.Y. Furgeson, M. Bikram, S.W. Kim, Combination of local, nonviral IL12 gene therapy and systemic paclitaxel treatment in a metastatic breast cancer model, Mol. Ther., 9 (2004) 829-836.

[62] H.Y. Huang, W.T. Kuo, M.J. Chou, Y.Y. Huang, Co-delivery of anti-vascular endothelial growth factor siRNA and doxorubicin by multifunctional polymeric micelle for tumor growth suppression, J Biomed Mater Res A, 97 (2011) 330-338.

[63] C.M. Hu, S. Aryal, L. Zhang, Nanoparticle-assisted combination therapies for effective cancer treatment, Ther Deliv, 1 (2010) 323-334.

[64] N. Cao, D. Cheng, S. Zou, H. Ai, J. Gao, X. Shuai, The synergistic effect of hierarchical assemblies of siRNA and chemotherapeutic drugs co-delivered into hepatic cancer cells, Biomaterials, 32 (2011) 2222-2232.

[65] D. Cheng, N. Cao, J. Chen, X. Yu, X. Shuai, Multifunctional nanocarrier mediated co-delivery of doxorubicin and siRNA for synergistic enhancement of glioma apoptosis in rat, Biomaterials, 33 (2012) 1170-1179.

[66] A.M. Chen, M. Zhang, D. Wei, D. Stueber, O. Taratula, T. Minko, H. He, Co-delivery of doxorubicin and Bcl-2 siRNA by mesoporous silica nanoparticles enhances the efficacy of chemotherapy in multidrug-resistant cancer cells, Small, 5 (2009) 2673-2677.

[67] Y. Wang, S. Gao, W.H. Ye, H.S. Yoon, Y.Y. Yang, Co-delivery of drugs and DNA from cationic core-shell nanoparticles self-assembled from a biodegradable copolymer, Nat. Mater., 5 (2006) 791-796.

[68] M. Saad, O.B. Garbuzenko, T. Minko, Co-delivery of siRNA and an anticancer drug for treatment of multidrug-resistant cancer, Nanomedicine (Lond), 3 (2008) 761-776.

[69] Y. Chen, S.R. Bathula, J. Li, L. Huang, Multifunctional nanoparticles delivering small interfering RNA and doxorubicin overcome drug resistance in cancer, J. Biol. Chem., 285 (2010) 22639-22650.

[70] Y. Chen, J.J. Wu, L. Huang, Nanoparticles targeted with NGR motif deliver c-myc siRNA and doxorubicin for anticancer therapy, Mol. Ther., 18 (2010) 828-834.

[71] Y. Chen, J. Sen, S.R. Bathula, Q. Yang, R. Fittipaldi, L. Huang, Novel cationic lipid that delivers siRNA and enhances therapeutic effect in lung cancer cells, Mol. Pharm., 6 (2009) 696-705.

[72] C. Kim, B.P. Shah, P. Subramaniam, K.B. Lee, Synergistic induction of apoptosis in brain cancer cells by targeted codelivery of siRNA and anticancer drugs, Mol. Pharm., 8 (2011) 1955-1961.

[73] G. Shim, S.E. Han, Y.H. Yu, S. Lee, H.Y. Lee, K. Kim, I.C. Kwon, T.G. Park, Y.B. Kim, Y.S. Choi, C.W. Kim, Y.K. Oh, Trilysinoyl oleylamide-based cationic liposomes for systemic co-delivery of siRNA and an anticancer drug, J Control Release, 155 (2011) 60-66.

[74] R.S. Chang, M.S. Suh, S. Kim, G. Shim, S. Lee, S.S. Han, K.E. Lee, H. Jeon, H.G. Choi, Y. Choi, C.W. Kim, Y.K. Oh, Cationic drug-derived nanoparticles for multifunctional delivery of anticancer siRNA, Biomaterials, 32 (2011) 9785-9795.

[75] Y.H. Yu, E. Kim, D.E. Park, G. Shim, S. Lee, Y.B. Kim, C.W. Kim, Y.K. Oh, Cationic solid lipid nanoparticles for co-delivery of paclitaxel and siRNA, Eur J Pharm Biopharm, 80 (2012) 268-273.

[76] X.B. Xiong, A. Lavasanifar, Traceable multifunctional micellar nanocarriers for cancer-targeted co-delivery of MDR-1 siRNA and doxorubicin, ACS Nano, 5 (2011) 5202-5213.

[77] J.M. Li, Y.Y. Wang, M.X. Zhao, C.P. Tan, Y.Q. Li, X.Y. Le, L.N. Ji, Z.W. Mao, Multifunctional QD-based co-delivery of siRNA and doxorubicin to HeLa cells for reversal of multidrug resistance and real-time tracking, Biomaterials, 33 (2012) 2780-2790.

[78] M. Han, Q. Lv, X.J. Tang, Y.L. Hu, D.H. Xu, F.Z. Li, W.Q. Liang, J.Q. Gao, Overcoming drug resistance of MCF-7/ADR cells by altering intracellular distribution of

doxorubicin via MVP knockdown with a novel siRNA polyamidoamine-hyaluronic acid complex, J Control Release, 163 (2012) 136-144.

[79] Y.B. Patil, S.K. Swaminathan, T. Sadhukha, L. Ma, J. Panyam, The use of nanoparticle-mediated targeted gene silencing and drug delivery to overcome tumor drug resistance, Biomaterials, 31 (2010) 358-365.

[80] H.A. Meng, M. Liong, T.A. Xia, Z.X. Li, Z.X. Ji, J.I. Zink, A.E. Nel, Engineered Design of Mesoporous Silica Nanoparticles to Deliver Doxorubicin and P-Glycoprotein siRNA to Overcome Drug Resistance in a Cancer Cell Line, ACS Nano, 4 (2010) 4539-4550.

[81] T.M. Sun, J.Z. Du, Y.D. Yao, C.Q. Mao, S. Dou, S.Y. Huang, P.Z. Zhang, K.W. Leong, E.W. Song, J. Wang, Simultaneous delivery of siRNA and paclitaxel via a "two-in-one" micelleplex promotes synergistic tumor suppression, ACS Nano, 5 (2011) 1483-1494.

[82] Q. Hu, W. Li, X. Hu, J. Shen, X. Jin, J. Zhou, G. Tang, P.K. Chu, Synergistic treatment of ovarian cancer by co-delivery of survivin shRNA and paclitaxel via supramolecular micellar assembly, Biomaterials, 33 (2012) 6580-6591.

[83] L. Han, R. Huang, J. Li, S. Liu, S. Huang, C. Jiang, Plasmid pORF-hTRAIL and doxorubicin co-delivery targeting to tumor using peptide-conjugated polyamidoamine dendrimer, Biomaterials, 32 (2011) 1242-1252.

[84] S. Liu, Y. Guo, R. Huang, J. Li, S. Huang, Y. Kuang, L. Han, C. Jiang, Gene and doxorubicin co-delivery system for targeting therapy of glioma, Biomaterials, 33 (2012) 4907-4916.

[85] C. Zhu, S. Jung, S. Luo, F. Meng, X. Zhu, T.G. Park, Z. Zhong, Co-delivery of siRNA and paclitaxel into cancer cells by biodegradable cationic micelles based on PDMAEMA-PCL-PDMAEMA triblock copolymers, Biomaterials, 31 (2010) 2408-2416.

[86] A. Venne, S. Li, R. Mandeville, A. Kabanov, V. Alakhov, Hypersensitizing effect of pluronic L61 on cytotoxic activity, transport, and subcellular distribution of doxorubicin in multiple drug-resistant cells, Cancer Res., 56 (1996) 3626-3629.

[87] E.V. Batrakova, S. Li, W.F. Elmquist, D.W. Miller, V.Y. Alakhov, A.V. Kabanov, Mechanism of sensitization of MDR cancer cells by Pluronic block copolymers: Selective energy depletion, Br. J. Cancer, 85 (2001) 1987-1997.

[88] D.Y. Alakhova, N.Y. Rapoport, E.V. Batrakova, A.A. Timoshin, S. Li, D. Nicholls, V.Y. Alakhov, A.V. Kabanov, Differential metabolic responses to pluronic in MDR and non-MDR cells: a novel pathway for chemosensitization of drug resistant cancers, J Control Release, 142 (2010) 89-100.

[89] Z. Yang, G. Sahay, S. Sriadibhatla, A.V. Kabanov, Amphiphilic block copolymers enhance cellular uptake and nuclear entry of polyplex-delivered DNA, Bioconjug Chem, 19 (2008) 1987-1994.

[90] M.E. Martin, K.G. Rice, A novel class of intrinsic proteasome inhibitory gene transfer peptides, Bioconjug Chem, 19 (2008) 370-376.

[91] J. Li, Y. Zhu, S.T. Hazeldine, C. Li, D. Oupicky, Dual-function CXCR4 antagonist polyplexes to deliver gene therapy and inhibit cancer cell invasion, Angew. Chem. Int. Ed. Engl., 51 (2012) 8740-8743.

[92] K.E. Luker, G.D. Luker, Functions of CXCL12 and CXCR4 in breast cancer, Cancer Lett, 238 (2006) 30-41.

[93] J.D. Benson, Y.N. Chen, S.A. Cornell-Kennon, M. Dorsch, S. Kim, M. Leszczyniecka, W.R. Sellers, C. Lengauer, Validating cancer drug targets, Nature, 441 (2006) 451-456.

[94] K. Igarashi, K. Kashiwagi, Modulation of cellular function by polyamines, Int. J. Biochem. Cell Biol., 42 (2010) 39-51.

[95] A.E. Pegg, R.A. Casero, Jr., Current status of the polyamine research field, Methods Mol Biol, 720 (2011) 3-35.

[96] C.W. Tabor, H. Tabor, Polyamines, Annu. Rev. Biochem., 53 (1984) 749-790.

[97] A.C. Childs, D.J. Mehta, E.W. Gerner, Polyamine-dependent gene expression, Cell. Mol. Life Sci., 60 (2003) 1394-1406.

[98] L. Brieger, Weitere Untersuchungen √ºber Ptomaine, A. Hirschwald, 1885.

[99] V. Battaglia, C. Destefano Shields, T. Murray-Stewart, R.A. Casero, Jr., Polyamine catabolism in carcinogenesis: potential targets for chemotherapy and chemoprevention, Amino Acids, (2013).

[100] M.H. Park, K. Igarashi, Polyamines and Their Metabolites as Diagnostic Markers of Human Diseases, Biomol Ther (Seoul), 21 (2013) 1-9.

[101] R.A. Casero, Jr., L.J. Marton, Targeting polyamine metabolism and function in cancer and other hyperproliferative diseases, Nat Rev Drug Discov, 6 (2007) 373-390.

[102] S. Watanabe, K. Kusama-Eguchi, H. Kobayashi, K. Igarashi, Estimation of polyamine binding to macromolecules and ATP in bovine lymphocytes and rat liver, J. Biol. Chem., 266 (1991) 20803-20809.

[103] S.L. Nowotarski, P.M. Woster, R.A. Casero, Jr., Polyamines and cancer: implications for chemotherapy and chemoprevention, Expert Rev Mol Med, 15 (2013) e3.

[104] N. Minois, D. Carmona-Gutierrez, F. Madeo, Polyamines in aging and disease, Aging (Albany NY), 3 (2011) 716-732.

[105] A. Clifford, D. Morgan, S.H. Yuspa, A.P. Soler, S. Gilmour, Role of ornithine decarboxylase in epidermal tumorigenesis, Cancer Res., 55 (1995) 1680-1686.

[106] C. Loser, A. Eisel, D. Harms, U.R. Folsch, Dietary polyamines are essential luminal growth factors for small intestinal and colonic mucosal growth and development, Gut, 44 (1999) 12-16.

[107] P. Marko, C.H. Loser, H. Fluckiger, P.M. Davies, Dietary influence on the urinary excretion of polyamines, Bratisl Lek Listy, 99 (1998) 339-342.

[108] M. Zhang, C.M. Pickart, P. Coffino, Determinants of proteasome recognition of ornithine decarboxylase, a ubiquitin-independent substrate, EMBO J., 22 (2003) 1488-1496.

[109] S. Roje, S-Adenosyl-L-methionine: beyond the universal methyl group donor, Phytochemistry, 67 (2006) 1686-1698.

[110] A.E. Pegg, Spermidine/spermine-N(1)-acetyltransferase: a key metabolic regulator, Am J Physiol Endocrinol Metab, 294 (2008) E995-1010.

[111] S. Vujcic, P. Liang, P. Diegelman, D.L. Kramer, C.W. Porter, Genomic identification and biochemical characterization of the mammalian polyamine oxidase involved in polyamine back-conversion, Biochem. J., 370 (2003) 19-28.

[112] M. Cervelli, R. Amendola, F. Polticelli, P. Mariottini, Spermine oxidase: ten years after, Amino Acids, 42 (2012) 441-450.

[113] Y. Chen, D.L. Kramer, P. Diegelman, S. Vujcic, C.W. Porter, Apoptotic signaling in polyamine analogue-treated SK-MEL-28 human melanoma cells, Cancer Res., 61 (2001) 6437-6444.

[114] H.C. Ha, P.M. Woster, J.D. Yager, R.A. Casero, Jr., The role of polyamine catabolism in polyamine analogue-induced programmed cell death, Proc. Natl. Acad. Sci. U. S. A., 94 (1997) 11557-11562.

[115] M. Kawakita, K. Hiramatsu, Diacetylated derivatives of spermine and spermidine as novel promising tumor markers, J Biochem, 139 (2006) 315-322.

[116] D. Russell, S.H. Snyder, Amine synthesis in rapidly growing tissues: ornithine decarboxylase activity in regenerating rat liver, chick embryo, and various tumors, Proc. Natl. Acad. Sci. U. S. A., 60 (1968) 1420-1427.

[117] C. Bello-Fernandez, G. Packham, J.L. Cleveland, The ornithine decarboxylase gene is a transcriptional target of c-Myc, Proc. Natl. Acad. Sci. U. S. A., 90 (1993) 7804-7808.

[118] X. Xu, Z. Liu, M. Fang, H. Yu, X. Liang, X. Li, X. Liu, C. Chen, J. Jia, Helicobacter pylori CagA induces ornithine decarboxylase upregulation via Src/MEK/ERK/c-Myc pathway: implication for progression of gastric diseases, Exp Biol Med (Maywood), 237 (2012) 435-441.

[119] E.D. Arisan, P. Obakan, A. Coker, N. Palavan-Unsal, Inhibition of ornithine decarboxylase alters the roscovitine-induced mitochondrial-mediated apoptosis in MCF-7 breast cancer cells, Mol Med Rep, 5 (2012) 1323-1329.

[120] J.A. Nilsson, U.B. Keller, T.A. Baudino, C. Yang, S. Norton, J.A. Old, L.M. Nilsson, G. Neale, D.L. Kramer, C.W. Porter, J.L. Cleveland, Targeting ornithine decarboxylase in Myc-induced lymphomagenesis prevents tumor formation, Cancer Cell, 7 (2005) 433-444.

[121] P.P. Grimminger, P.M. Schneider, R. Metzger, D. Vallbohmer, K.D. Danenberg, P.V. Danenberg, A.H. Holscher, J. Brabender, Ornithine decarboxylase mRNA expression in curatively resected non-small-cell lung cancer, Clin Lung Cancer, 11 (2010) 114-119.

[122] S. Gupta, N. Ahmad, S.R. Marengo, G.T. MacLennan, N.M. Greenberg, H. Mukhtar, Chemoprevention of prostate carcinogenesis by alpha-difluoromethylornithine in TRAMP mice, Cancer Res., 60 (2000) 5125-5133.

[123] W. Deng, X. Jiang, Y. Mei, J. Sun, R. Ma, X. Liu, H. Sun, H. Tian, X. Sun, Role of ornithine decarboxylase in breast cancer, Acta Biochim Biophys Sin (Shanghai), 40 (2008) 235-243.

[124] T.G. O'Brien, L.C. Megosh, G. Gilliard, A.P. Soler, Ornithine decarboxylase overexpression is a sufficient condition for tumor promotion in mouse skin, Cancer Res., 57 (1997) 2630-2637.

[125] D.L. Koomoa, T. Borsics, D.J. Feith, C.C. Coleman, C.J. Wallick, I. Gamper, A.E. Pegg, A.S. Bachmann, Inhibition of S-adenosylmethionine decarboxylase by inhibitor SAM486A connects polyamine metabolism with p53-Mdm2-Akt/protein kinase B regulation and apoptosis in neuroblastoma, Mol. Cancer Ther., 8 (2009) 2067-2075.

[126] K. Ravanko, K. Jarvinen, J. Helin, N. Kalkkinen, E. Holtta, Cysteine cathepsins are central contributors of invasion by cultured adenosylmethionine decarboxylase-transformed rodent fibroblasts, Cancer Res., 64 (2004) 8831-8838.

[127] X. Hu, S. Washington, M.F. Verderame, L.M. Demers, D. Mauger, A. Manni, Biological activity of the S-adenosylmethionine decarboxylase inhibitor SAM486A in human breast cancer cells in vitro and in vivo, Int J Oncol, 25 (2004) 1831-1838.

[128] N. Seiler, Thirty years of polyamine-related approaches to cancer therapy. Retrospect and prospect. Part 1. Selective enzyme inhibitors, Curr. Drug Targets, 4 (2003) 537-564.

[129] A.M. De Marzo, V.L. Marchi, J.I. Epstein, W.G. Nelson, Proliferative inflammatory atrophy of the prostate: implications for prostatic carcinogenesis, Am. J. Pathol., 155 (1999) 1985-1992.

[130] A.C. Goodwin, S. Jadallah, A. Toubaji, K. Lecksell, J.L. Hicks, J. Kowalski, G.S. Bova, A.M. De Marzo, G.J. Netto, R.A. Casero, Jr., Increased spermine oxidase expression in human prostate cancer and prostatic intraepithelial neoplasia tissues, Prostate, 68 (2008) 766-772.

[131] H. Xu, R. Chaturvedi, Y. Cheng, F.I. Bussiere, M. Asim, M.D. Yao, D. Potosky, S.J. Meltzer, J.G. Rhee, S.S. Kim, S.F. Moss, A. Hacker, Y. Wang, R.A. Casero, Jr., K.T. Wilson, Spermine oxidation induced by Helicobacter pylori results in apoptosis and DNA damage: implications for gastric carcinogenesis, Cancer Res., 64 (2004) 8521-8525.

[132] M. Cervelli, G. Bellavia, E. Fratini, R. Amendola, F. Polticelli, M. Barba, R. Federico, F. Signore, G. Gucciardo, R. Grillo, P.M. Woster, R.A. Casero, Jr., P.

Mariottini, Spermine oxidase (SMO) activity in breast tumor tissues and biochemical analysis of the anticancer spermine analogues BENSpm and CPENSpm, BMC Cancer, 10 (2010) 555.

[133] H.M. Wallace, J. Duthie, D.M. Evans, S. Lamond, K.M. Nicoll, S.D. Heys, Alterations in polyamine catabolic enzymes in human breast cancer tissue, Clinical cancer research : an official journal of the American Association for Cancer Research, 6 (2000) 3657-3661.

[134] M. Pietila, J.J. Parkkinen, L. Alhonen, J. Janne, Relation of skin polyamines to the hairless phenotype in transgenic mice overexpressing spermidine/spermine N-acetyltransferase, J. Invest. Dermatol., 116 (2001) 801-805.

[135] C.S. Coleman, A.E. Pegg, L.C. Megosh, Y. Guo, J.A. Sawicki, T.G. O'Brien, Targeted expression of spermidine/spermine N1-acetyltransferase increases susceptibility to chemically induced skin carcinogenesis, Carcinogenesis, 23 (2002) 359-364.

[136] N.A. Ignatenko, N. Babbar, D. Mehta, R.A. Casero, Jr., E.W. Gerner, Suppression of polyamine catabolism by activated Ki-ras in human colon cancer cells, Mol. Carcinog., 39 (2004) 91-102.

[137] K. Soda, The mechanisms by which polyamines accelerate tumor spread, J Exp Clin Cancer Res, 30 (2011) 95.

[138] L.D. Gamble, M.D. Hogarty, X. Liu, D.S. Ziegler, G. Marshall, M.D. Norris, M. Haber, Polyamine pathway inhibition as a novel therapeutic approach to treating neuroblastoma, Front Oncol, 2 (2012) 162.

[139] U.K. Basuroy, E.W. Gerner, Emerging concepts in targeting the polyamine metabolic pathway in epithelial cancer chemoprevention and chemotherapy, J Biochem, 139 (2006) 27-33.

[140] H.G. Williams-Ashman, A. Schenone, Methyl glyoxal bis(guanylhydrazone) as a potent inhibitor of mammalian and yeast S-adenosylmethionine decarboxylases, Biochem. Biophys. Res. Commun., 46 (1972) 288-295.

[141] C.W. Porter, D. Dworaczyk, B. Ganis, M.M. Weiser, Polyamines and biosynthetic enzymes in the rat intestinal mucosa and the influence of methylglyoxal-bis(guanylhydrazone), Cancer Res., 40 (1980) 2330-2335.

[142] M.M. Nass, Analysis of methylglyoxal bis(guanylhydrazone)-induced alterations of hamster tumor mitochondria by correlated studies of selective rhodamine binding, ultrastructural damage, DNA replication, and reversibility, Cancer Res., 44 (1984) 2677-2688.

[143] U. Regenass, H. Mett, J. Stanek, M. Mueller, D. Kramer, C.W. Porter, CGP 48664, a new S-adenosylmethionine decarboxylase inhibitor with broad spectrum antiproliferative and antitumor activity, Cancer Res., 54 (1994) 3210-3217.

[144] R. Paridaens, D.R. Uges, N. Barbet, L. Choi, M. Seeghers, W.T. van der Graaf, H.J. Groen, H. Dumez, I.V. Buuren, F. Muskiet, R. Capdeville, A.T. Oosterom, E.G. de Vries, A phase I study of a new polyamine biosynthesis inhibitor, SAM486A, in cancer patients with solid tumours, Br. J. Cancer, 83 (2000) 594-601.

[145] M. Pless, K. Belhadj, H.D. Menssen, W. Kern, B. Coiffier, J. Wolf, R. Herrmann, E. Thiel, D. Bootle, I. Sklenar, C. Muller, L. Choi, C. Porter, R. Capdeville, Clinical efficacy, tolerability, and safety of SAM486A, a novel polyamine biosynthesis inhibitor, in patients

with relapsed or refractory non-Hodgkin's lymphoma: results from a phase II multicenter study, Clinical cancer research : an official journal of the American Association for Cancer Research, 10 (2004) 1299-1305.

[146] P. Bey, C. Danzin, V. Van Dorsselaer, P. Mamont, M. Jung, C. Tardif, Analogues of ornithine as inhibitors of ornithine decarboxylase. New deductions concerning the topography of the enzyme's active site, J. Med. Chem., 21 (1978) 50-55.

[147] B.W. Metcalf, P. Bey, C. Danzin, M.J. Jung, P. Casara, J.P. Vevert, Catalytic irreversible inhibition of mammalian ornithine decarboxylase (E.C.4.1.1.17) by substrate and product analogs, J. Am. Chem. Soc., 100 (1978) 2551-2553.

[148] E.W. Gerner, P.S. Mamont, Restoration of the polyamine contents in rat hepatoma tissue-culture cells after inhibition of polyamine biosynthesis. Relationship with cell proliferation, Eur. J. Biochem., 156 (1986) 31-35.

[149] H.M. Wallace, A.V. Fraser, Inhibitors of polyamine metabolism: review article, Amino Acids, 26 (2004) 353-365.

[150] C. Danzin, P. Casara, N. Claverie, B.W. Metcalf, M.J. Jung, (2R,5R)-6-heptyne-2,5-diamine, an extremely potent inhibitor of mammalian ornithine decarboxylase, Biochem. Biophys. Res. Commun., 116 (1983) 237-243.

[151] A.E. Pegg, K.C. Tang, J.K. Coward, Effects of S-adenosyl-1,8-diamino-3-thiooctane on polyamine metabolism, Biochemistry, 21 (1982) 5082-5089.

[152] A.E. Pegg, R. Wechter, R. Poulin, P.M. Woster, J.K. Coward, Effect of S-adenosyl-1,12-diamino-3-thio-9-azadodecane, a multisubstrate adduct inhibitor of spermine synthase, on polyamine metabolism in mammalian cells, Biochemistry, 28 (1989) 8446-8453.

[153] C.W. Porter, R.J. Bergeron, Regulation of polyamine biosynthetic activity by spermidine and spermine analogs--a novel antiproliferative strategy, Adv. Exp. Med. Biol., 250 (1988) 677-690.

[154] R.A. Casero, Jr., P.M. Woster, Recent advances in the development of polyamine analogues as antitumor agents, J. Med. Chem., 52 (2009) 4551-4573.

[155] R.J. Bergeron, A.H. Neims, J.S. McManis, T.R. Hawthorne, J.R. Vinson, R. Bortell, M.J. Ingeno, Synthetic polyamine analogues as antineoplastics, J. Med. Chem., 31 (1988) 1183-1190.

[156] V.K. Reddy, A. Valasinas, A. Sarkar, H.S. Basu, L.J. Marton, B. Frydman, Conformationally restricted analogues of 1N,12N-bisethylspermine: synthesis and growth inhibitory effects on human tumor cell lines, J. Med. Chem., 41 (1998) 4723-4732.

[157] H.M. Wallace, A.V. Fraser, Polyamine analogues as anticancer drugs, Biochem. Soc. Trans., 31 (2003) 393-396.

[158] D.L. Kramer, S. Vujcic, P. Diegelman, J. Alderfer, J.T. Miller, J.D. Black, R.J. Bergeron, C.W. Porter, Polyamine analogue induction of the p53-p21WAF1/CIP1-Rb pathway and G1 arrest in human melanoma cells, Cancer Res., 59 (1999) 1278-1286.

[159] M. Fogel-Petrovic, D.L. Kramer, S. Vujcic, J. Miller, J.S. McManis, R.J. Bergeron, C.W. Porter, Structural basis for differential induction of spermidine/spermine N1-acetyltransferase activity by novel spermine analogs, Mol. Pharmacol., 52 (1997) 69-74.

[160] Y. Huang, A. Pledgie, E. Rubin, L.J. Marton, P.M. Woster, S. Sukumar, R.A. Casero, Jr., N.E. Davidson, Role of p53/p21(Waf1/Cip1) in the regulation of polyamine

analogue-induced growth inhibition and cell death in human breast cancer cells, Cancer biology & therapy, 4 (2005) 1006-1013.

[161] K.B. Wee, B.D. Aguda, Akt versus p53 in a network of oncogenes and tumor suppressor genes regulating cell survival and death, Biophys. J., 91 (2006) 857-865.

[162] T.M. Gottlieb, J.F. Leal, R. Seger, Y. Taya, M. Oren, Cross-talk between Akt, p53 and Mdm2: possible implications for the regulation of apoptosis, Oncogene, 21 (2002) 1299-1303.

[163] A. Valasinas, V.K. Reddy, A.V. Blokhin, H.S. Basu, S. Bhattacharya, A. Sarkar, L.J. Marton, B. Frydman, Long-chain polyamines (oligoamines) exhibit strong cytotoxicities against human prostate cancer cells, Bioorg. Med. Chem., 11 (2003) 4121-4131.

[164] Y. Huang, E.R. Hager, D.L. Phillips, V.R. Dunn, A. Hacker, B. Frydman, J.A. Kink, A.L. Valasinas, V.K. Reddy, L.J. Marton, R.A. Casero, Jr., N.E. Davidson, A novel polyamine analog inhibits growth and induces apoptosis in human breast cancer cells, Clinical cancer research : an official journal of the American Association for Cancer Research, 9 (2003) 2769-2777.

[165] Y. Huang, J.C. Keen, A. Pledgie, L.J. Marton, T. Zhu, S. Sukumar, B.H. Park, B. Blair, K. Brenner, R.A. Casero, Jr., N.E. Davidson, Polyamine analogues down-regulate estrogen receptor alpha expression in human breast cancer cells, J. Biol. Chem., 281 (2006) 19055-19063.

[166] B. Frydman, S. Bhattacharya, A. Sarkar, K. Drandarov, S. Chesnov, A. Guggisberg, K. Popaj, S. Sergeyev, A. Yurdakul, M. Hesse, H.S. Basu, L.J. Marton,

Macrocyclic polyamines deplete cellular ATP levels and inhibit cell growth in human prostate cancer cells, J. Med. Chem., 47 (2004) 1051-1059.

[167] L. Alhonen, A. Karppinen, M. Uusi-Oukari, S. Vujcic, V.P. Korhonen, M. Halmekyto, D.L. Kramer, R. Hines, J. Janne, C.W. Porter, Correlation of polyamine and growth responses to N1,N11-diethylnorspermine in primary fetal fibroblasts derived from transgenic mice overexpressing spermidine/spermine N1-acetyltransferase, J. Biol. Chem., 273 (1998) 1964-1969.

[168] S. Suppola, M. Pietila, J.J. Parkkinen, V.P. Korhonen, L. Alhonen, M. Halmekyto, C.W. Porter, J. Janne, Overexpression of spermidine/spermine N1-acetyltransferase under the control of mouse metallothionein I promoter in transgenic mice: evidence for a striking post-transcriptional regulation of transgene expression by a polyamine analogue, Biochem. J., 338 ( Pt 2) (1999) 311-316.

[169] W. Devereux, Y. Wang, T.M. Stewart, A. Hacker, R. Smith, B. Frydman, A.L. Valasinas, V.K. Reddy, L.J. Marton, T.D. Ward, P.M. Woster, R.A. Casero, Induction of the PAOh1/SMO polyamine oxidase by polyamine analogues in human lung carcinoma cells, Cancer Chemother Pharmacol, 52 (2003) 383-390.

[170] Y. Chen, K. Alm, S. Vujcic, D.L. Kramer, K. Kee, P. Diegelman, C.W. Porter, The role of mitogen-activated protein kinase activation in determining cellular outcomes in polyamine analogue-treated human melanoma cells, Cancer Res., 63 (2003) 3619-3625.

[171] N. Shah, T.J. Thomas, J.S. Lewis, C.M. Klinge, A. Shirahata, C. Gelinas, T. Thomas, Regulation of estrogenic and nuclear factor kappa B functions by polyamines

and their role in polyamine analog-induced apoptosis of breast cancer cells, Oncogene, 20 (2001) 1715-1729.

[172] E. Gabrielson, E. Tully, A. Hacker, A.E. Pegg, N.E. Davidson, R.A. Casero, Jr., Induction of spermidine/spermine N1-acetyltransferase in breast cancer tissues treated with the polyamine analogue N1, N11-diethylnorspermine, Cancer Chemother Pharmacol, 54 (2004) 122-126.

[173] C. Hegardt, O.T. Johannsson, S.M. Oredsson, Rapid caspase-dependent cell death in cultured human breast cancer cells induced by the polyamine analogue N(1),N(11)-diethylnorspermine, Eur. J. Biochem., 269 (2002) 1033-1039.

[174] D.L. Kramer, M. Fogel-Petrovic, P. Diegelman, J.M. Cooley, R.J. Bernacki, J.S. McManis, R.J. Bergeron, C.W. Porter, Effects of novel spermine analogues on cell cycle progression and apoptosis in MALME-3M human melanoma cells, Cancer Res., 57 (1997) 5521-5527.

[175] V.M. Johansson, S.M. Oredsson, K. Alm, Polyamine depletion with two different polyamine analogues causes DNA damage in human breast cancer cell lines, DNA Cell Biol., 27 (2008) 511-516.

[176] A. Pledgie, Y. Huang, A. Hacker, Z. Zhang, P.M. Woster, N.E. Davidson, R.A. Casero, Jr., Spermine oxidase SMO(PAOh1), Not N1-acetylpolyamine oxidase PAO, is the primary source of cytotoxic H2O2 in polyamine analogue-treated human breast cancer cell lines, J. Biol. Chem., 280 (2005) 39843-39851.

[177] B.K. Chang, R.J. Bergeron, C.W. Porter, J.R. Vinson, Y. Liang, P.R. Libby, Regulatory and antiproliferative effects of N-alkylated polyamine analogues in human

and hamster pancreatic adenocarcinoma cell lines, Cancer Chemother Pharmacol, 30 (1992) 183-188.

[178] B.K. Chang, R.J. Bergeron, C.W. Porter, Y. Liang, Antitumor effects of N-alkylated polyamine analogues in human pancreatic adenocarcinoma models, Cancer Chemother Pharmacol, 30 (1992) 179-182.

[179] E. Soderstjerna, C.M. Holst, K. Alm, S.M. Oredsson, Apoptosis induced by the potential chemotherapeutic drug N1, N11-Diethylnorspermine in a neuroblastoma cell line, Anticancer Drugs, 21 (2010) 917-926.

[180] L. Myhre, K. Alm, C. Hegardt, J. Staaf, G. Jonsson, S. Larsson, S.M. Oredsson, Different cell cycle kinetic effects of N1,N11-diethylnorspermine-induced polyamine depletion in four human breast cancer cell lines, Anticancer Drugs, 19 (2008) 359-368.

[181] Y. Chen, D.L. Kramer, F. Li, C.W. Porter, Loss of inhibitor of apoptosis proteins as a determinant of polyamine analog-induced apoptosis in human melanoma cells, Oncogene, 22 (2003) 4964-4972.

[182] Y. Tian, S. Wang, B. Wang, J. Zhang, R. Jiang, W. Zhang, Overexpression of SSAT by DENSPM treatment induces cell detachment and apoptosis in glioblastoma, Oncology reports, 27 (2012) 1227-1232.

[183] R. Jiang, W. Choi, L. Hu, E.W. Gerner, S.R. Hamilton, W. Zhang, Activation of polyamine catabolism by N1, N11-diethylnorspermine alters the cellular localization of mTOR and downregulates mTOR protein level in glioblastoma cells, Cancer biology & therapy, 6 (2007) 1644-1648.

[184] G.P. Zagaja, M. Shrivastav, M.J. Fleig, L.J. Marton, C.W. Rinker-Schaeffer, M.E. Dolan, Effects of polyamine analogues on prostatic adenocarcinoma cells in vitro and in vivo, Cancer Chemother Pharmacol, 41 (1998) 505-512.

[185] R.G. Schipper, G. Deli, P. Deloyer, W.P. Lange, J.A. Schalken, A.A. Verhofstad, Antitumor activity of the polyamine analog N(1), N(11)-diethylnorspermine against human prostate carcinoma cells, Prostate, 44 (2000) 313-321.

[186] R. Jiang, W. Choi, A. Khan, K. Hess, E.W. Gerner, R.A. Casero, Jr., W.K. Yung, S.R. Hamilton, W. Zhang, Activation of polyamine catabolism by N1,N11-diethylnorspermine leads to cell death in glioblastoma, Int J Oncol, 31 (2007) 431-440.

[187] R.J. Bernacki, E.J. Oberman, K.E. Seweryniak, A. Atwood, R.J. Bergeron, C.W. Porter, Preclinical antitumor efficacy of the polyamine analogue N1, N11-diethylnorspermine administered by multiple injection or continuous infusion, Clinical cancer research : an official journal of the American Association for Cancer Research, 1 (1995) 847-857.

[188] R.J. Bernacki, R.J. Bergeron, C.W. Porter, Antitumor activity of N,N'-bis(ethyl)spermine homologues against human MALME-3 melanoma xenografts, Cancer Res., 52 (1992) 2424-2430.

[189] A. Sharma, D. Glaves, C.W. Porter, D. Raghavan, R.J. Bernacki, Antitumor efficacy of N1,N11-diethylnorspermine on a human bladder tumor xenograft in nude athymic mice, Clinical cancer research : an official journal of the American Association for Cancer Research, 3 (1997) 1239-1244.

[190] C.W. Porter, R.J. Bernacki, J. Miller, R.J. Bergeron, Antitumor activity of N1,N11-bis(ethyl)norspermine against human melanoma xenografts and possible biochemical correlates of drug action, Cancer Res., 53 (1993) 581-586.

[191] N. Shah, T. Antony, S. Haddad, P. Amenta, A. Shirahata, T.J. Thomas, T. Thomas, Antitumor effects of bis(ethyl)polyamine analogs on mammary tumor development in FVB/NTgN (MMTVneu) transgenic mice, Cancer Lett, 146 (1999) 15-23.

[192] R.R. Streiff, J.F. Bender, Phase 1 study of N1-N11-diethylnorspermine (DENSPM) administered TID for 6 days in patients with advanced malignancies, Invest. New Drugs, 19 (2001) 29-39.

[193] P.J. Creaven, R. Perez, L. Pendyala, N.J. Meropol, G. Loewen, E. Levine, E. Berghorn, D. Raghavan, Unusual central nervous system toxicity in a phase I study of N1N11 diethylnorspermine in patients with advanced malignancy, Invest. New Drugs, 15 (1997) 227-234.

[194] L. Goyal, J.G. Supko, J. Berlin, L.S. Blaszkowsky, A. Carpenter, D.M. Heuman, S.L. Hilderbrand, K.E. Stuart, S. Cotler, N.N. Senzer, E. Chan, C.L. Berg, J.W. Clark, A.F. Hezel, D.P. Ryan, A.X. Zhu, Phase 1 study of N ,N -diethylnorspermine (DENSPM) in patients with advanced hepatocellular carcinoma, Cancer Chemother Pharmacol, (2013).

[195] H.A. Hahm, D.S. Ettinger, K. Bowling, B. Hoker, T.L. Chen, Y. Zabelina, R.A. Casero, Jr., Phase I study of N(1),N(11)-diethylnorspermine in patients with non-small cell lung cancer, Clinical cancer research : an official journal of the American Association for Cancer Research, 8 (2002) 684-690.

[196] A.C. Wolff, D.K. Armstrong, J.H. Fetting, M.K. Carducci, C.D. Riley, J.F. Bender, R.A. Casero, Jr., N.E. Davidson, A Phase II study of the polyamine analog N1,N11-diethylnorspermine (DENSpm) daily for five days every 21 days in patients with previously treated metastatic breast cancer, Clinical cancer research : an official journal of the American Association for Cancer Research, 9 (2003) 5922-5928.

[197] S.K. Nair, A. Verma, T.J. Thomas, T.C. Chou, M.A. Gallo, A. Shirahata, T. Thomas, Synergistic apoptosis of MCF-7 breast cancer cells by 2-methoxyestradiol and bis(ethyl)norspermine, Cancer Lett, 250 (2007) 311-322.

[198] W. Choi, E.W. Gerner, L. Ramdas, J. Dupart, J. Carew, L. Proctor, P. Huang, W. Zhang, S.R. Hamilton, Combination of 5-fluorouracil and N1,N11-diethylnorspermine markedly activates spermidine/spermine N1-acetyltransferase expression, depletes polyamines, and synergistically induces apoptosis in colon carcinoma cells, J. Biol. Chem., 280 (2005) 3295-3304.

[199] A. Pledgie-Tracy, M. Billam, A. Hacker, M.D. Sobolewski, P.M. Woster, Z. Zhang, R.A. Casero, N.E. Davidson, The role of the polyamine catabolic enzymes SSAT and SMO in the synergistic effects of standard chemotherapeutic agents with a polyamine analogue in human breast cancer cell lines, Cancer Chemother Pharmacol, 65 (2010) 1067-1081.

[200] T.R. Hawthorne, J.K. Austin, Jr., Synergism of the polyamine analogue, N1,N11-bisethylnorspermine with cis-diaminedichloroplatinum (II) against murine neoplastic cell lines in vitro and in vivo, Cancer Lett, 99 (1996) 99-107.

[201] S. Hector, C.W. Porter, D.L. Kramer, K. Clark, J. Prey, N. Kisiel, P. Diegelman, Y. Chen, L. Pendyala, Polyamine catabolism in platinum drug action: Interactions between

oxaliplatin and the polyamine analogue N1,N11-diethylnorspermine at the level of spermidine/spermine N1-acetyltransferase, Mol. Cancer Ther., 3 (2004) 813-822.

[202] R. Tummala, P. Diegelman, S. Hector, D.L. Kramer, K. Clark, P. Zagst, G. Fetterly, C.W. Porter, L. Pendyala, Combination effects of platinum drugs and N1, N11 diethylnorspermine on spermidine/spermine N1-acetyltransferase, polyamines and growth inhibition in A2780 human ovarian carcinoma cells and their oxaliplatin and cisplatin-resistant variants, Cancer Chemother Pharmacol, 67 (2011) 401-414.

[203] S. Hector, R. Tummala, N.D. Kisiel, P. Diegelman, S. Vujcic, K. Clark, M. Fakih, D.L. Kramer, C.W. Porter, L. Pendyala, Polyamine catabolism in colorectal cancer cells following treatment with oxaliplatin, 5-fluorouracil and N1, N11 diethylnorspermine, Cancer Chemother Pharmacol, 62 (2008) 517-527.

[204] W.L. Allen, E.G. McLean, J. Boyer, A. McCulla, P.M. Wilson, V. Coyle, D.B. Longley, R.A. Casero, Jr., P.G. Johnston, The role of spermidine/spermine N1-acetyltransferase in determining response to chemotherapeutic agents in colorectal cancer cells, Mol. Cancer Ther., 6 (2007) 128-137.

[205] J. Rautio, H. Kumpulainen, T. Heimbach, R. Oliyai, D. Oh, T. Jarvinen, J. Savolainen, Prodrugs: design and clinical applications, Nat Rev Drug Discov, 7 (2008) 255-270.

[206] Q. Sun, J. Wang, M. Radosz, Y. Shen, Chapter 11 Polymer-Based Prodrugs for Cancer Chemotherapy, in: Functional Polymers for Nanomedicine, The Royal Society of Chemistry, 2013, pp. 245-260.

[207] R. Mahato, W. Tai, K. Cheng, Prodrugs for improving tumor targetability and efficiency, Adv Drug Deliv Rev, 63 (2011) 659-670.

[208] B.M. Liederer, R.T. Borchardt, Enzymes involved in the bioconversion of ester-based prodrugs, J. Pharm. Sci., 95 (2006) 1177-1195.

[209] C. Li, S. Wallace, Polymer-drug conjugates: recent development in clinical oncology, Adv Drug Deliv Rev, 60 (2008) 886-898.

[210] A.L. Simplicio, J.M. Clancy, J.F. Gilmer, Prodrugs for amines, Molecules, 13 (2008) 519-547.

[211] I.R. Vlahov, C.P. Leamon, Engineering folate-drug conjugates to target cancer: from chemistry to clinic, Bioconjug Chem, 23 (2012) 1357-1369.

[212] I.R. Vlahov, H.K. Santhapuram, P.J. Kleindl, S.J. Howard, K.M. Stanford, C.P. Leamon, Design and regioselective synthesis of a new generation of targeted chemotherapeutics. Part 1: EC145, a folic acid conjugate of desacetylvinblastine monohydrazide, Bioorg. Med. Chem. Lett., 16 (2006) 5093-5096.

[213] J. Kalia, R.T. Raines, Hydrolytic stability of hydrazones and oximes, Angew Chem Int Ed Engl, 47 (2008) 7523-7526.

[214] S. Jaracz, J. Chen, L.V. Kuznetsova, I. Ojima, Recent advances in tumor-targeting anticancer drug conjugates, Bioorg. Med. Chem., 13 (2005) 5043-5054.

[215] K.M. Huttunen, H. Raunio, J. Rautio, Prodrugs--from serendipity to rational design, Pharmacol Rev, 63 (2011) 750-771.

[216] R.J. Griffin, E. Evers, R. Davison, A.E. Gibson, D. Layton, W.J. Irwin, The 4-azidobenzyloxycarbonyl function; application as a novel protecting group and potential prodrug modification for amines, Journal of the Chemical Society, Perkin Transactions 1, (1996) 1205-1211.

[217] L. Bildstein, C. Dubernet, P. Couvreur, Prodrug-based intracellular delivery of anticancer agents, Adv Drug Deliv Rev, 63 (2011) 3-23.

[218] Y. Matsumura, H. Maeda, A new concept for macromolecular therapeutics in cancer chemotherapy: mechanism of tumoritropic accumulation of proteins and the antitumor agent smancs, Cancer Res., 46 (1986) 6387-6392.

[219] P.A. Vasey, S.B. Kaye, R. Morrison, C. Twelves, P. Wilson, R. Duncan, A.H. Thomson, L.S. Murray, T.E. Hilditch, T. Murray, S. Burtles, D. Fraier, E. Frigerio, J. Cassidy, Phase I clinical and pharmacokinetic study of PK1 [N-(2-hydroxypropyl)methacrylamide copolymer doxorubicin]: first member of a new class of chemotherapeutic agents-drug-polymer conjugates. Cancer Research Campaign Phase I/II Committee, Clinical cancer research : an official journal of the American Association for Cancer Research, 5 (1999) 83-94.

[220] J.G. Shiah, M. Dvorak, P. Kopeckova, Y. Sun, C.M. Peterson, J. Kopecek, Biodistribution and antitumour efficacy of long-circulating N-(2-hydroxypropyl)methacrylamide copolymer-doxorubicin conjugates in nude mice, European journal of cancer, 37 (2001) 131-139.

[221] S.N.S. Alconcel, A.S. Baas, H.D. Maynard, FDA-approved poly(ethylene glycol)-protein conjugate drugs, Polymer Chemistry, 2 (2011) 1442-1448.

[222] A. Awada, A.A. Garcia, S. Chan, G.H. Jerusalem, R.E. Coleman, M.T. Huizing, A. Mehdi, S.M. O'Reilly, J.T. Hamm, P.J. Barrett-Lee, V. Cocquyt, K. Sideras, D.E. Young, C. Zhao, Y.L. Chia, U. Hoch, A.L. Hannah, E.A. Perez, Two schedules of etirinotecan pegol (NKTR-102) in patients with previously treated metastatic breast cancer: a randomised phase 2 study, Lancet Oncol, 14 (2013) 1216-1225.

[223] Y. Matsumura, Poly (amino acid) micelle nanocarriers in preclinical and clinical studies, Adv Drug Deliv Rev, 60 (2008) 899-914.

[224] C. Young, T. Schluep, J. Hwang, S. Eliasof, CRLX101 (formerly IT-101)-A Novel Nanopharmaceutical of Camptothecin in Clinical Development, Curr. Bioact. Compd., 7 (2011) 8-14.

[225] P.J. Stevens, M. Sekido, R.J. Lee, A folate receptor-targeted lipid nanoparticle formulation for a lipophilic paclitaxel prodrug, Pharm. Res., 21 (2004) 2153-2157.

[226] A. Uimari, T.A. Keinanen, A. Karppinen, P. Woster, P. Uimari, J. Janne, L. Alhonen, Spermine analogue-regulated expression of spermidine/spermine N1-acetyltransferase and its effects on depletion of intracellular polyamine pools in mouse fetal fibroblasts, Biochem. J., 422 (2009) 101-109.

[227] H.A. Hahm, V.R. Dunn, K.A. Butash, W.L. Deveraux, P.M. Woster, R.A. Casero, Jr., N.E. Davidson, Combination of standard cytotoxic agents with polyamine analogues in the treatment of breast cancer cell lines, Clinical cancer research : an official journal of the American Association for Cancer Research, 7 (2001) 391-399.

[228] G.S. Wu, TRAIL as a target in anti-cancer therapy, Cancer Lett., 285 (2009) 1-5.

[229] C.R. de Almodovar, C. Ruiz-Ruiz, A. Rodriguez, G. Ortiz-Ferron, J.M. Redondo, A. Lopez-Rivas, Tumor necrosis factor-related apoptosis-inducing ligand (TRAIL) decoy receptor TRAIL-R3 is up-regulated by p53 in breast tumor cells through a mechanism involving an intronic p53-binding site, Journal of Biological Chemistry, 279 (2004) 4093-4101.

[230] R.S. Herbst, S.G. Eckhardt, R. Kurzrock, S. Ebbinghaus, P.J. O'Dwyer, M.S. Gordon, W. Novotny, M.A. Goldwasser, T.M. Tohnya, B.L. Lum, A. Ashkenazi, A.M.

Jubb, D.S. Mendelson, Phase I dose-escalation study of recombinant human Apo2L/TRAIL, a dual proapoptotic receptor agonist, in patients with advanced cancer, J Clin Oncol, 28 (2010) 2839-2846.

[231] E. Bremer, Targeting of the tumor necrosis factor receptor superfamily for cancer immunotherapy, ISRN Oncol, 2013 (2013) 371854.

[232] A. Ashkenazi, P. Holland, S.G. Eckhardt, Ligand-based targeting of apoptosis in cancer: the potential of recombinant human apoptosis ligand 2/Tumor necrosis factor-related apoptosis-inducing ligand (rhApo2L/TRAIL), J Clin Oncol, 26 (2008) 3621-3630.

[233] L. Zhang, B. Fang, Mechanisms of resistance to TRAIL-induced apoptosis in cancer, Cancer Gene Ther., 12 (2005) 228-237.

[234] C.T. Hellwig, M. Rehm, TRAIL signaling and synergy mechanisms used in TRAIL-based combination therapies, Mol. Cancer Ther., 11 (2012) 3-13.

[235] S. Bacus, D. Altomare, L. Lyass, D. Chin, M. Farrell, K. Gurova, A. Gudkov, J. Testa, Akt is frequently upregulated in HER-2/ neu-positive breast cancers and may contribute to tumor aggressiveness by enhancing cell survival, Oncogene, 21 (2002) 3532 - 3540.

[236] A. Bellacosa, D. de Feo, A. Godwin, D. Bell, J. Cheng, D. Altomare, M. Wan, L. Dubeau, G. Scambia, V. Masciullo, G. Ferrandina, P. Benedetti Panici, S. Mancuso, G. Neri, J. Testa, Molecular alterations of the AKT2 oncogene in ovarion and breast carcinomas, Int. J. Cancer, 64 (1995) 280 - 285.

[237] J. Cheng, B. Ruggeri, W. Klein, G. Sonoda, D. Altomare, D. Watson, J. Testa, Amplification of AKT2 in human pancreatic cells and inhibition of AKT2 expression and tumorigenicity by antisense RNA, Proc Natl Acad Sci USA, 93 (1996) 3636 - 3641.

[238] J.Q. Cheng, A.K. Godwin, A. Bellacosa, T. Taguchi, T.F. Franke, T.C. Hamilton, P.N. Tsichlis, J.R. Testa, AKT2, a putative oncogene encoding a member of a subfamily of protein-serine/threonine kinases, is amplified in human ovarian carcinomas, Proc. Natl. Acad. Sci. U. S. A., 89 (1992) 9267-9271.

[239] M. Arboleda, J. Lyons, F. Kabbinavar, M. Bray, B. Snow, R. Ayala, M. Danino, B. Karlan, D. Slamon, Overexpression of AKT2/protein kinase B beta leads to up-regulation of beta1 integrins, increased invasion, and metastasis of human breast and ovarian cancer cells, Cancer Res., 63 (2003) 196 - 206.

[240] N.-M. Chau, M. Ashcroft, Akt2: a role in breast cancer metastasis, Breast cancer research : BCR, 6 (2004) 55 - 57.

[241] A. Goncalves, P. Finetti, R. Sabatier, M. Gilabert, J. Adelaide, J.P. Borg, M. Chaffanet, P. Viens, D. Birnbaum, F. Bertucci, Poly(ADP-ribose) polymerase-1 mRNA expression in human breast cancer: a meta-analysis, Breast Cancer Res Treat, 127 (2011) 273-281.

[242] D.R. Fogelman, R.A. Wolff, S. Kopetz, M. Javle, C. Bradley, I. Mok, F. Cabanillas, J.L. Abbruzzese, Evidence for the Efficacy of Iniparib, a PARP-1 Inhibitor, in BRCA2-associated Pancreatic Cancer, Anticancer Res., 31 (2011) 1417-1420.

[243] E. Perkins, D. Sun, A. Nguyen, S. Tulac, M. Francesco, H. Tavana, H. Nguyen, S. Tugendreich, P. Barthmaier, J. Couto, E. Yeh, S. Thode, K. Jarnagin, A. Jain, D. Morgans, T. Melese, Novel inhibitors of poly(ADP-ribose) polymerase/PARP1 and PARP2 identified using a cell-based screen in yeast, Cancer Res., 61 (2001) 4175-4183.

[244] Y. Yuan, Y.M. Liao, C.T. Hsueh, H.R. Mirshahidi, Novel targeted therapeutics: inhibitors of MDM2, ALK and PARP, J Hematol Oncol, 4 (2011) 16.

[245] M.S. Goldberg, D. Xing, Y. Ren, S. Orsulic, S.N. Bhatia, P.A. Sharp, Nanoparticle-mediated delivery of siRNA targeting Parp1 extends survival of mice bearing tumors derived from Brca1-deficient ovarian cancer cells, Proceedings of the National Academy of Sciences, 108 (2011) 745-750.

[246] S. Koshida, D. Kobayashi, R. Moriai, N. Tsuji, N. Watanabe, Specific overexpression of OLFM4(GW112/HGC-1) mRNA in colon, breast and lung cancer tissues detected using quantitative analysis, Cancer Sci., 98 (2007) 315-320.

[247] J. Lu, M. Tan, W.C. Huang, P. Li, H. Guo, L.M. Tseng, X.H. Su, W.T. Yang, W. Treekitkarnmongkol, M. Andreeff, F. Symmans, D. Yu, Mitotic deregulation by survivin in ErbB2-overexpressing breast cancer cells contributes to Taxol resistance, Clinical cancer research : an official journal of the American Association for Cancer Research, 15 (2009) 1326-1334.

[248] G.D. Kenny, N. Kamaly, T.L. Kalber, L.P. Brody, M. Sahuri, E. Shamsaei, A.D. Miller, J.D. Bell, Novel multifunctional nanoparticle mediates siRNA tumour delivery, visualisation and therapeutic tumour reduction in vivo, J. Controlled Release, 149 (2011) 111-116.

[249] B. Li, J. Fan, X. Liu, R. Qi, L. Bo, J. Gu, C. Qian, Suppression of colorectal tumor growth by regulated survivin targeting, J Mol Med, 84 (2006) 1077-1086.

[250] F. Paduano, R. Villa, M. Pennati, M. Folini, M. Binda, M.G. Daidone, N. Zaffaroni, Silencing of survivin gene by small interfering RNAs produces supra-additive growth

suppression in combination with 17-allylamino-17-demethoxygeldanamycin in human prostate cancer cells, Mol. Cancer Ther., 5 (2006) 179-186.

[251] J. Shen, J. Liu, Y. Long, Y. Miao, M. Su, Q. Zhang, H. Han, X. Hao, Knockdown of survivin expression by siRNAs enhances chemosensitivity of prostate cancer cells and attenuates its tumorigenicity, Acta Biochim Biophys Sin (Shanghai), 41 (2009) 223-230.

[252] M.C. Zhang, C.P. Hu, Q. Chen, [Effect of down-regulation of survivin gene on apoptosis and cisplatin resistance in cisplatin resistant human lung adenocarcinoma A549/CDDP cells], Zhonghua Zhong Liu Za Zhi, 28 (2006) 408-412.

[253] D. Chen, M. Niu, X. Jiao, K. Zhang, J. Liang, D. Zhang, Inhibition of AKT2 Enhances Sensitivity to Gemcitabine via Regulating PUMA and NF-kappaB Signaling Pathway in Human Pancreatic Ductal Adenocarcinoma, Int J Mol Sci, 13 (2012) 1186-1208.

[254] M.T. Park, Y.H. Kang, I.C. Park, C.H. Kim, Y.S. Lee, H.Y. Chung, S.J. Lee, Combination treatment with arsenic trioxide and phytosphingosine enhances apoptotic cell death in arsenic trioxide-resistant cancer cells, Mol. Cancer Ther., 6 (2007) 82-92.

[255] J. Michels, I. Vitale, L. Senovilla, D.P. Enot, P. Garcia, D. Lissa, K.A. Olaussen, C. Brenner, J.C. Soria, M. Castedo, G. Kroemer, Synergistic interaction between cisplatin and PARP inhibitors in non-small cell lung cancer, Cell Cycle, 12 (2013) 877-883.

[256] T.C. Chou, Derivation and properties of Michaelis-Menten type and Hill type equations for reference ligands, J. Theor. Biol., 59 (1976) 253-276.

[257] T.C. Chou, On the determination of availability of ligand binding sites in steady-state systems, J. Theor. Biol., 65 (1977) 345-356.

[258] T.C. Chou, P. Talalay, Quantitative analysis of dose-effect relationships: the combined effects of multiple drugs or enzyme inhibitors, Adv Enzyme Regul, 22 (1984) 27-55.

[259] T.C. Chou, P. Talalay, Generalized equations for the analysis of inhibitions of Michaelis-Menten and higher-order kinetic systems with two or more mutually exclusive and nonexclusive inhibitors, Eur. J. Biochem., 115 (1981) 207-216.

[260] L. Zhao, J.L. Au, M.G. Wientjes, Comparison of methods for evaluating drug-drug interaction, Front Biosci (Elite Ed), 2 (2010) 241-249.

[261] T.C. Chou, Theoretical basis, experimental design, and computerized simulation of synergism and antagonism in drug combination studies, Pharmacol Rev, 58 (2006) 621-681.

[262] D.S. Manickam, A. Hirata, D.A. Putt, L.H. Lash, F. Hirata, D. Oupicky, Overexpression of Bcl-2 as a proxy redox stimulus to enhance activity of non-viral redox-responsive delivery vectors, Biomaterials, 29 (2008) 2680-2688.

[263] J. Li, Y. Zhu, S.T. Hazeldine, S.M. Firestine, D. Oupicky, Cyclam-based polymeric copper chelators for gene delivery and potential PET imaging, Biomacromolecules, 13 (2012) 3220-3227.

[264] T.C. Chou, Drug combination studies and their synergy quantification using the Chou-Talalay method, Cancer Res., 70 (2010) 440-446.

[265] Y. Dong, Y. Zhu, J. Li, Q.H. Zhou, C. Wu, D. Oupicky, Synthesis of bisethylnorspermine lipid prodrug as gene delivery vector targeting polyamine metabolism in breast cancer, Mol. Pharm., 9 (2012) 1654-1664.

[266] S. Shamimi-Noori, W.S. Yeow, M.F. Ziauddin, H. Xin, T.L. Tran, J. Xie, A. Loehfelm, P. Patel, J. Yang, D.S. Schrump, B.L. Fang, D.M. Nguyen, Cisplatin enhances the antitumor effect of tumor necrosis factor-related apoptosis-inducing ligand gene therapy via recruitment of the mitochondria-dependent death signaling pathway, Cancer Gene Ther., 15 (2008) 356-370.

[267] S.R. Murugesan, C.R. King, R. Osborn, W.R. Fairweather, E.M. O'Reilly, M.O. Thornton, L.L. Wei, Combination of human tumor necrosis factor-alpha (hTNF-alpha) gene delivery with gemcitabine is effective in models of pancreatic cancer, Cancer Gene Ther., 16 (2009) 841-847.

[268] C.D. Davidson, N.F. Ali, M.C. Micsenyi, G. Stephney, S. Renault, K. Dobrenis, D.S. Ory, M.T. Vanier, S.U. Walkley, Chronic cyclodextrin treatment of murine Niemann-Pick C disease ameliorates neuronal cholesterol and glycosphingolipid storage and disease progression, PLoS One, 4 (2009) e6951.

[269] Y. Dong, J. Li, C. Wu, D. Oupicky, Bisethylnorspermine lipopolyamine as potential delivery vector for combination drug/gene anticancer therapies, Pharm. Res., 27 (2010) 1927-1938.

[270] K.E. Tobias, J. Shor, C. Kahana, c-Myc and Max transregulate the mouse ornithine decarboxylase promoter through interaction with two downstream CACGTG motifs, Oncogene, 11 (1995) 1721-1727.

[271] P. Celano, C.M. Berchtold, F.M. Giardiello, R.A. Casero, Jr., Modulation of growth gene expression by selective alteration of polyamines in human colon carcinoma cells, Biochem. Biophys. Res. Commun., 165 (1989) 384-390.

[272] B. Le Bon, N. Van Craynest, O. Boussif, P. Vierling, Polycationic diblock and random polyethylene glycol- or tris(hydroxymethyl)methyl-grafted (co)telomers for gene transfer: synthesis and evaluation of their in vitro transfection efficiency, Bioconjug Chem, 13 (2002) 1292-1301.

[273] T.V. DeCollo, W.J. Lees, Effects of aromatic thiols on thiol-disulfide interchange reactions that occur during protein folding, J. Org. Chem., 66 (2001) 4244-4249.

[274] R.A. Casero, Jr., P. Celano, S.J. Ervin, C.W. Porter, R.J. Bergeron, P.R. Libby, Differential induction of spermidine/spermine N1-acetyltransferase in human lung cancer cells by the bis(ethyl)polyamine analogues, Cancer Res., 49 (1989) 3829-3833.

[275] T. Murray-Stewart, N.B. Applegren, W. Devereux, A. Hacker, R. Smith, Y. Wang, R.A. Casero, Jr., Spermidine/spermine N1-acetyltransferase (SSAT) activity in human small-cell lung carcinoma cells following transfection with a genomic SSAT construct, Biochem. J., 373 (2003) 629-634.

[276] M. Kovar, J. Strohalm, T. Etrych, K. Ulbrich, B. Rihova, Star structure of antibody-targeted HPMA copolymer-bound doxorubicin: a novel type of polymeric conjugate for targeted drug delivery with potent antitumor effect, Bioconjug Chem, 13 (2002) 206-215.

[277] P.S. Cogan, T.H. Koch, Rational design and synthesis of androgen receptor-targeted nonsteroidal anti-androgen ligands for the tumor-specific delivery of a doxorubicin-formaldehyde conjugate, J. Med. Chem., 46 (2003) 5258-5270.

[278] A.-Z.A. Elassar, A.A. El-Khair, Recent developments in the chemistry of enaminones, Tetrahedron, 59 (2003) 8463-8480.

[279] A.L. Simplicio, J.M. Clancy, J.F. Gilmer, Beta-aminoketones as prodrugs with pH-controlled activation, Int. J. Pharm., 336 (2007) 208-214.

[280] R.E. Hansen, D. Roth, J.R. Winther, Quantifying the global cellular thiol-disulfide status, Proc. Natl. Acad. Sci. U. S. A., 106 (2009) 422-427.

[281] D.P. Jones, J.L. Carlson, P.S. Samiec, P. Sternberg, Jr., V.C. Mody, Jr., R.L. Reed, L.A. Brown, Glutathione measurement in human plasma. Evaluation of sample collection, storage and derivatization conditions for analysis of dansyl derivatives by HPLC, Clin. Chim. Acta, 275 (1998) 175-184.

[282] D.S. Manickam, J. Li, D.A. Putt, Q.H. Zhou, C. Wu, L.H. Lash, D. Oupicky, Effect of innate glutathione levels on activity of redox-responsive gene delivery vectors, J Control Release, 141 (2010) 77-84.

[283] J.H. Brumbach, C. Lin, J. Yockman, W.J. Kim, K.S. Blevins, J.F. Engbersen, J. Feijen, S.W. Kim, Mixtures of poly(triethylenetetramine/cystamine bisacrylamide) and poly(triethylenetetramine/cystamine bisacrylamide)-g-poly(ethylene glycol) for improved gene delivery, Bioconjug Chem, 21 (2010) 1753-1761.

[284] C. Lin, Z. Zhong, M.C. Lok, X. Jiang, W.E. Hennink, J. Feijen, J.F. Engbersen, Linear poly(amido amine)s with secondary and tertiary amino groups and variable amounts of disulfide linkages: synthesis and in vitro gene transfer properties, J Control Release, 116 (2006) 130-137.

[285] S. Zalipsky, N. Mullah, C. Engbers, M.U. Hutchins, R. Kiwan, Thiolytically cleavable dithiobenzyl urethane-linked polymer-protein conjugates as macromolecular prodrugs: reversible PEGylation of proteins, Bioconjug Chem, 18 (2007) 1869-1878.

[286] S. Zalipsky, M. Qazen, J.A. Walker, 2nd, N. Mullah, Y.P. Quinn, S.K. Huang, New detachable poly(ethylene glycol) conjugates: cysteine-cleavable lipopolymers

regenerating natural phospholipid, diacyl phosphatidylethanolamine, Bioconjug Chem, 10 (1999) 703-707.

[287] P.D. Senter, W.E. Pearce, R.S. Greenfield, Development of a drug-release strategy based on the reductive fragmentation of benzyl carbamate disulfides, The Journal of Organic Chemistry, 55 (1990) 2975-2978.

[288] R.B. Greenwald, A. Pendri, C.D. Conover, H. Zhao, Y.H. Choe, A. Martinez, K. Shum, S. Guan, Drug delivery systems employing 1,4- or 1,6-elimination: poly(ethylene glycol) prodrugs of amine-containing compounds, J. Med. Chem., 42 (1999) 3657-3667.

[289] R.S. Shirazi, K.K. Ewert, C. Leal, R.N. Majzoub, N.F. Bouxsein, C.R. Safinya, Synthesis and characterization of degradable multivalent cationic lipids with disulfide-bond spacers for gene delivery, Biochim. Biophys. Acta, 1808 (2011) 2156-2166.

[290] X.L. Wang, T. Nguyen, D. Gillespie, R. Jensen, Z.R. Lu, A multifunctional and reversibly polymerizable carrier for efficient siRNA delivery, Biomaterials, 29 (2008) 15-22.

[291] Z. Huang, W. Li, J.A. MacKay, F.C. Szoka, Jr., Thiocholesterol-based lipids for ordered assembly of bioresponsive gene carriers, Mol. Ther., 11 (2005) 409-417.

[292] H.F. Gilbert, Molecular and cellular aspects of thiol-disulfide exchange, Adv. Enzymol. Relat. Areas Mol. Biol., 63 (1990) 69-172.

[293] C. Hwang, H.F. Lodish, A.J. Sinskey, Measurement of glutathione redox state in cytosol and secretory pathway of cultured cells, Methods Enzymol., 251 (1995) 212-221.

[294] N.S. Kosower, E.M. Kosower, The glutathione status of cells, Int Rev Cytol, 54 (1978) 109-160.

[295] G. Bellomo, M. Vairetti, L. Stivala, F. Mirabelli, P. Richelmi, S. Orrenius, Demonstration of nuclear compartmentalization of glutathione in hepatocytes, Proc. Natl. Acad. Sci. U. S. A., 89 (1992) 4412-4416.

[296] C.V. Smith, D.P. Jones, T.M. Guenthner, L.H. Lash, B.H. Lauterburg, Compartmentation of glutathione: implications for the study of toxicity and disease, Toxicol. Appl. Pharmacol., 140 (1996) 1-12.

[297] S. Soboll, S. Grundel, J. Harris, V. Kolb-Bachofen, B. Ketterer, H. Sies, The content of glutathione and glutathione S-transferases and the glutathione peroxidase activity in rat liver nuclei determined by a non-aqueous technique of cell fractionation, Biochem. J., 311 ( Pt 3) (1995) 889-894.

[298] W. Sun, P.B. Davis, Reducible DNA nanoparticles enhance in vitro gene transfer via an extracellular mechanism, J Control Release, 146 (2010) 118-127.

[299] M. Calderon, M.A. Quadir, S.K. Sharma, R. Haag, Dendritic polyglycerols for biomedical applications, Adv Mater, 22 (2010) 190-218.

[300] H. Frey, R. Haag, Dendritic polyglycerol: a new versatile biocompatible-material, J. Biotechnol., 90 (2002) 257-267.

[301] A. Sunder, R. Hanselmann, H. Frey, R. Mülhaupt, Controlled Synthesis of Hyperbranched Polyglycerols by Ring-Opening Multibranching Polymerization, Macromolecules, 32 (1999) 4240-4246.

[302] W. Fischer, M. Calderon, A. Schulz, I. Andreou, M. Weber, R. Haag, Dendritic polyglycerols with oligoamine shells show low toxicity and high siRNA transfection efficiency in vitro, Bioconjug Chem, 21 (2010) 1744-1752.

[303] A.L. Wolfe, K.K. Duncan, N.K. Parelkar, S.J. Weir, G.A. Vielhauer, D.L. Boger, A novel, unusually efficacious duocarmycin carbamate prodrug that releases no residual byproduct, J. Med. Chem., 55 (2012) 5878-5886.

[304] G. Mata, V.E. do Rosario, J. Iley, L. Constantino, R. Moreira, A carbamate-based approach to primaquine prodrugs: antimalarial activity, chemical stability and enzymatic activation, Bioorg. Med. Chem., 20 (2012) 886-892.

[305] S. Roller, H. Zhou, R. Haag, High-loading polyglycerol supported reagents for Mitsunobu- and acylation-reactions and other useful polyglycerol derivatives, Mol Divers, 9 (2005) 305-316.

[306] M.R. Hakkinen, T.A. Keinanen, J. Vepsalainen, A.R. Khomutov, L. Alhonen, J. Janne, S. Auriola, Quantitative determination of underivatized polyamines by using isotope dilution RP-LC-ESI-MS/MS, J. Pharm. Biomed. Anal., 48 (2008) 414-421.

[307] A. Akinc, M. Thomas, A.M. Klibanov, R. Langer, Exploring polyethylenimine-mediated DNA transfection and the proton sponge hypothesis, J Gene Med, 7 (2005) 657-663.

[308] N.D. Sonawane, F.C. Szoka, Jr., A.S. Verkman, Chloride accumulation and swelling in endosomes enhances DNA transfer by polyamine-DNA polyplexes, J. Biol. Chem., 278 (2003) 44826-44831.

[309] R.V. Benjaminsen, M.A. Mattebjerg, J.R. Henriksen, S.M. Moghimi, T.L. Andresen, The possible "proton sponge " effect of polyethylenimine (PEI) does not include change in lysosomal pH, Mol. Ther., 21 (2013) 149-157.

[310] A.M. Funhoff, C.F. van Nostrum, G.A. Koning, N.M. Schuurmans-Nieuwenbroek, D.J. Crommelin, W.E. Hennink, Endosomal escape of polymeric gene delivery

complexes is not always enhanced by polymers buffering at low pH, Biomacromolecules, 5 (2004) 32-39.

[311] Y. Liu, T.M. Reineke, Poly(glycoamidoamine)s for gene delivery. structural effects on cellular internalization, buffering capacity, and gene expression, Bioconjug Chem, 18 (2007) 19-30.

[312] B.G. Zanetti-Ramos, M.B. Fritzen-Garcia, C.S. de Oliveira, A.A. Pasa, V. Soldi, R. Borsali, T.B. Creczynski-Pasa, Dynamic light scattering and atomic force microscopy techniques for size determination of polyurethane nanoparticles, Materials Science and Engineering: C, 29 (2009) 638-640.

[313] H. Mok, S.H. Lee, J.W. Park, T.G. Park, Multimeric small interfering ribonucleic acid for highly efficient sequence-specific gene silencing, Nat. Mater., 9 (2010) 272-278.

[314] C. Scholz, E. Wagner, Therapeutic plasmid DNA versus siRNA delivery: common and different tasks for synthetic carriers, J Control Release, 161 (2012) 554-565.

[315] J. Nguyen, F.C. Szoka, Nucleic acid delivery: the missing pieces of the puzzle?, Acc. Chem. Res., 45 (2012) 1153-1162.

[316] P.J. O'Brien, W. Irwin, D. Diaz, E. Howard-Cofield, C.M. Krejsa, M.R. Slaughter, B. Gao, N. Kaludercic, A. Angeline, P. Bernardi, P. Brain, C. Hougham, High concordance of drug-induced human hepatotoxicity with in vitro cytotoxicity measured in a novel cell-based model using high content screening, Arch. Toxicol., 80 (2006) 580-604.

[317] V. Mersch-Sundermann, S. Knasmuller, X.J. Wu, F. Darroudi, F. Kassie, Use of a human-derived liver cell line for the detection of cytoprotective, antigenotoxic and cogenotoxic agents, Toxicology, 198 (2004) 329-340.

[318] S. Knasmuller, V. Mersch-Sundermann, S. Kevekordes, F. Darroudi, W.W. Huber, C. Hoelzl, J. Bichler, B.J. Majer, Use of human-derived liver cell lines for the detection of environmental and dietary genotoxicants; current state of knowledge, Toxicology, 198 (2004) 315-328.

[319] M.Y. Khuhawar, G.A. Qureshi, Polyamines as cancer markers: applicable separation methods, J Chromatogr B Biomed Sci Appl, 764 (2001) 385-407.

[320] I. Molnar-Perl, Quantitation of amino acids and amines in the same matrix by high-performance liquid chromatography, either simultaneously or separately, J Chromatogr A, 987 (2003) 291-309.

[321] A. El-Aneed, An overview of current delivery systems in cancer gene therapy, J Control Release, 94 (2004) 1-14.

[322] M.S. Al-Dosari, X. Gao, Nonviral gene delivery: principle, limitations, and recent progress, AAPS J, 11 (2009) 671-681.

[323] Y. Lee, K. Miyata, M. Oba, T. Ishii, S. Fukushima, M. Han, H. Koyama, N. Nishiyama, K. Kataoka, Charge-conversion ternary polyplex with endosome disruption moiety: a technique for efficient and safe gene delivery, Angew Chem Int Ed Engl, 47 (2008) 5163-5166.

[324] D. Peer, J.M. Karp, S. Hong, O.C. Farokhzad, R. Margalit, R. Langer, Nanocarriers as an emerging platform for cancer therapy, Nat. Nanotechnol., 2 (2007) 751-760.

[325] S. Ganesh, A.K. Iyer, J. Weiler, D.V. Morrissey, M.M. Amiji, Combination of siRNA-directed Gene Silencing With Cisplatin Reverses Drug Resistance in Human Non-small Cell Lung Cancer, Mol Ther Nucleic Acids, 2 (2013) e110.

[326] A.K. Iyer, A. Singh, S. Ganta, M.M. Amiji, Role of integrated cancer nanomedicine in overcoming drug resistance, Adv Drug Deliv Rev, (2013).

[327] S.C. De Smedt, J. Demeester, W.E. Hennink, Cationic polymer based gene delivery systems, Pharm. Res., 17 (2000) 113-126.

[328] S. Ganta, H. Devalapally, A. Shahiwala, M. Amiji, A review of stimuli-responsive nanocarriers for drug and gene delivery, J Control Release, 126 (2008) 187-204.

[329] J. Sunshine, N. Bhise, J.J. Green, Degradable polymers for gene delivery, Conf Proc IEEE Eng Med Biol Soc, 2009 (2009) 2412-2415.

[330] C.M. Varga, K. Hong, D.A. Lauffenburger, Quantitative analysis of synthetic gene delivery vector design properties, Mol. Ther., 4 (2001) 438-446.

[331] J.M. Dang, K.W. Leong, Natural polymers for gene delivery and tissue engineering, Adv Drug Deliv Rev, 58 (2006) 487-499.

[332] E. Fleige, M.A. Quadir, R. Haag, Stimuli-responsive polymeric nanocarriers for the controlled transport of active compounds: concepts and applications, Adv Drug Deliv Rev, 64 (2012) 866-884.

[333] D. Jere, R. Arote, H.L. Jiang, Y.K. Kim, M.H. Cho, C.S. Cho, Bioreducible polymers for efficient gene and siRNA delivery, Biomed Mater, 4 (2009) 025020.

[334] Y. Lei, T. Segura, DNA delivery from matrix metalloproteinase degradable poly(ethylene glycol) hydrogels to mouse cloned mesenchymal stem cells, Biomaterials, 30 (2009) 254-265.

[335] H. Lee, A.K. Lytton-Jean, Y. Chen, K.T. Love, A.I. Park, E.D. Karagiannis, A. Sehgal, W. Querbes, C.S. Zurenko, M. Jayaraman, C.G. Peng, K. Charisse, A. Borodovsky, M. Manoharan, J.S. Donahoe, J. Truelove, M. Nahrendorf, R. Langer, D.G.

Anderson, Molecularly self-assembled nucleic acid nanoparticles for targeted in vivo siRNA delivery, Nat. Nanotechnol., 7 (2012) 389-393.

[336] M. Yan, M. Liang, J. Wen, Y. Liu, Y. Lu, I.S. Chen, Single siRNA nanocapsules for enhanced RNAi delivery, J. Am. Chem. Soc., 134 (2012) 13542-13545.

[337] K. Liang, G.K. Such, Z. Zhu, S.J. Dodds, A.P. Johnston, J. Cui, H. Ejima, F. Caruso, Engineering cellular degradation of multilayered capsules through controlled cross-linking, ACS Nano, 6 (2012) 10186-10194.

[338] N. Sanvicens, M.P. Marco, Multifunctional nanoparticles--properties and prospects for their use in human medicine, Trends Biotechnol., 26 (2008) 425-433.

[339] M.H. Lee, J.H. Han, P.S. Kwon, S. Bhuniya, J.Y. Kim, J.L. Sessler, C. Kang, J.S. Kim, Hepatocyte-targeting single galactose-appended naphthalimide: a tool for intracellular thiol imaging in vivo, J. Am. Chem. Soc., 134 (2012) 1316-1322.

[340] E.K.Y. Chen, R.A. McBride, E.R. Gillies, Self-Immolative Polymers Containing Rapidly Cyclizing Spacers: Toward Rapid Depolymerization Rates, Macromolecules, 45 (2012) 7364-7374.

[341] P.M. Kabra, H.K. Lee, W.P. Lubich, L.J. Marton, Solid-phase extraction and determination of dansyl derivatives of unconjugated and acetylated polyamines by reversed-phase liquid chromatography: improved separation systems for polyamines in cerebrospinal fluid, urine and tissue, J. Chromatogr., 380 (1986) 19-32.

[342] M.L. Read, S. Singh, Z. Ahmed, M. Stevenson, S.S. Briggs, D. Oupicky, L.B. Barrett, R. Spice, M. Kendall, M. Berry, J.A. Preece, A. Logan, L.W. Seymour, A versatile reducible polycation-based system for efficient delivery of a broad range of nucleic acids, Nucleic Acids Res., 33 (2005) e86.

[343] S.b. Perrier, D. Haddleton, In Situ NMR Monitoring of Living Radical Polymerization, in: J.E. Puskas, T.E. Long, R.F. Storey, S. Shaikh, C. Simmons (Eds.) In Situ Spectroscopy of Monomer and Polymer Synthesis, Springer US, 2003, pp. 125-146.

[344] M.A. Dewit, E.R. Gillies, A cascade biodegradable polymer based on alternating cyclization and elimination reactions, J. Am. Chem. Soc., 131 (2009) 18327-18334.

[345] R.J. Christie, N. Nishiyama, K. Kataoka, Delivering the code: polyplex carriers for deoxyribonucleic acid and ribonucleic acid interference therapies, Endocrinology, 151 (2010) 466-473.

[346] D. Soundara Manickam, D. Oupicky, Polyplex gene delivery modulated by redox potential gradients, J Drug Target, 14 (2006) 519-526.

[347] J.J. Green, J. Shi, E. Chiu, E.S. Leshchiner, R. Langer, D.G. Anderson, Biodegradable polymeric vectors for gene delivery to human endothelial cells, Bioconjug Chem, 17 (2006) 1162-1169.

[348] L.S. Nair, C.T. Laurencin, Biodegradable polymers as biomaterials, Prog. Polym. Sci., 32 (2007) 762-798.

[349] Z.W. Ma, Y. Hong, D.M. Nelson, J.E. Pichamuthu, C.E. Leeson, W.R. Wagner, Biodegradable Polyurethane Ureas with Variable Polyester or Polycarbonate Soft Segments: Effects of Crystallinity, Molecular Weight, and Composition on Mechanical Properties, Biomacromolecules, 12 (2011) 3265-3274.

[350] C. Zhu, S. Jung, F. Meng, X. Zhu, T.G. Park, Z. Zhong, Reduction-responsive cationic biodegradable micelles based on PDMAEMA-SS-PCL-SS-PDMAEMA triblock copolymers for gene delivery, J Control Release, 152 Suppl 1 (2011) e188-190.

[351] J. Yang, W. Hendricks, G. Liu, J.M. McCaffery, K.W. Kinzler, D.L. Huso, B. Vogelstein, S. Zhou, A nanoparticle formulation that selectively transfects metastatic tumors in mice, Proceedings of the National Academy of Sciences, (2013).

[352] T. Murray-Stewart, C.L. Hanigan, P.M. Woster, L.J. Marton, R.A. Casero, Jr., Histone Deacetylase Inhibition Overcomes Drug Resistance through a miRNA-Dependent Mechanism, Mol. Cancer Ther., 12 (2013) 2088-2099.

[353] L.C. Penning, R.G. Schipper, D. Vercammen, A.A. Verhofstad, T. Denecker, R. Beyaert, P. Vandenabeele, Sensitization of tnf-induced apoptosis with polyamine synthesis inhibitors in different human and murine tumour cell lines, Cytokine, 10 (1998) 423-431.

[354] Y. Degenhardt, T. Lampkin, Targeting Polo-like kinase in cancer therapy, Clinical cancer research : an official journal of the American Association for Cancer Research, 16 (2010) 384-389.

[355] K. Strebhardt, A. Ullrich, Targeting polo-like kinase 1 for cancer therapy, Nat. Rev. Cancer, 6 (2006) 321-330.

[356] H. Thomadaki, A. Scorilas, BCL2 family of apoptosis-related genes: functions and clinical implications in cancer, Crit Rev Clin Lab Sci, 43 (2006) 1-67.

[357] J.M. Adams, S. Cory, The Bcl-2 apoptotic switch in cancer development and therapy, Oncogene, 26 (2007) 1324-1337.

[358] Z. Song, W. Yue, B. Wei, N. Wang, T. Li, L. Guan, S. Shi, Q. Zeng, X. Pei, L. Chen, Sonic hedgehog pathway is essential for maintenance of cancer stem-like cells in human gastric cancer, PLoS One, 6 (2011) e17687.

[359] D. Davar, J.H. Beumer, L. Hamieh, H. Tawbi, Role of PARP inhibitors in cancer biology and therapy, Curr. Med. Chem., 19 (2012) 3907-3921.

[360] J.A. Fresno Vara, E. Casado, J. de Castro, P. Cejas, C. Belda-Iniesta, M. Gonzalez-Baron, PI3K/Akt signalling pathway and cancer, Cancer Treat Rev, 30 (2004) 193-204.

[361] D.A. Altomare, J.R. Testa, Perturbations of the AKT signaling pathway in human cancer, Oncogene, 24 (2005) 7455-7464.

[362] D.C. Altieri, Survivin, cancer networks and pathway-directed drug discovery, Nat. Rev. Cancer, 8 (2008) 61-70.

[363] G.L. Semenza, Targeting HIF-1 for cancer therapy, Nat. Rev. Cancer, 3 (2003) 721-732.

[364] H. Yu, D. Pardoll, R. Jove, STATs in cancer inflammation and immunity: a leading role for STAT3, Nat. Rev. Cancer, 9 (2009) 798-809.

[365] P. Kucharzewska, J.E. Welch, K.J. Svensson, M. Belting, Ornithine decarboxylase and extracellular polyamines regulate microvascular sprouting and actin cytoskeleton dynamics in endothelial cells, Exp. Cell Res., 316 (2010) 2683-2691.

[366] D.C. Dale, A.A. Bolyard, M.L. Kelley, E.C. Westrup, V. Makaryan, A. Aprikyan, B. Wood, F.J. Hsu, The CXCR4 antagonist plerixafor is a potential therapy for myelokathexis, WHIM syndrome, Blood, 118 (2011) 4963-4966.

[367] F.A. Sinicrope, R. Broaddus, N. Joshi, E. Gerner, E. Half, I. Kirsch, J. Lewin, B. Morlan, W.K. Hong, Evaluation of difluoromethylornithine for the chemoprevention of Barrett's esophagus and mucosal dysplasia, Cancer Prev Res (Phila), 4 (2011) 829-839.

# ABSTRACT

## DUAL DELIVERY SYSTEMS BASED ON POLYAMINE ANALOG BENSPM AS PRODRUG AND GENE DELIVERY VECTORS

by

**YU ZHU**

**May 2014**

**Advisor:** Dr. David Oupický

**Major:** Pharmaceutical Sciences

**Degree:** Doctor of Philosophy

Combination drug and gene therapy shows promise in cancer treatment. However, the success of such strategy requires careful selection of the therapeutic agents, as well as development of efficient delivery vectors. BENSpm ($N^1$, $N^{11}$-bisethylnorspermine), a polyamine analogue targeting the intracellular polyamine pathway, draws our special attention because of the following reasons: (1) polyamine pathway is frequently dysregulated in cancer; (2) BENSpm exhibits multiple functions to interfere with the polyamine pathway, such as to up-regulate polyamine metabolism enzymes and down-regulate polyamine biosynthesis enzymes. Therefore BENSpm depletes all natural polyamines and leads to apoptosis and cell growth inhibition in a wide range of cancers; (3) preclinical studies proved that BENSpm can act synergistically with various chemotherapy agents, making it a promising candidate in

combination therapy; (4) multiple positive charges in BENSpm enable it as a suitable building block for cationic polymers, which can be further applied to gene delivery.

In this dissertation, our goal was to design dual-function delivery vector based on BENSpm that can function as a gene delivery vector and, after intracellular degradation, as an active anticancer agent targeting dysregulated polyamine metabolism. We first demonstrated strong synergism between BENSpm and a potential therapeutic gene product TRAIL. Strong synergism was obtained in both estrogen-dependent MCF-7 breast cancer cells and triple-negative MDA-MB-231 breast cancer cells. Significant dose reduction of TRAIL in combination with BENSpm in MDA-MB-231 cells, together with the fact that BENSpm rendered MCF-7 cells more sensitive to TRAIL treatment verified our rationale of designing BENSpm-based delivery platform. This was expected to be beneficial for overcoming drug resistance in chemotherapy, as well as boosting the therapeutic effect of therapeutic genes.

We first designed a lipid-based BENSpm dual vector (Lipo-SS-BEN) capable of intracellular release of BENSpm using thiolytically sensitive dithiobenzyl carbamate linker. Similar activity on SSAT enzyme induction by Lipo-SS-BEN compared with BENSpm free drug verified the success of this prodrug design. Biodegradability of Lipo-SS-BEN contributed to decreased toxicity compared with nondegradable control LipoBEN. However, decreased enhancement of TRAIL activity was observed for Lipo-SS-BEN when compared with BENSpm, indicating that the lipid-related toxicity diminished the synergism. In addition, compared with LipoBEN and DOTAP, decreased transfection efficiency of Lipo-SS-BEN demonstrated instability of Lipo-SS-BEN in extracellular environment.

In order to design a dual delivery vector with reduced vector toxicity and improved linker stability, we employed dendritic polyglycerol (PG) as a safe carrier backbone, onto which BENSpm was conjugated through carbamate linkage (PG-BEN). Polymers with norspermine (PG-Nor) shell and amine-terminated PG (PG-$NH_2$) were synthesized as controls. The BENSpm dual vector PG-BEN demonstrated superior gene delivery function, and showed decreased toxicity compared with the control polymers. However, compared with BENSpm, which depleted all natural polyamines, PG-BEN only down-regulated intracellular putrescine levels. In addition, no free BENSpm was detected in PG-BEN treated cells. These results suggested that in order to take full advantage of BENSpm anticancer activity, alternative linker chemistry needs to be further explored.

We then incorporated bis(2-hydroxyethyl) disulfide as a self-immolative linker to synthesize polymer prodrugs of BENSpm (DSS-BEN). The proposed mechanism of BENSpm release from DSS-BEN contains two steps: disulfide bond is first cleaved in the reducing intracellular space, then the intermediate further undergoes slow intramolecular cyclization to release free BENSpm. Cell line-dependent BENSpm release after DSS-BEN treatment was observed using HPLC analysis, demonstrating the success of our linker strategy. DSS-BEN showed comparable transfection efficiency as polyethylenimine and showed decreased toxicity in several cell lines compared with the nondegradable control DCC-BEN. We further demonstrated that DSS-BEN could act synergistically with several therapeutic agents, making it a promising delivery platform for combination therapy in cancer. In all, we have successfully developed a dual delivery vector based on BENSpm, which fulfills its function as a gene delivery

vector as well as a prodrug of BENSpm, and possesses synergistic potential to augment the effect of the co-delivered agents.

# AUTOBIOGRAPHICAL STATEMENT

**Education**

2005-2009 B.Sc. in Pharmacy, China Pharmaceutical University, Nanjing, China

2009-pres. Ph.D. Pharmaceutical Sciences; Wayne State University, Detroit, MI

**Publications**

1. Li, J.; **Zhu, Y.;** Hazeldine, S. T.; Firestine, S. M.; Oupicky, D., Cyclam-based polymeric copper chelators for gene delivery and potential PET imaging. *Biomacromolecules* 2012, *13* (10), 3220-3227.
2. Li, J.; **Zhu, Y.**; Hazeldine, S. T.; Li, C.; Oupicky, D., Dual-function CXCR4 antagonist polyplexes to deliver gene therapy and inhibit cancer cell invasion. *Angew Chem Int Ed Engl* 2012, *51* (35), 8740-8743.
3. Dong, Y. M.; **Zhu, Y**.; Li, J.; Zhou, Q. H.; Wu, C.; Oupicky, D., Synthesis of bisethylnorspermine lipid prodrug as gene delivery vector targeting polyamine metabolism in breast cancer. *Mol. Pharm.* 2012, *9* (6), 1654-1664.
4. Li, J.; Wang, Y.; **Zhu, Y**.; Oupicky, D., Recent advances in delivery of drug-nucleic acid combinations for cancer treatment. *J Control Release* 2013.
5. Wu, C.; Li, J.; **Zhu, Y**.; Chen, J.; Oupicky, D., Opposing influence of intracellular and membrane thiols on the toxicity of reducible polycations. *Biomaterials* 2013, *34* (34), 8843-8850.
6. **Zhu, Y**.; Li, J.; Oupicky, D., Intracellular delivery considerations for RNAi therapeutics. "RNA Interference from Biology to Therapeutics", K. Howard, Ed., 2013, pp 79-95
7. **Zhu, Y.**; Hazeldine, S. T.; Li, J.; Oupicky, D., Dendritic polyglycerol with polyamine shell as a potential macromolecular prodrug and gene delivery vector. *Submitted to Eur J Pharm Sci.*
8. **Zhu, Y.**; Hazeldine, S. T.; Li, J.; Oupicky, D., Self-immolative linker based BENSpm prodrug as dual drug/gene delivery system. *In preparation.*
9. Li, J.; **Zhu, Y.**; Lepadatu, A. M.; Wang, Y.; Ciobanu, M.; Asaftei, S.; Oupicky, D., Viologen-based dendrimers function dually as CXCR4 antagonists and gene delivery vectors. *Submitted to Bioconjugate Chem.*
10. **Zhu, Y.**; Li, J.; Wang, Y.; Manickam, D.S.; You, Y. Z.; Oupicky, D., Redox-responsive polymer-based gene delivery systems. "Gene and Cell Therapy: Therapeutic Mechanisms and Strategies", Templeton N. S., 4th Ed., *Submitted.*

**Patents**

1. Oupicky, D. and **Zhu, Y.** (co-inventor), "Dual function biodegradable polycations synthesized from polyamine analogs for combination drug-RNAi, drug-gene, and drug-protein therapies." Invention disclosure (13-1186) filed 7/29/2013

**Awards**

1. **First place at NanoDDS'11 Poster Award and Oral Presentation**, Nanomedicine and drug delivery symposium, Salt Lake City, UT, 2011
2. **Outstanding student poster award**, 8th Annual Research Forum, Eugene Applebaum College of Pharmacy and Health Sciences, Wayne State University, Detroit, MI, 2011
3. **Frank O. Taylor Scholarship**, Wayne State University, Detroit, MI, 2012
4. **Summer Dissertation Fellowship**, Wayne State University, Detroit, MI, 2013